Microbial Formation of Nitrous Acid and its Exchange Processes between Soils and Atmosphere

Dissertation

zur Erlangung des Grades eines
'Doktor rerum naturalium (Dr. rer. nat.)' der Fachbereiche:
08 - Physik, Mathematik und Informatik,
09 - Chemie, Pharmazie und Geowissenschaften,
10 - Biologie,
Universitätsmedizin

verfasst und vorgelegt von

Michael Ermel

geboren am 19. März 1986
in Kirn

Max Planck Graduate Center
mit der Johannes Gutenberg-Universität Mainz

angefertigt am Max-Planck-Institut für Chemie

Mainz, 2014

Tag der mündlichen Prüfung: 28.11.2014

I hereby declare that I wrote the dissertation submitted without any unauthorized external assistance and used only sources acknowledged in the work. All textual passages which are appropriated verbatim or paraphrased from published and unpublished texts as well as all information obtained from oral sources are duly indicated and listed in accordance with bibliographical rules. In carrying out this research, I complied with the rules of standard scientific practice as formulated in the statutes of the Johannes Gutenberg University Mainz to insure standard scientific practice.

Mainz, 26. September 2014

Michael Ermel

„In der Wissenschaft gleichen wir alle nur den Kindern, die am Rande des Wissens hier und da einen Kiesel aufheben, während sich der weite Ozean des Unbekannten vor unseren Augen erstreckt."

Isaac Newton

Abstract

Nitrous acid (HONO) is an important reactive nitrogen species, which is short lived due to the photolysis yielding nitric oxide (NO) and hydroxyl radicals (OH). While the latter is the major oxidant of the atmosphere and thus of crucial importance for the self-cleansing ability of the atmosphere, NO is considered as an air pollutant enhancing the formation of ozone. Hence, HONO has an ambivalent role in atmospheric chemistry, but is usually considered as a major source of OH. A sound understanding of sources and sinks of HONO is a basic prerequisite to assess its impacts on the environment. However, a strong daytime source of HONO is still missing and nighttime HONO deposition on the ground was only postulated. Soil emissions of HONO were recently suggested to explain the missing source. This thesis aims to reveal the processes of HONO release and uptake from soil and to understand the underlying mechanisms.

In order to quantify the role of HONO soil emissions, 17 soils covering a wide range of soil parameters were investigated in a dynamic chamber system. HONO emissions were found to be in the same order of magnitude as the well-studied NO emissions from soil and for some samples NO release was exceeded by HONO. Generally, HONO emissions occurred at low soil water contents below 30% of water holding capacity. Unexpectedly, strongest emissions were found for soils of neutral pH from arid and arable regions. Such areas comprise about 20% of the earth's terrestrial surface, thus demonstrating the global importance of HONO emission from soil. Temperature dependencies of HONO and NO release lead to the assumption of a microbial release of HONO, which was confirmed by pure culture experiments with the ammonia-oxidizing bacterium *Nitrosomonas europaea* and soil sterilization experiments. A conceptual model on release of reactive nitrogen species (NO, N_2O, N_2) by microbes from soil as a function of the soil water content was extended by HONO soil emissions.

Further analysis of the bacterial release of HONO from soil showed that only ammonia-oxidizing bacteria are capable of emitting HONO within microbial nitrification, by evidence from pure culture and inhibition experiments. Cell internal accumulated hydroxylamine (NH_2OH) was shown to be responsible for HONO release, by a controlled introduction of cell lysis. NH_2OH was measured for the first time in the gas phase and was released by ammonia-oxidizing bacteria during the entire soil water content range investigated. The heterogeneous reaction of NH_2OH with water vapor on glass bead surface was shown to form HONO. In addition, the occurrence of HONO emissions at low soil moistures is explained by this reaction, as only then the surface is available for the reaction and not covered by water.

A ^{15}N tracer method was developed to measure isotopic labeled gas-phase HONO, which enables the investigation of formation processes of HONO and its role in biogeochemical cycles. The azo dye formed during the detection by the long path absorption photometer (LOPAP) is utilized for further analysis, as the nitrogen atom of HONO is quantitatively conserved into the dye. Purification by solid phase extraction of the dye solution and subsequent analysis by high performance liquid chromatography coupled to mass spectrometry yield the ^{15}N relative exceedance. Application of the method to a soil sample with ^{15}N labeled urea, which was investigated in a dynamic chamber system, confirmed our recent findings of the strong contribution of soil bacteria to HONO release.

Bidirectional fluxes of HONO were found for six investigated soil samples. The direction of the flux is depending on the ambient mixing ratio of HONO and the soil water content. An important value to describe the bidirectional flux is the "ecosystem specific compensation mixing ratio of HONO", χ_{comp}. This new term was defined and introduced as the various processes involved in the soil exchange of HONO are not compatible with the classic definition of the compensation point. Low χ_{comp}, below typical daytime mixing ratios of HONO for some soils and, hence, uptake of HONO, reveal the ambivalent role of soil in the exchange of HONO. The results confirm recent field observation, that HONO, which was adsorbed to soil at high ambient mixing ratios, is desorbed from the soil at low ambient mixing ratios of HONO. Thus HONO deposited during night time can be transformed to a source of HONO during daytime. Four processes, partitioning of HONO according to Henry's law, bacterial HONO formation via NH_2OH, adsorption and desorption of HONO were identified to be dominant at certain soil moistures. Thus, a conceptual model about the processes involved in release and uptake of HONO from soil as a function of the soil water content was developed.

Overall, this thesis revealed crucial processes in the exchange of HONO between soil and atmosphere and the mechanism of bacterial HONO formation was elucidated. Soil was shown to be an important source and sink of HONO and, hence, its consideration in future field observations is highly encouraged.

Zusammenfassung

Salpetrige Säure (HONO) ist eine wichtige Form von reaktivem Stickstoff, die aufgrund ihrer Photolyse zu Stickstoffmonoxid (NO) und dem Hydroxylradikal (OH), sehr kurzlebig ist. Während letzteres das wichtigste Oxidans in der Gasphase und deshalb von größter Bedeutung für die Selbstreinigungsfähigkeit der Atmosphäre ist, wird NO als Luftschadstoff angesehen, der die Bildung von Ozon fördert. Weshalb HONO eine ambivalente Rolle in der atmosphärischen Chemie hat, jedoch wird es oftmals als starke Quelle für OH-Radikale betrachtet. Ein genaues Verständnis der Quellen und Senken von HONO ist eine grundlegende Voraussetzung, um dessen Einfluss auf die Umwelt zu beurteilen. Allerdings wird immer noch nach einer starken HONO-Quelle am Tag gesucht und nächtliche HONO-Deposition auf den Boden wurde bisher stets nur postuliert. Bodenemissionen von HONO wurden kürzlich vorgeschlagen um die fehlende Quelle zu erklären. Diese Dissertation folgt der Zielsetzung die Prozesse der HONO-Aufnahme und -Freisetzung von Böden aufzudecken und die zugrunde liegenden Mechanismen zu verstehen.

Um die Rolle von HONO-Bodenemissionen zu quantifizieren, wurden 17 Böden, die ein großes Spektrum von Bodenparametern abdecken, in einem dynamischen Kammersystem untersucht. Es konnten HONO-Emissionen derselben Größenordnung wie die bereits gut untersuchten NO-Emissionen festgestellt werden. In einigen Proben überstiegen die HONO-Emissionen die NO-Freisetzung. Im Allgemeinen wurden die Emissionen von HONO bei niedrigen Bodenwassergehalten unter 30% der Feldkapazität gefunden. Unerwarteter Weise wurden die stärksten Emissionen bei Böden mit neutralem pH aus ariden und landwirtschaftlichen Gebieten beobachtet. Dies sind etwa 20% der terrestrischen Erdoberfläche, was die globale Relevanz von HONO-Bodenemissionen zeigt. Die Temperaturabhängigkeit der Bodenemissionen von HONO und NO führten zu der Annahme einer mikrobiellen Freisetzung von HONO, welche durch Reinkulturexperimente mit dem ammoniumoxidierenden Bakterium *Nitrosomonas europaea* und Sterilisationsexperimente bestätigt werden konnte. Ein konzeptionelles Model für die Freisetzung reaktiver Stickstoffverbindungen aus Böden in Abhängigkeit des Bodenwassergehaltes wurde um HONO-Emissionen erweitert.

Durch Nachweise mittels Reinkultur- und Inhibitionsexperimenten konnten weitere Untersuchungen der bakteriellen Freisetzung von HONO aus Böden zeigen, dass innerhalb der bakteriellen Nitrifikation nur ammoniumoxidierende Bakterien zur Emission von HONO fähig sind. Durch kontrolliert initiierte Zelllyse konnte gezeigt werden, dass intrazellulär akkumuliertes Hydroxylamin (NH_2OH) für die HONO-Freisetzung verantwortlich sind. Zum

ersten Mal wurde NH_2OH in der Gasphase nachgewiesen und dass dieses über den gesamten Bodenfeuchtebereich von ammoniumoxidierenden Bakterien freigesetzt wird. Es wurde gezeigt, dass die heterogene Reaktion von NH_2OH mit Wasserdampf auf einer Glasperlenoberfläche HONO bildet. Diese Reaktion erklärt die beobachtete Freisetzung von HONO bei niedrigen Bodenfeuchten, da nur dann die Oberfläche zur Reaktion zur Verfügung steht und nicht von Wasser bedeckt ist.

Eine ^{15}N Isotopenmarkierungsmethode wurde entwickelt um isotopenmarkiertes gasförmiges HONO zu messen, was die Untersuchung der Bildungsprozesse von HONO und dessen Rolle in biogeochemischen Zyklen ermöglicht. Der Azofarbstoff, der während der Detektion durch das Langwegabsorptionsphotometer (LOPAP) gebildet wird, kann für die weitere Analyse verwendet werden, da das Stickstoffatom in HONO quantitativ im Farbstoff konserviert wird. Durch die Reinigung mittels Festphasenextraktion der Farbstofflösung und die darauffolgende Analyse mithilfe von Hochleistungsflüssigkeitschromatographie gekoppelt mit Massenspektrometrie erhält man den relativen ^{15}N Überschuss von HONO. Die Anwendung dieser neuen Methode auf eine Bodenprobe die mit ^{15}N Harnstoff angereichert und in einem dynamischen Kammersystem untersucht wurde, bestätigt die obigen Ergebnisse einer starken mikrobiellen Beteiligung von Bodenbakterien zur HONO Freisetzung.

Bidirektionale Flüsse von HONO wurden für sechs untersuchte Bodenproben gefunden. Die Richtung der Flüsse hängt dabei vom Umgebungsmischungsverhältnis von HONO und dem Bodenwassergehalt ab. Eine wichtige Größe, die die bidirektionalen Flüsse von HONO beschreibt, ist das „Ökosystem spezifische Kompensationsmischungsverhältnis von HONO“, χ_{comp}. Dieser neue Begriff wurde definiert und eingeführt, da die verschiedenen in den Bodenaustausch von HONO involvierten Prozesse nicht mit dem klassischen Kompensationspunktkonzept kompatibel sind. Niedrige χ_{comp} unterhalb den typischen Tagesmischungsverhältnissen von HONO, was eine HONO-Aufnahme über Tag zur Folge hat, zeigen die ambivalente Rolle von Böden im HONO-Austausch. Die Untersuchungen bestätigen neueste Feldbeobachtungen, dass HONO, welches bei hohen Umgebungsmischungsverhältnissen vom Boden adsorbiert wird, bei niedrigen Mischungsverhältnissen wieder vom Boden desorbiert wird. Folglich wird nächtlich akkumuliertes HONO tagsüber in eine Quelle für HONO umgewandelt. Vier Prozesse - Verteilung von HONO zwischen Gas- und Flüssigphase nach Henrys Gesetz, bakterielle HONO Bildung aus NH_2OH, Adsorption und Desorption von HONO - und deren Dominanz in speziellen Bodenfeuchtebereichen wurden identifiziert. Dadurch wurde ein konzeptionelles Model für die Prozesse, die in Aufnahme

und Freisetzung von HONO aus Böden involviert sind, als Funktion der Bodenfeuchte entwickelt.

Zusammenfassend hat diese Dissertation die entscheidenden Prozesse im Austausch von HONO zwischen Boden und Atmosphäre aufgeklärt und den der bakteriellen HONO Bildung zugrunde liegenden Mechanismus aufgedeckt. Es konnte gezeigt werden, dass Böden sowohl eine wichtige Quelle als auch eine Senke für HONO sind und sollten folglich in zukünftigen Feldmessungen stärker berücksichtigt werden.

Table of Contents

1. Introduction and Motivation

1.1 The nitrogen cycle

Nitrogen (N) is essential for the growth and health of all forms of living. The earths' largest reservoir of nitrogen in form of the inert molecular nitrogen (N_2) in the atmosphere can naturally only be assimilated by a few plants and microbes which are capable of biological nitrogen fixation (BNF)(Vitousek et al 2002). This process converts N_2 into reactive nitrogen (N_r), ammonium (NH_4^+) namely during BNF, which can be metabolized by the biosphere. Nitrifying microbes in soil, marine and fresh water oxidize NH_4^+ to nitrite (NO_2^-) and nitrate (NO_3^-)(Koops et al 2006, Prosser and Nicol 2012), for example, providing another accessible form of N_r to plants and other microbes. Some of the latter are capable of reducing NO_3^- back to N_2, a process known as denitrification (Knowles 1982), and recycle N_2 to the atmosphere. During these processes the microbes emit the trace gases nitrous oxide (N_2O) and nitric oxide (NO). These two, together with ammonia (NH_3) emissions from soil, are part of different atmospheric chemistry cycles, forming other N_r species like nitrous acid (HONO) or nitric acid (HNO_3) with different impacts on the atmosphere and biosphere. Ammonium nitrate (NH_4NO_3), a product of the acid-base reaction of NH_3 and HNO_3, is an important cloud condensation nucleus (CCN), which is responsible for cloud formation and precipitation. Wet and dry deposition of the different N_r species is another nutrient input for terrestrial and marine ecosystems and withdraws N_r from the atmosphere. Oxidized forms of nitrogen are effectively washed out by rain, while other compounds accumulate to larger particles, which sediment. Figure 1 comprises the different pathways and shows some additional transport processes between the atmosphere and marine and terrestrial ecosystems. The lifetime of a N_r species, can vary strongly, depending on its current position in the nitrogen cycle. While some freshly applied fertilizer can be degraded in a few weeks or even days, N_r in the deeper soil layers under the surface, where microbial activity is lower, might not be converted for years. The relatively inert N_2O passes the troposphere without major losses until it reaches the stratosphere, where it finally reacts with ozone. This process takes place in the order of years. HONO on the other hand is photolyzed within 20 – 30 min under strong solar irradiation (Stutz et al 2000).

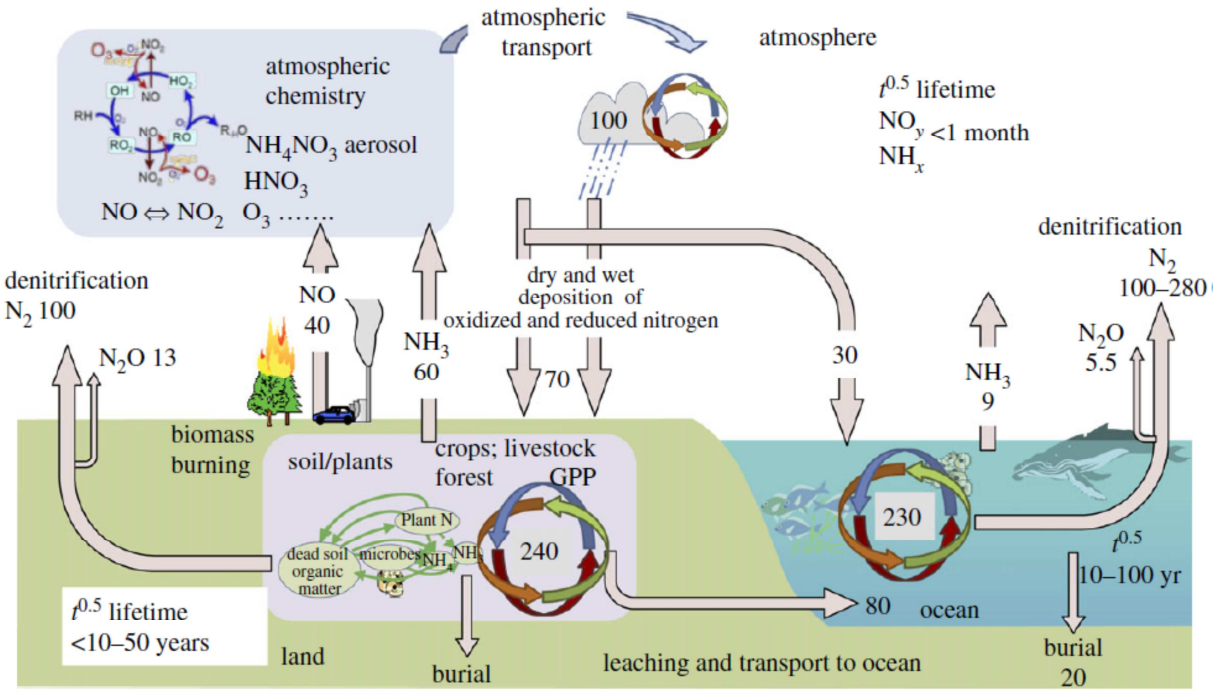

Figure 1: Scheme of the nitrogen cycle and the fluxes of reactive nitrogen in Tg N yr^{-1} between and within the atmosphere and terrestrial and marine ecosystems. (from Fowler et al (2013))

Besides BNF, nitrogen fixation can also occur during thunderstorms. Lightning strikes release enough energy to break the nitrogen-nitrogen triple bond, which is among the strongest in chemistry, and as a result NO is formed in a reaction with atmospheric oxygen (Tie et al 2002). The naturally low rates of N_r production have formed ecosystems coping with low N availability worldwide, although for every 100 atoms of carbon used for cell construction, between 1 to 20 atoms of N are needed (Sterner and Elser 2002). This has limited the ecosystems productivity, but enriched its biodiversity. N-limitation has driven the evolution to extremes in the hunt for N, some plants for example have evolved to carnivores, extracting N from catching and digesting animals. Mankind had to face this problem as well and learned to overcome N-limitation by fertilizing agricultural fields for 6500 years (Smith 1995) in order to ensure good food production.

In 1909, the German chemist Fritz Haber found a reaction producing ammonia (NH_3) from N_2 and hydrogen (H_2) in the laboratory. The up scaling to an industrial process by Carl Bosch and the first industrial plant for the so called Haber-Bosch process in 1913, were the beginning of the anthropogenic nitrogen fixation (Smil 2004). Although the first use was the production of munitions, this process became the foundation for the synthetic fertilizer production. In the 1970's the production of NH_3 by terrestrial BNF was overtaken by the

Haber-Bosch process. In 2005 the nitrogen fixation by the Haber-Bosch process of 120 Tg N yr^{-1} (Galloway et al 2008) doubled the terrestrial BNF of 63 Tg N yr^{-1}(Fowler et al 2013). Besides this, the unintentional production of N_r as a side product of fuel combustion is a major anthropogenic contributor to the total N_r budget. The total anthropogenic nitrogen fixation (210 Tg N yr^{-1}) is now as large as the natural nitrogen fixation (203 Tg N yr^{-1})(Fowler et al 2013). Hence, the input of N_r into ecosystems has doubled in the last century.

The enhanced availability of cheap fertilizer supported the growth of the world's population and today the food of about half of the humans on our planet depends on artificially produced fertilizer N (Erisman et al 2008). Albeit the intensified N_r input in ecosystems has led to severe negative effects for the environment, climate and human health (Erisman et al 2013). The diversity of possible transformation steps of one atom of N within the nitrogen cycle before it is released as the ineffective N_2, leads to an accumulation of adverse impacts of just a single N atom. This chain is called the nitrogen cascade (Galloway et al 2003) and its most important effects are shortly discussed:

Eutrophication of fresh water disequilibrates the ecosystems by acidification and favoring the growth of algae and other water plants (Camargo and Alonso 2006). A high abundance of algae can cause low oxygen levels, which is harmful for different aquatic forms of living. The defined threshold for eutrophication is 1 mg NO_3-N l^{-1} and at levels of 10 mg NO_3-N l^{-1} severe effects for aquatic animals are observed (Camargo et al 2005). These values can be quickly reached if agricultural fields close to the fresh water are intensively fertilized. The same effect is reported for N_r input into marine ecosystems and in 2012 about 540 coastal dead zones were known (Galloway et al 2013) and in some regions the area has increased by the 10-fold in the last two decades (Carstensen et al 2014).

In 1872 it was first mentioned by Robert Angus Smith, that rain is more acidic around cities and "artificial circumstances" are likely (Smith 1872). Acid rain is indeed mainly caused by human sulfur dioxide (SO_2) and nitrogen oxide (NO_x = NO + NO_2) emissions, which form sulfuric acid (H_2SO_4) and HNO_3 due to the oxidative character of the atmosphere. While anthropogenic SO_2 was strongly reduced by flue-gas desulfurization, the contribution of NO_x to acid rain increased. HNO_3 is formed by the oxidation of NO_2 with the hydroxyl radical (OH):

$$NO_2 + OH \rightarrow HNO_3 \qquad \text{(R1)}$$

The N_r deposited by acid rain enhances the eutrophication of ecosystems, besides the negative effect of increasing acidity.

The formation of N_2O, one of the most important non-CO_2 greenhouse gases, influences the global radiative forcing and hence, climate change, strongly (Stocker et al 2013). The trace gas is mainly emitted from denitrification in soils and anthropogenic induced emission of N_2O by fertilizer application exceeded natural sources in the 1990s (Reay et al 2012). Further sources are biomass burning, industry and formation from other N_r emissions (Galloway et al 2004). The mixing ratio of N_2O has increased from ~ 270 ppb in pre-industrial era to currently 325 ppb (Davidson 2009), which equals a surplus of 20%. Besides the radiative characteristics, the depletion of stratospheric ozone by N_2O has strong effects on human health, as more harmful UV radiation passes the stratospheric ozone layer. Throughout the 21st century it is expected to remain the strongest ozone-depleting agent in the stratosphere (Ravishankara et al 2009).

In the troposphere NO and NO_2 influence atmospheric chemistry strongly, through the formation and depletion of ozone:

$$NO + O_3 \rightarrow NO_2 + O_2 \quad \text{(R2)}$$

$$NO_2 + h\nu \rightarrow NO + O \quad \text{(R3)}$$

$$O + O_2 \rightarrow O_3 \quad \text{(R4)}$$

The N_r enhanced formation of O_3 leads to crop losses (Ainsworth 2008, Paoletti 2005), stronger formation of particulate matter (PM) (Meng et al 1997) and adverse effects on human health by ozone itself (Levy et al 2005, Uysal and Schapira 2003). Besides the formed O_3, also PM and NO_x have severe health impacts like lung cancer and other respiratory diseases (Anenberg et al 2010, Fajersztajn et al 2013, Lelieveld et al 2013). Various sources of NO exist, like fossil fuel burning, lightning, biomass burning and release by soil bacteria. Nitrous acid (HONO), another important N_r species, can form carcinogenic nitrosamines (Sleiman et al 2010), which is of special concern indoors, where unexpectedly high concentrations of HONO are found (Febo and Perrino 1991). Beside the formation of carcinogens, HONO strongly influences the oxidative capacity of the atmosphere and is a direct precursor of NO. Hence, HONO is directly and indirectly involved in many of the previously described processes, but formation processes and fate of HONO are yet not fully understood.

1.2 The chemistry and impact of nitrous acid in the atmosphere

Since its first detection as a trace gas in the atmosphere in 1979 by Perner and Platt (1979), nitrous acid (HONO) has been intensively studied and is now well accepted as an important source of the OH radical. This is considered as the major oxidant of the atmosphere and thus is mainly responsible for the oxidative capacity of the atmosphere.

HONO undergoes a diurnal cycle with accumulation overnight and decay during the day. The photolysis of HONO is responsible for lower mixing ratios of HONO during daytime and yields the OH radical:

$$HONO + h\nu \rightarrow NO + OH \qquad (R5)$$

While early studies assumed, that production of OH from HONO is only relevant in the morning hours after sunrise (Harrison et al 1996), recent studies showed a contribution of up to 60% to the total OH production (Ren et al 2003) and significant production during the whole day (Sörgel et al 2011a). This progress in the understanding of the atmospheric chemistry of HONO can mainly be attributed to more sophisticated measurement techniques, which are able to measure HONO down to detection limits of a few ppt (Heland et al 2001, Kleffmann et al 2002). The increased sensitivity led to the discovery of HONO daytime mixing ratios of up to a few hundred ppt (Kleffmann et al 2003), which were not detectable before. Hence, the expected low daytime mixing ratios in the order of several ppt (Vogel et al 2003), according to known gas phase (see chapter 1.2.1) and heterogeneous reactions (see chapter 1.2.2), were exceeded and a missing daytime source was postulated (Kleffmann et al 2003). In the following time, this missing source of HONO during daytime was observed many times and correlations with the photolysis frequency of NO_2 ($J(NO_2)$) were found (Kleffmann et al 2005, Li et al 2012, Su et al 2008b, Villena et al 2011, Wong et al 2012). Consequently, different new reactions were characterized and postulated to explain the missing daytime source of HONO (Bejan et al 2006, George et al 2005, Ramazan et al 2004, Stemmler et al 2006, Zhang and Tao 2010), however, none of them was capable to close the budget of HONO (Sörgel et al 2011a).

In the nighttime high levels of HONO are observed and a pseudo stationary state, with a constant mixing ratio of HONO, is reached. The underlying process of the accumulation is the heterogeneous formation of HONO from NO_2 on surfaces (Finlayson-Pitts et al 2003, Harrison et al 1996, Lammel and Cape 1996). Several studies suggest dry deposition of

HONO, which is accumulated in the gas phase, to the ground surface (Sörgel et al 2011a, Stutz et al 2002, Stutz et al 2004, Su et al 2008a, Su et al 2008b, Wong et al 2011). This process is yet only poorly investigated and just recently a first study on the uptake of HONO on soil particles started to explore this surface reaction (Donaldson et al 2014). However, only dry soils were studied, which might impede the application of these results to field observations, as the partitioning of HONO to soil water has to be considered due to its Henry coefficient (Lide 2004). Earlier laboratory studies focused on the uptake of HONO into water, as thin films, dew or at different pH (Bongartz et al 1994, He et al 2006, Hirokawa et al 2008, Kleffmann et al 1998, Mertes and Wahner 1995), and the process was mostly found to be reversible. Several field studies observed the uptake of HONO into the liquid phase, like fog or dew (Rubio et al 2009, Sörgel et al 2011b).

The uncertainties in the knowledge of the formation of HONO during daytime and the loss of HONO during nighttime need further investigation in order to understand the impact of nitrous acid on the atmosphere. Although many field studies showed the large contribution of HONO to the total OH production, it is usually not considered in atmospheric models. Recent studies showed the significant impact in global scale models on the oxidative capacity of the atmosphere (Elshorbany et al 2012) but also on cloud and aerosol formation (Elshorbany et al 2014).

1.2.1 Gas phase reactions of HONO

The photolysis of HONO (R5) is the most prominent gas phase reaction of HONO. Wavelengths of 300 – 405 nm are necessary for the dissociation to take place (Stockwell and Calvert 1978, Stutz et al 2000). The lifetime of HONO can vary from about 2 h after sunrise to 20 – 30 min at noon for mid latitudes (Stutz et al 2000), with a typical photolysis frequency of $J(HONO) = 1 - 4 \cdot 10^{-3}\ s^{-1}$ (Platt et al 1980). The recombination of NO and OH is a ternary reaction yielding HONO (Nguyen et al 1998, Pagsberg et al 1997, Stuhl and Niki 1972):

$$NO + OH + M \rightarrow HONO + M \qquad (R6)$$

The collision partner M can either be N_2 or O_2, which is necessary to conserve energy and momentum. Due to the small reaction rate constant ($k \approx 8 \cdot 10^{-12}\ cm^6\ molec^{-2}\ s^{-2}$, (Pagsberg et al 1997, Sander et al 2006)), the recombination reaction of the photolysis yields only small amounts of HONO. A steady state of HONO, NO and OH is established through reactions (R5) and (R6), which reaches HONO mixing ratios in the order of 10 – 30 ppt for moderate

atmospheric levels of NO and OH. Another process yielding HONO is the ternary reaction of NO_x and water vapor (R7).

$$NO + NO_2 + H_2O \rightarrow 2\ HONO \qquad (R7)$$

However, the rate constant ($k = 1.2 \cdot 10^{-34}$ cm^6 $molec^{-2}$ s^{-2}, (Chan et al 1976)) is too small for a significant HONO formation under atmospheric conditions, due to the unlikelihood of a three-body collision of the three educts.

Another reaction forming HONO is the reaction of photoexcited NO_2 and water vapor (R8) (Li et al 2008), however, two photons are needed for this processes. Hence, this process is negligible under atmospheric conditions (Amedro et al 2011). Recently, the photolysis of ortho-nitrophenols (R9) has been proposed as significant daytime source of HONO, as the reaction forms HONO efficiently (Bejan et al 2006). Nevertheless, the atmospheric concentration of these aromatic compounds is too low for a considerable contribution to the HONO budget (Wong et al 2012).

$$NO_2^* + H_2O \rightarrow HONO + OH \qquad (R8)$$

$$\text{o-nitrophenols} + h\nu \rightarrow R + HONO \qquad (R9)$$

The reaction of HO_2 and NO_2 (R10) has been investigated since the 1970s (Simonaitis and Heicklen 1974), but only recently suggested to explain the missing daytime source of HONO (Li et al 2014).

$$HO_2 + NO_2 \rightarrow HONO + O_2 \qquad (R10)$$

However, to explain the missing daytime source the yield of (R10) was assumed to be 100% by the authors of the study and potentially significant ground sources (see chapter 1.2.2) were estimated based on studies of a different ecosystem. Several studies on (R10) have been performed, but only a few identified HONO as a product (Cox and Derwent 1975, Levine et al 1977, Simonaitis and Heicklen 1974), while others did not observe HONO formation (Dransfield et al 2000, Graham et al 1977, Howard 1977, Niki et al 1977) or suggested pernitric acid (HNO_4, (R11)) as major product (> 99% yield) (Tyndall et al 1995, Zhu et al 1993).

$$HO_2 + NO_2 \rightarrow HNO_4 \quad \text{(R11)}$$

According to the available studies showing ambivalent findings and the resulting uncertainty, further laboratory and field measurements are essential to evaluate the contribution of (R10) on daytime formation of HONO.

The photolysis of HONO (R5) is the most important sink under atmospheric conditions, while gas phase reactions (R12) (Burkholder et al 1992) and (R13) (Ten Brink and Spoelstra 1998) are only of minor importance compared to (R5) (Sörgel et al 2011a).

$$HONO + OH \rightarrow H_2O + NO_2 \quad \text{(R12)}$$

$$2\ HONO \rightarrow NO + NO_2 + H_2O \quad \text{(R13)}$$

1.2.2 Heterogeneous reactions of HONO

The heterogeneous formation of HONO has become crucially important in the last decade, as many reactions suggested to explain the missing daytime source occur on different kinds of surfaces. The most studied reaction is the disproportionation of NO_2 in thin water layers:

$$2\ NO_2 + H_2O_{(ads)} \rightarrow HONO + HNO_{3(ads)} \quad \text{(R14)}$$

This reaction is the most dominant pathway of HONO production during nighttime and was shown to explain high HONO mixing ratios at night during several field observations (Harrison and Kitto 1994, Sörgel et al 2011a, Stutz et al 2002, Stutz et al 2004, Su et al 2008a). The formation mechanism has been intensively investigated (Barney and Finlayson-Pitts 2000, Kamboures et al 2008, Kleffmann et al 1998, Miller et al 2009, Mochida and Finlayson-Pitts 2000) and the proposed mechanism by Finlayson-Pitts et al (2003) involves the formation of N_2O_4 and the intermediate $NO^-NO_3^+$:

$$2\ NO_{2(g)} \rightarrow N_2O_{4(g)} \quad \text{(R15)}$$

$$N_2O_{4(g)} \rightarrow N_2O_{4(ads)} \quad \text{(R16)}$$

$$N_2O_{4(ads)} \rightarrow ONONO_{2(ads)} \quad \text{(R17)}$$

$$ONONO_{2(ads)} + NO_{2(g)} \rightarrow N_2O_{4(ads)} + NO_{2(g)} \quad \text{(R18)}$$

$$ONONO_{2(ads)} + H_2O_{(ads)} \rightarrow HONO_{(g,ads)} + HNO_{3(ads)} \quad \text{(R19)}$$

Several field studies found a correlation between the unknown daytime source of HONO and mixing ratio of NO_2, as well as the photolysis frequency of NO_2 $j(NO_2)$ (Li et al 2012, Sörgel et al 2011a, Stutz et al 2002, Su et al 2008a, Wong et al 2012). Hence, photosensitized reactions received strong scientific interest and many different reactions were proposed. In general, a substrate becomes a hydration agent after photo excitation and NO_2 is reduced by the transfer of a proton yielding HONO. A variety of substrate has been shown to be photo catalytic, like humic acids (Bartels-Rausch et al 2010, Stemmler et al 2006, Stemmler et al 2007), soot and aerosols (Broske et al 2003, Gerecke et al 1998, Kalberer et al 1999), TiO_2 and other metal surfaces(Bedjanian and El Zein 2012, Ndour et al 2008, Nishino and Finlayson-Pitts 2012).

$$R\text{-}H + h\nu \rightarrow [R\text{-}H]^* \quad \text{(R20)}$$

$$[R\text{-}H]^* + NO_2 \rightarrow HONO + R' \quad \text{(R21)}$$

Although all these reactions match the previously found correlations between the unknown daytime source of HONO and a product of the mixing ratio of NO_2 and the irradiation, none of them was yet shown to account for the unknown source. Sörgel et al (2011a) estimated the upper limit of the HONO formation from the heterogeneous transformation of NO_2 on humic acids (Stemmler et al 2006). The calculated maximal contribution was 30% and, hence, can only partly explain the high mixing ratios of HONO during daytime.

Recently the photolysis of nitrate and HNO_3 was suggested as daytime source of HONO (Zhou et al 2011). Li et al (2012) confirmed a formation from this pathway under atmospheric conditions at a field site in southern China. However, a recent study showed, that the photolysis of HNO_3 cannot account for the missing daytime source of HONO in a boreal forest environment (Oswald et al 2014).

In the past, several field studies performing gradient measurements of HONO suggested the ground to be a source of HONO (Febo et al 1996, Kleffmann et al 2003, VandenBoer et al 2013, Wong et al 2011, Wong et al 2012, Zhang et al 2009). A reasonable explanation is the partitioning of soil nitrite on the soil surface (Kubota and Asami 1985a, Kubota and Asami 1985b, Su et al 2011). Nitrite in soil is in an acid-base equilibrium with nitrous acid ($HONO_{aq}$) depending on the soil pH. According to Henry's law (Henry 1803, Smith and Harvey 2007), aqueous nitrous acid is in an additional equilibrium with gaseous HONO. The release of HONO varies with soil moisture and, hence, is variable. A crucial parameter for emission of HONO is the soil temperature, as the equilibria are temperature dependent and

emissions rise at higher temperatures. In the upper layers of soil, the temperature is mainly driven by irradiation, thus a maximum during noon time can be reached. Su et al (2011) showed in different model runs, that partitioning of soil nitrite can indeed explain the missing daytime source from a field observation in China (Su et al 2008b). However, only one soil sample was investigated and evidence from field measurements is still lacking.

$$H_3O^+_{(aq)} + NO_2^-{}_{(aq)} \leftrightarrow HONO_{(aq)} + H_2O_{(l)} \quad \text{(R22)}$$

$$HONO_{(aq)} \leftrightarrow HONO_{(g)} \quad \text{(R23)}$$

The assumption of HONO deposition on soils or the ground surface was suggested from many field observations, however has just recently be confirmed by a laboratory study (Donaldson et al 2014). A competitive adsorption process with water vapor was suggested. The results of VandenBoer et al (2014) point to a release of HONO during daytime from HONO adsorbed overnight. They found a strong contribution of this process to the missing daytime source of HONO. However, further investigation of this process and its temporal and quantitative limitations are needed to assess the significance of this adsorption-desorption process and the HONO budget.

1.3 Microbial nitrification in soil

Nitrification in soil is a process, that can be separated in two steps: the oxidation of NH_4^+ to NO_2^- by ammonia-oxidizing bacteria (AOB) (Koops et al 2006) and ammonia-oxidizing archaea (AOA) (Stahl and de la Torre 2012), followed by the transformation of NO_2^- to NO_3^- by nitrite-oxidizing bacteria (NOB) (Spieck and Lipski 2011). These processes occur under aerobic conditions, in contrast to denitrification (Knowles 1982), a microbial process that reduces NO_3^- to N_2, taking place under anaerobic conditions.

The oxidation of NH_4^+ by AOB is mediated by the membrane-bound enzyme ammonia monooxygenase (AMO) (Hofman and Lees 1953) and forms the intermediate hydroxylamine (NH_2OH) (Hollocher et al 1981). However, the enzyme needs NH_3 as substrate for the oxidation (R24). This step is endergonic and needs two electrons to take place (Arp and Stein 2003). AMO can also oxidize a wide range of small organic molecules like e.g. phenol, methanol and halogenated aliphatic compounds (Rasche et al 1990). Acetylene (C_2H_2) strongly inhibits AMO (Hyman and Wood 1985) and is applied in agriculture to avoid microbial loss of ammonia fertilizer(Freney et al 2000).

$$NH_3 + 2\,H^+ + O_2 + 2\,e^- \rightarrow NH_2OH + H_2O \qquad \text{(R24)}$$

In a second step NH_2OH is oxidized by hydroxylamine oxidoreductase (HAO) to nitrite (R25). This exergonic reaction provides four electrons, thus the overall oxidation of NH_3 yields two electrons for the metabolism of AOB. Hydrazine (N_2H_4) is another possible substrate for HAO, resulting in an alternative metabolism for pure culture studies of AOB (Anderson 1964). The exact mechanism of NH_2OH oxidation by HAO remains unclear. Several intermediates like HNO and NO were suggested (Hooper and Terry 1979, Hynes and Knowles 1984), but recent studies provide contradictory results, whether these compounds are involved (Cabail and Pacheco 2003, Hendrich et al 2002).

$$NH_2OH + H_2O \rightarrow NO_2^- + 4\,e^- + 5\,H^+ \qquad \text{(R25)}$$

The resulting overall conversion of NH_3 to NO_2^- by AOB needs 1.5 oxygen molecules:

$$NH_3 + 1.5\,O_2 \rightarrow NO_2^- + H^+ + H_2O \qquad \text{(R26)}$$

The atmospherically relevant trace gases NO and N_2O are known to be released by AOB, this is either possible during the oxidation of NH_2OH (R25) or by nitrifier denitrification. The latter process consists of the enzymes nitrite reductase (NirK or NirS) and nitric oxide reductase (NorB), which reduce nitrite to NO and subsequently to N_2O (Ferguson 1998, Stein and Yung 2003). The nitrite reducing enzyme of ammonia-oxidizers reveals a similarity to the nitrite reductase of denitrifiers (Chain et al 2003). The relevant metabolic processes of AOB are summarized in figure 2.

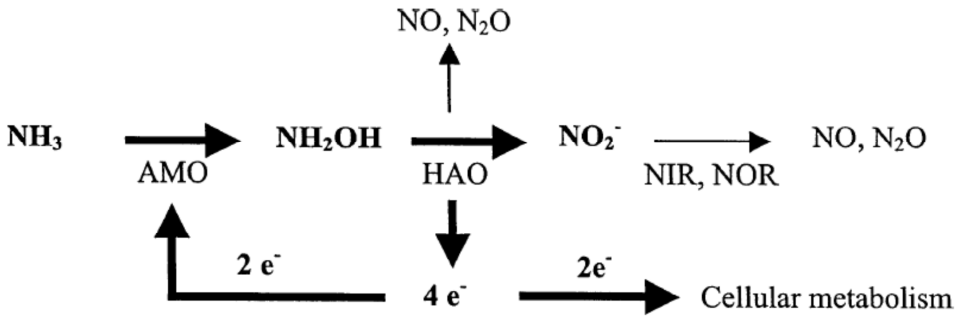

Figure 2: The metabolism of ammonia-oxidizing bacteria with the relevant enzymes ammonia monooxygenase (AMO), hydroxylamine oxidoreductase (HAO), nitrite reductase (NIR) and nitric oxide reductase (NOR) is schematically shown (Arp and Stein 2003).

The need of NH_3 as substrate instead of NH_4^+ restricts AOB to mostly neutral and alkaline soils. Some strains of *Nitrosospira* and *Nitrosovibrio* inhabit more acidic soils, where nearly no *Nitrosomonas* are found (Koops and Pommerening-Roser 2001). Some AOB exhibit an urease and are able to use urea (CH_4N_2O) as source of NH_3. As the urease is an intracytoplasmic enzyme, the metabolism gets independent of the external pH and thus the respective AOB reveal lower pH optima (Pommerening-Roser and Koops 2005). However, AOB were isolated from soils, rocks, fresh and seawaters, as well as sediments, thus revealing the broad abundance of this group of bacteria (Koops et al 2006).

Ammonia-oxidizing archaea received strong scientific interest since their recent discovery. The first marine AOA was isolated in 2005 (Konneke et al 2005) and two terrestrial strains were isolated in the following years (Lehtovirta-Morley et al 2011, Tourna et al 2011). The exact metabolism of AOA is not fully understood (Stahl and de la Torre 2012), but NH_2OH was recently shown to be produced as an intermediate in the ammonia oxidation (Vajrala et al 2013). The role of AOA in the nitrogen cycle is currently assessed and although AOA were shown to be more abundant in soils (Leininger et al 2006), AOB were shown to dominate the ammonia oxidation (Jia and Conrad 2009). However, *Nitrosopumilus maritimus* was also

shown to emit N_2O in significant amounts (Loscher et al 2012) and, thus, is of relevance for biogeochemistry.

The last step in nitrification is undertaken by NOB. A nitrite oxidoreductase oxidizes NO_2^- to NO_3^- and thus NO_2^- produced by AOB is directly converted (Spieck and Lipski 2011). Consequently, the nitrite pool undergoes fast transformation by AOB, NOB and denitrifying bacteria (Russow et al 2009).

$$NO_3^- + H_2O \rightarrow NO_3^- + 2\,H^+ + 2\,e^- \qquad \text{(R27)}$$

1.4. Knowledge gaps and research objectives

The release of nitrous acid from soils was already discovered in the 1980s (Kubota and Asami 1985a, Kubota and Asami 1985b), but has not received any scientific attention subsequently. The deposition of HONO to the soil surface was frequently reported to explain constant mixing ratios of HONO during nighttime, however laboratory studies confirming this process are still lacking. Recently soil nitrite was proposed to be a major source of atmospheric HONO during daytime (Su et al 2011). The acid-base equilibrium between nitrite and nitrous acid favors the formation of nitrous acid in acidic soils. The produced aqueous nitrous acid undergoes a partitioning with the gas phase yielding gaseous HONO. This process was shown to explain the missing daytime source of HONO in model calculations. However, this process is yet as poorly understood as HONO uptake by soil. Therefore this work addresses the following knowledge gaps:

- The source strength, which was estimated by Su et al. (2011) to be in the range of 1 – 3000 ng (N) m^{-2} s^{-1}, matches the values reported for the missing daytime source strength of 1 – 1000 ng (N) m^{-2} s^{-1}. However, only one sample was measured and the crucial parameters pH and nitrite content were adjusted artificially. As the applied reagents hydrochloric acid and NO_2^- are well known to produce HONO (Febo et al 1995), experiments without manipulation of the soil sample are of crucial importance to evaluate the strength of HONO release from soil.
- According to the conclusions of Su et al. (2011), high HONO emissions are expected from highly acidic soils, like boreal or tropical forest soils. Even low NO_2^- concentrations should yield strong release of HONO due to the strong influence of the pH. So far only one soil sample was investigated at nearly neutral pH, hence further measurements are necessary to verify the mechanism and draw further conclusions.
- The release of NO from soil is well studied (Feig et al 2008, Meixner and Yang 2006, Meixner 1997, Pilegaard 2013, Remde et al 1989) and contributes significantly to the global NO budget (Solomon 2007). Thus, a relation between NO and HONO emission might increase the understanding of HONO formation in soil. After photolysis, HONO is virtually a source of NO and, hence, HONO release from soil might influence the global NO budget substantially.
- The release of numerous atmospherically relevant trace gases like e.g. NO (Lipschultz et al 1981), N_2O (Bremner and Blackmer 1978), CH_4 (Schütz et al 1989) is primarily attributed to soil microbes. Hence, a possible microbial formation of HONO and subsequent release from soil should be considered. According to the acid-base

mechanism proposed by Su et al. (2011), microbes have a strong influence on the nitrite concentration in soil. Thus, soil microbes are at least involved indirectly.

- The partitioning of nitrous acid between soil solution and atmosphere is an equilibrium process, which can turn the proposed source of HONO into a sink. A prerequisite is a high pH, which favors the formation of nitrite after HONO uptake. Due to the limitations of Henry's law this process must be restricted to higher soil water contents. In addition, a possible uptake under dry conditions should be investigated as well.
- The release and uptake of HONO from soil implies the existence of a mixing ratio, where uptake and release compensate each other. For certain trace gases like e.g. NO, N_2O, CO the compensation point concept was introduced (Conrad 1994). As this parameter is of high value for upscaling and global models, further studies will strongly improve the understanding of the soils role in HONO chemistry.
- Isotope studies are of crucial importance in the process elucidation. The nitrogen atom of HONO is conserved in the azo-dye produced during the detection of HONO in the LOPAP instrument. Hence, the development of an isotope tracer method for HONO appears feasible and could strongly contribute to the investigation of processes forming HONO in soil, but also in the atmosphere.

In this thesis the principle to address the above knowledge gaps is the investigation of various soil samples, which cover a wide range of parameters to identify underlying processes. These processes will be further studied in detail in order to reveal their mechanism.

The overall aim of this thesis is (i) to reveal the processes in the release and uptake of HONO from soil, (ii) to understand the underlying mechanisms, (iii) to develop an isotope tracer method for HONO and (iv) to derive a conceptual model of the exchange of HONO between soil and atmosphere.

2. Methods

2.1 Dynamic Chamber Method

Measuring fluxes from soil is a demanding task, which needs sophisticated instrumentation and methods. While micrometeorological methods, like e.g. eddy covariance, are restricted to large areas (Horst and Weil 1994) and require very fast and precise analyzers (Ermel et al 2013, Müller et al 2010), chamber systems are suitable to investigate smaller samples and commercial analyzers are usually satisfying. Thus the deployment of chamber systems allows the investigation of samples in the laboratory. This is a big advantage to either measure samples from a wide variety of ecosystems without moving the measurement setup (van Dijk and Meixner 2001), or to study the processes controlling the fluxes of trace gases from soil (Behrendt et al 2014, Remde et al 1989).

In general static and dynamic chamber systems can be distinguished and only the latter are suitable to measure fluxes of reactive trace gases (Meixner 1994), as a continuous air flow reduces the contact time to the chamber walls and thus measurement artifacts. The flux F of a sample can be calculated from the mixing ratio difference between the entering χ_{in} and exiting air χ_{out}, the purging air flow Q, the molar volume of air V_m and the surface area of the sample A:

$$F = \frac{Q}{A \cdot V_m}(\chi_{out} - \chi_{in}) \quad (1)$$

However, the turbulent regime inside a dynamic chamber is significantly altered compared to undisturbed conditions in the field (Pape et al 2008). According to the common bulk resistance model (Hicks et al 1987, Wesely and Hicks 2000), the total exchange resistance under ambient conditions is the sum of the turbulent resistance (R_a), the quasi-laminar boundary layer resistance (R_b) and the surface resistance (R_c) (Fig. 3). The flux in ambient conditions is:

$$F_{amb} = \frac{1}{R_a + R_b + R_c}\frac{1}{V_m}(\chi_{out} - \chi_{in}) \quad (2)$$

In a dynamic chamber, the total resistance is the sum of four different resistance, the purging resistance (R_{purge}) between chamber and ambient air, the mixing resistance (R_{mix}), describing the turbulent mixing in the chamber, the modified boundary layer resistance (R_b^*) and the

chamber surface resistance (R_c^*) (Fig. 3). The flux in a dynamic chamber can be described by equation (3):

$$F_{cham} = \frac{1}{R_{purge}+R_{mix}+R_b^*+R_c^*}\frac{1}{V_m}(\chi_{out} - \chi_{in}) \quad (3)$$

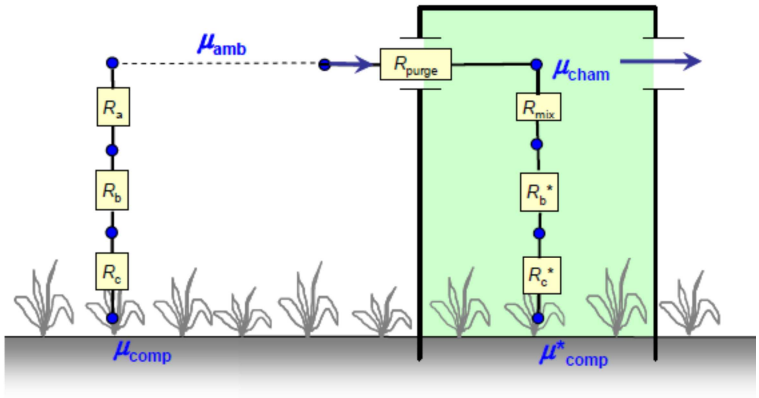

Figure 3: The resistances of trace gas exchange in undisturbed conditions (left) differ from the resistances present in the dynamic chamber (adapted from Pape et al (2008)).

Usually R_c^* is considered to be close to R_c and thus $R_c^* \approx R_c$ is assumed. The measured chamber flux can be corrected to match ambient conditions by equating eqs. (2) and (3):

$$\frac{F_{cham}}{F_{amb}} = \frac{R_a+R_b+R_c}{R_{purge}+R_{mix}+R_b^*+R_c} \quad (4)$$

According to eq. (4), fluxes measured in dynamic chambers can be corrected for the modified turbulent conditions, if all resistances are quantified. A good agreement between large scale micrometeorological methods and fluxes from dynamic chamber measurements was found by Rummel et al (2002).

2.2 Long Path Absorption Photometry

Several methods to measure HONO in the gas phase exist, like e.g. differential optical absorption spectroscopy (DOAS) (Perner and Platt 1979), chemical ionization mass spectrometry (Roberts et al 2010), wet chemical denuder techniques (Takenaka et al 2004) and long path absorption photometry (LOPAP) (Heland et al 2001). The latter instrument was used for the measurements in this thesis.

The LOPAP is a wet chemical instrument that quantitatively converts HONO to an azo dye. The concentration of this dye is measured by absorption photometry (Kleffmann et al 2002). A 1M hydrochloric acid (HCl) solution in a stripping coil takes up HONO and the subsequent reaction forms the nitrosyl cation (NO^+):

$$H^+ + HONO \quad \leftrightarrow \quad H_2O + NO^{+-} \qquad \text{(R28)}$$

Sulfanilamide from the stripping solution reacts with the nitrosyl cation:

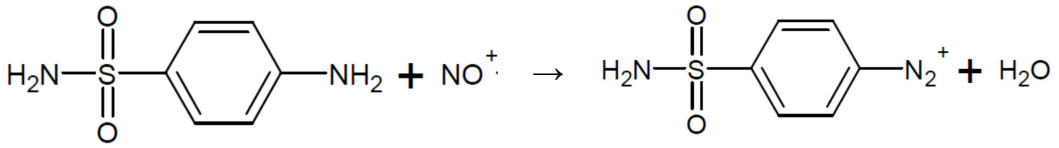

(R29)

The formed diazonium salt is transported into the instrument, where a second solution of N-(1-naphthyl)-ethylendiamine dihydrochloride is added and the reaction yields the azo dye:

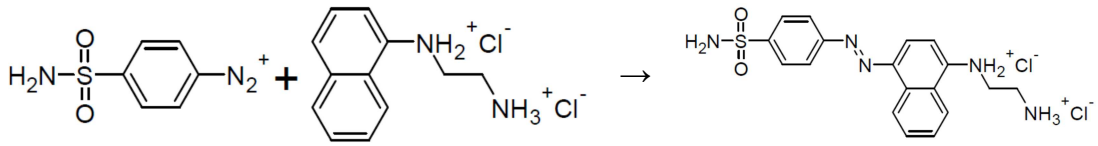

(R30)

Due to the low mixing ratios of HONO in the atmosphere a long absorption path is needed to achieve satisfying detection limits. This absorption volume is a Teflon tube of 1 – 2m with a high reflective index. Pump speed of the HPLC pump used to create the liquid flow and tube length determine the limit of detection (LOD) and response time of the instrument. Long tubes favor a low LOD but increase the response time. Depending on the specifications, LOD from 1 – 500 ppt are achievable.

To avoid measurement artifacts, a second stripping coil is mounted directly behind the first one, which is operated in the same way. While HONO is effectively collected in the first coil

(99.7% collection efficiency), other trace gases causing interferences (e.g. NO_2 and NO) are collected in both coils in equal ratios. Hence, a correction of the data for most interferences is possible (Kleffmann et al 2002). The stripping coils are placed in an external sampling unit, which avoids the problem of HONO wall losses in tubing. A scheme of the instrument setup is shown in figure 4.

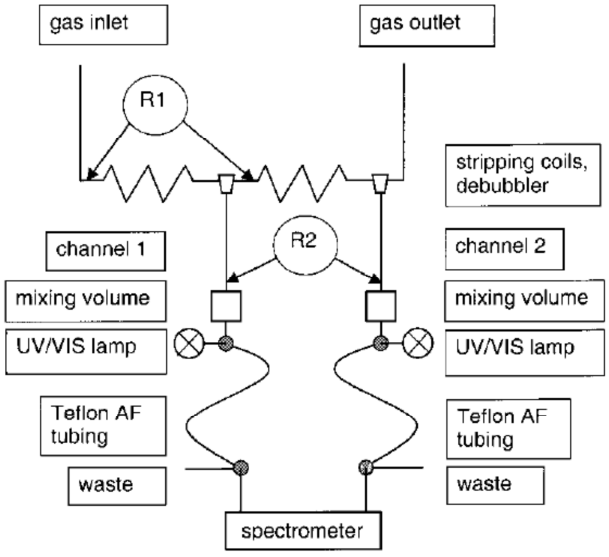

Figure 4: The external sampling unit of the LOPAP and the analysis unit are shown in a scheme (adapted from Heland et al (2001))

In a comparison study (Kleffmann et al 2006), the LOPAP was shown to measure HONO mixing ratios in good agreement with the DOAS technique. The comparison was performed in the field and in a smog chamber, simulating different atmospheric conditions. It was shown, that the correction for interference by the second stripping coil is of crucial importance to avoid an overestimation of HONO mixing ratios especially during daytime.

3. Results

3.1 Soil bacteria as a major source of HONO emissions

In a first approach, soil samples were measured in a dynamic chamber system setup to assess the significance of HONO release from soil. Measurements on temperature dependence of HONO emissions and sterilizations experiments were conducted to investigate a possible bacterial contribution to HONO release from soil. The aim of this study was (i) to quantify the strength of HONO emissions, (ii) to identify soil parameters controlling HONO emissions, (iii) to compare HONO and NO release from soil and (iv) to reveal the role of microbes in HONO release from soil.

In total, 17 soil samples were selected in order to cover a wide range of parameters, like pH, NH_4^+, NO_2^-, NO_3^-, loss on ignition (LOI), C/N ratio and particle distribution. The investigation of this samples showed, that HONO fluxes follow an optimum curve similar to the well-studied NO fluxes. In general, HONO fluxes were found to be in der same order of magnitude as NO fluxes for all soil samples. Contrary to the predicted strong HONO emissions from acidic forest soils, strongest emissions were found for nonacidic soils from arid and arable areas. High nutrient contents of NH_4^+ and NO_2^- favored the release of both N_r species. From these findings we deduced HONO hotspot areas, which we expect to exhibit strong HONO release and hence, a strong influence on tropospheric chemistry. The areas can be found around the world and comprise about 20% of the earth's terrestrial surface. Additionally, we expect HONO soil emissions, as an indirect source of NO, to account for discrepancies between global models of reactive nitrogen emissions and "top-down" approaches by satellite observations using NO_2 column densities.

The investigation of the temperature dependency of HONO fluxes from one soil sample resulted in similar activation energies for the processes of HONO and NO release, which were in a range that is reported for bacterial nitrification in soil. Consequently, we examined a pure culture of *Nitrosmonas europaea*, a well-studied ammonia-oxidizing bacterium (AOB), on its ability to emit HONO and found four times higher HONO flux compared to a sterile control. To corroborate these findings, we sterilized a soil sample and found a significant reduction of HONO and NO fluxes of 75% each, compared to the untreated sample. Measurements of microbial activity supported these findings, thus revealing a strong microbial source. Since the pH optimum of AOB is between pH 7-8, this process explains the unexpected strong release of HONO in soils of neutral pH.

From our results we concluded a conceptual model of reactive nitrogen release from soil as a function of the soil water content. HONO and NO fluxes occur at lower SWC (below 30 and 50% of water holding capacity (whc), respectively), whereas N_2O and N_2 are released at higher SWC.

For details, see: Oswald[*], Behrendt[*], Ermel[*], et al., Science (2013): HONO Emissions from Soil Bacteria as a Major Source of Atmospheric Reactive Nitrogen.

[*]: authors contributed equally

3.2 Bacterial hydroxylamine as a precursor of HONO soil emissions

This study follows up on Oswald et al (2013) and aims (i) to elucidate which groups of bacteria within bacterial nitrification are capable of emitting HONO and (ii) to clarify the underlying processes of bacterial HONO emissions.

We investigated five strains of AOB and three strains NOB on their ability to emit HONO. Only AOB were found to emit HONO significantly, while no emissions were observed for NOB. The examined AOB strains represent all phylogenetic lineages comprising terrestrial and limnic AOB species. We confirmed the findings of the pure culture experiments by the application of AOB and NOB specific inhibitors on soil samples, showing reduced HONO emissions during inhibition of AOB.

The investigation of pure AOB cultures was continued to elucidate the process of HONO release. An increase of the HONO flux with increasing cell density was found up to a threshold, when the flux started to decrease strongly. A similar pattern was found for the metabolism product NO_2^-, thus a formation via the acid-base equilibrium due to a lower pH in the cell membrane can be eliminated. The nitrifier denitrification pathway was excluded by experiments with knock-out mutants lacking the necessary enzymes, as these cultures emitted HONO as the wild-type. However, we found the HONO flux to be restricted by the ammonia availability in the cell and thus by the NH_2OH concentration inside the cell.

To confirm our theory, we initiated cell lysis of an AOB culture and measured subsequent release of HONO. By the use of mass spectrometry, we present the first detection of gaseous NH_2OH, which was released by AOB. NH_2OH was released during the whole SWC range and declined at lower SWC, where HONO release occurs. A coincidence of maximal HONO and NH_2OH release with an increase of cells with damaged membranes was found, pointing to a formation of HONO from cell internal NH_2OH. We show that a heterogeneous reaction of NH_2OH and water vapor on a glass surface forms HONO. This reaction explains HONO fluxes at low SWC, as only then the surface is available.

For details, see: Ermel, et al., *to be submitted*, (2014a): Hydroxylamine released by ammonia-oxidizing bacteria as precursor for HONO emissions from soils.

3.3 A novel ^{15}N tracer method to investigate the formation of HONO

So far many systems to measure HONO were optimized to lower the limit of detection, but a method to reveal processes by isotope labeling is still lacking. This study aims to develop a new method, which allows the investigation of isotopic labeled HONO.

The long path absorption photometer (LOPAP) utilizes an azo coupling of sulfanilamide and N-(1-naphthyl)-ethylendiamine dihydrochloride to form a strong absorbing azo dye. The crucial NO^+ is derived from the sampling of HONO in an acidic solution. Hence, the nitrogen atom in HONO remains in the azo dye and can be detected by mass spectrometry. The azo dye was purified by solid phase extraction and analyzed by high performance liquid chromatography coupled to mass spectrometry (HPLC-MS). As a result the ^{15}N relative exceedance, $\Psi(^{15}N)$, of gas phase HONO is measurable. The optimal working range of the method was found to be $\Psi(^{15}N) = 0.2 – 0.5$ and resulting standard deviation of $\Psi(^{15}N) < 4\%$. These parameters are comparable to other state-of-the art ^{15}N isotopic tracer methods.

The new method was applied to a dynamic chamber system, which is used to measure HONO soil emissions. After the application of ^{15}N labeled urea to a soil sample and the subsequent analysis of the azo dye, $HO^{15}NO$ was found in the gas phase. This measurement confirmed the contribution of bacteria to the soil emissions of HONO.

This method permits new approaches in the investigation of processes forming HONO, either in the atmosphere or in the biogeochemical nitrogen cycle, like studies on the effects of fertilizers on HONO formation.

For details, see: Wu, et al., Environ. Sci. Technol. (2014): Novel Tracer Method To Measure Isotopic Labeled Gas-Phase Nitrous Acid ($HO^{15}NO$) in Biogeochemical Studies.

3.4 Process studies on the exchange fluxes of HONO from soil

Most studies have focused on the processes regulating the release of HONO from soils and processes related to uptake of HONO on the soil are yet not understood. The goal of this study is (i) to identify processes controlling exchange fluxes of HONO, (ii) to assess the applicability of the compensation point concept to exchange fluxes of HONO, (iii) to discuss implications of exchange fluxes on atmospheric chemistry and (iv) to derive a conceptual model of the processes involved in the bidirectional fluxes of HONO between soil and air.

In this study, we investigated six soil samples on the presence of bidirectional fluxes of HONO. Therefore we used a dynamic chamber system, which was equipped with a HONO source and a valve, switching between air free of HONO and elevated mixing ratios of HONO. We intensively investigated one soil sample on effects of elevated mixing ratios of HONO and found desorption to take place, when HONO free air was applied. A linear relationship was found between the applied elevated mixing ratio of HONO and the desorbed HONO. These results support a recent field observation (VandenBoer et al 2014), which suggests a deposition of HONO during nighttime, followed by desorption during day to explain the missing daytime source of HONO.

A crucial prerequisite for the application of the compensation point concept are constant bidirectional fluxes of HONO with increasing soil layer thickness. Although our experiments confirmed this, the identified processes are of physic-chemical origin. Hence, the concept cannot be applied in its original microbial sense, but a calculation of the compensation mixing ratio is still possible. We defined this as the “ecosystem specific compensation mixing ratio of HONO”, χ_{comp}, as it still is a meaningful quantity to describe the exchange flux of HONO.

The ecosystem specific compensation mixing ratio of HONO was calculated for all soil samples of the whole SWC range, but only a correlation between the maximum emissions and χ_{comp} at the maximum emission was found. Hence the formation of HONO from bacterial NH_2OH is dominating and higher ambient mixing ratios of HONO are necessary to compensate the emission. For all soil samples χ_{comp} was found to be a function of the soil water content. As χ_{comp} below typical daytime mixing ratios of HONO (30 – 300 ppt) were found for some samples, soil has to be considered as significant sink not only during night time. Thus the unknown daytime source of HONO might be larger than previously considered.

The four identified processes, namely the partitioning of nitrous acid between aqueous and gas phase according to Henry’s law, the formation from bacterial NH_2OH, adsorption and

desorption, occur at different soil water contents. Hence, we derived a conceptual model of bidirectional fluxes of HONO, which shows the processes as a function of the soil moisture and their respective contribution.

For details, see: Ermel, et al., *to be submitted* to Biogeosciences Discussion (2014b): Bidirectional exchange of HONO between soil and air.

4. Conclusions

The main findings and their conclusions of this study can be summarized as follows:

1. Arable and arid soils of nonacidic pH emit HONO and NO in the same order of magnitude (Oswald et al 2013a). For a first approach of an upscaling by global models a ratio of 1:1 for F(HONO) and F(NO) could be used for soils obeying the above criteria. This easy approach would quantify the contribution of HONO to the global budget of N_r emission from soil. Furthermore this approach could verify, if HONO is responsible for the discrepancies between global models of N_r emissions and top-down approaches by satellite observations of NO_2 columns.
2. Strong HONO release was found for soils from arid ecosystems and in general the emission optimum was found at low soil water contents (Oswald et al 2013a). Thus, HONO soil emissions likely increase the oxidative capacity of troposphere in arid regions. In these areas agriculture is dominated by drip irrigation, which supplies just the necessary water to plants and, hence, keeps soils at low soil water content. Additionally the agricultural soils are strongly fertilized. Consequently, strong point sources are formed, which could particularly contribute to NO and OH formation.
3. Laboratory studies have convincingly shown, that soil is a significant source of HONO (Ermel et al 2014b, Oswald et al 2013a). However, final evidence from field observations is still lacking, although the ground was often suggested as source of HONO. Most recent field studies (Levy et al 2014, Li et al 2012, Li et al 2014, VandenBoer et al 2013, VandenBoer et al 2014, Wong et al 2012, Zhang et al 2012) have not considered soil as a source of HONO, mostly due to a lack of necessary measurements. Oswald et al (2014) investigated the role of soil within the HONO budget at a boreal forest, however, this soil emits only negligible amounts of HONO. Thus field observations in the identified hotspot areas are suggested to assess the contribution of HONO soil emissions to the missing daytime source of HONO.
4. Soil bacteria were identified as source of HONO soil emissions in soils of neutral pH (Ermel et al 2014a, Oswald et al 2013a). Thus a strong link between microbiology and important cycles of atmospheric chemistry was revealed, with impacts on cloud formation and, hence, climate. However, bacterial processes are harder to quantify as chemical processes, which only rely on few parameters. This means for future field observations, that microbial parameters should be considered as well.

5. The derived conceptual model of N_r release from soil (Oswald et al 2013a) enhances the understanding of the biogeochemical nitrogen cycling. The addition of HONO to the hole-in-a-pipe model is an important step to improve our insight into the microbial processes in the terrestrial nitrogen cycle.
6. Ammonia-oxidizing bacteria release cell internal NH_2OH during cell lysis, which forms HONO in the presence of water vapor on surfaces (Ermel et al 2014a). Recently NH_2OH was found to be the intermediate in the metabolism of ammonia-oxidizing archaea (Vajrala et al 2013). Thus, AOA should be considered as an additional source of HONO release from soil. This is of considerable significance, as AOA usually inhabit soils, which are more acidic compared to AOB and AOA can handle lower nutrient concentrations. Hence, the second smaller maximum among the investigated soils at pH 5-6 (Oswald et al 2013a) might be explained by HONO formation from AOA.
7. The heterogeneous reaction of NH_2OH and water vapor forms HONO and likely unknown products on surfaces (Ermel et al 2014a). However, NH_2OH is yet unknown in atmospheric chemistry. Although no release from soil was observed, NH_2OH should be considered to be present in the atmosphere. In this case, NH_2OH could contribute to HONO formation and might help to explain the missing daytime of HONO in ecosystems with low soil emission (Oswald et al 2014).
8. The release of NH_2OH and, hence, HONO formation occur after the cell membrane was damaged, due to water limitation at low soil water content (Ermel et al 2014a). Although this release was shown only for terrestrial and limnic strains of ammonia-oxidizing bacteria, the same mechanism is expected for marine strains, as all ammonia-oxidizing bacteria occupy the same metabolism, in respect to NH_2OH formation (Koops et al 2006). Therefore an enhanced release of HONO in coastal areas should be considered, as the cycle of high and low tide leads to a daily dry out of large areas. Especially areas with a large tidal range like the Wadden Sea should be examined.
9. Although no emissions of HONO from nitrite-oxidizing bacteria were found (Ermel et al 2014a), they still might influence bidirectional fluxes of HONO. An uptake of gaseous HONO as a source of nitrite might be a possible process for NOB to receive nutrients under dry conditions. Uptake processes of e.g. NO and N_2O are well known for nitrifying and denitrifying bacteria in soil.

10. The ecosystem specific compensation mixing ratio of HONO, χ_{comp}, is an important quantity to describe bidirectional fluxes of HONO (Ermel et al 2014b). Results from six soil samples showed only a correlation between maximal emission and χ_{comp} at the point of maximal emission. Studies with more samples, covering a wide range of parameters, might reveal more correlations and enhance the systematic understanding. The dependency of χ_{comp} on the soil water content implies the measurement of this quantity during field observations, in order quantify χ_{comp} successfully.
11. Uptake of HONO occurs in the whole soil water content range from 0 – 100% of water holding capacity (whc) and can be either attributed to adsorption or partitioning according to Henry's law (Ermel et al 2014b). While the first process is known to occur at lower soil water content (Donaldson et al 2014), the partitioning of HONO is restricted to higher soil water content. Soils of high pH are expected to be a strong sink for HONO at high soil moistures, as the acid base equilibrium favors the HONO dissociation to H^+ and NO_2^- strongly. A subsequent fast microbial transformation to other N species results in a sink for atmospheric N_r. The observed χ_{comp} below typical daytime mixing ratios of HONO (Ermel et al 2014b) indicate the ambivalent role of soil in the exchange of HONO between surface and atmosphere. Thus, HONO needs to be considered as sink and quantification of bidirectional fluxes of HONO from soil is crucial in the interpretation and calculation of HONO budgets derived from field observations.
12. The previously proposed desorption of adsorbed HONO (VandenBoer et al 2014), was proven by laboratory experiments (Ermel et al 2014b). This has strong consequences for field observations, as soils that were shown to have no significant emission according to maximum emission experiments (Oswald et al 2014), might be a source of HONO after exposure to high HONO mixing ratios at night. Further studies on the strength of desorption and its temporal scales under atmospheric conditions are highly advisable. A relocation of HONO deposited at night to daytime formation of HONO likely contributes to explain the missing daytime source of HONO.
13. A ^{15}N tracer method was developed and is applicable for biogeochemical process studies (Wu et al 2014). This method is a suitable tool investigate the not fully understood processes behind the desorption of HONO.
14. The investigation of bidirectional fluxes of HONO with a dynamic chamber setup is suitable, if alternating HONO mixing ratios are applied at the inlet of the chamber (Ermel et al 2014b). However, the following desorption is critical and was shown to

alter χ_{comp}. Thus an additional optimum flux experiment with 0 ppb ambient HONO mixing ratio is necessary to determine χ_{comp}. An optimization of the method should be considered, after the mechanisms of HONO desorption are better understood.

15. Previously observed HONO to NO conversion on dry soil surfaces was found to be 16% (Donaldson et al 2014). Ermel et al (2014b) established the dependency of HONO conversion on soil moisture. Conversions of up to 100% of the deposited HONO were observed. High HONO mixing ratios at night should be considered as a source of NO, although no radiation for photolysis is available. The underlying mechanism, however, remains unknown and further research is need to address this issue.
16. The conceptual model on bidirectional fluxes of HONO from soil comprises four processes occurring at different soil moistures (Ermel et al 2014b). The limitation of partitioning of HONO between aqueous and gas phase (Su et al 2011), bacterial HONO formation (Oswald et al 2013a) via NH_2OH (Ermel et al 2014a), adsorption (Donaldson et al 2014) and desorption (Ermel et al 2014b) of HONO to soil water contents where the respective process dominates, facilitates the applicability and understanding of the ecosystem specific compensation mixing ratio of HONO.

5. References

Abeliovich A, Vonshak A (1992). Anaerobic Metabolism of *Nitrosomonas Europaea*. *Arch Microbiol* **158:** 267-270.

Ainsworth EA (2008). Rice production in a changing climate: a meta-analysis of responses to elevated carbon dioxide and elevated ozone concentration. *Global Change Biology* **14:** 1642-1650.

Amedro D, Parker AE, Schoemaecker C, Fittschen C (2011). Direct observation of OH radicals after 565nm multi-photon excitation of NO_2 in the presence of H_2O. *Chem Phys Lett* **513:** 12-16.

Anderson J (1964). The metabolism of hydroxylamine to nitrite by *Nitrosomonas*. *Biochem J* **91:** 8.

Andersson KK, Hooper AB (1983). O_2 and H_2O are each the source of one O in NO_2^- produced from NH_3 by Nitrosomonas: ^{15}N-NMR evidence. *Febs Lett* **164:** 236-240.

Anenberg SC, Horowitz LW, Tong DQ, West JJ (2010). An Estimate of the Global Burden of Anthropogenic Ozone and Fine Particulate Matter on Premature Human Mortality Using Atmospheric Modeling. *Environ Health Persp* **118:** 1189-1195.

Arnold P (1954). Losses of nitrous oxide from soil. *J Soil Sci* **5:** 116-128.

Arp DJ, Stein LY (2003). Metabolism of inorganic N compounds by ammonia-oxidizing bacteria. *Critical Reviews in Biochemistry and Molecular Biology* **38:** 471-495.

Barney W, Finlayson-Pitts B (2000). Enhancement of N_2O_4 on porous glass at room temperature: A key intermediate in the heterogeneous hydrolysis of NO_2? *The Journal of Physical Chemistry A* **104:** 171-175.

Bartels-Rausch T, Brigante M, Elshorbany YF, Ammann M, D'Anna B, George C *et al* (2010). Humic acid in ice Photo-enhanced conversion of nitrogen dioxide into nitrous acid. *Atmos Environ* **44:** 5443-5450.

Beaumont HJE, Hommes NG, Sayavedra-Soto LA, Arp DJ, Arciero DM, Hooper AB *et al* (2002). Nitrite reductase of *Nitrosomonas europaea* is not essential for production of gaseous nitrogen oxides and confers tolerance to nitrite. *J Bacteriol* **184:** 2557-+.

Beaumont HJE, van Schooten B, Lens SI, Westerhoff HV, van Spanning RJM (2004). *Nitrosomonas europaea* expresses a nitric oxide reductase during nitrification. *J Bacteriol* **186:** 4417-4421.

Bedjanian Y, El Zein A (2012). Interaction of NO_2 with TiO_2 surface under UV irradiation: products study. *The Journal of Physical Chemistry A* **116:** 1758-1764.

Behrendt T, Veres PR, Ashuri F, Song G, Flanz M, Mamtimin B *et al* (2014). Characterisation of NO production and consumption: new insights by an improved laboratory dynamic chamber technique. *Biogeosciences Discuss* **11:** 1187-1275.

Bejan I, Abd El Aal Y, Barnes I, Benter T, Bohn B, Wiesen P *et al* (2006). The photolysis of ortho-nitrophenols: a new gas phase source of HONO. *Phys Chem Chem Phys* **8:** 2028-2035.

Belser LW, Mays EL (1980). Specific-Inhibition of Nitrite Oxidation by Chlorate and Its Use in Assessing Nitrification in Soils and Sediments. *Appl Environ Microbiol* **39:** 505-510.

Belser LW, Schmidt EL (1980). Growth and Oxidation-Kinetics of 3 Genera of Ammonia Oxidizing Nitrifiers. *Fems Microbiology Letters* **7:** 213-216.

Bollmann A, Conrad R (1998). Influence of O_2 availability on NO and N_2O release by nitrification and denitrification in soils. *Global Change Biology* **4:** 387-396.

Bongartz A, Kames J, Schurath U, George C, Mirabel P, Ponche JL (1994). Experimental-Determination of Hono Mass Accommodation Coefficients Using 2 Different Techniques. *J Atmos Chem* **18:** 149-169.

Braker G, Conrad R (2011). Diversity, Structure, and Size of N_2O-Producing Microbial Communities in Soils-What Matters for Their Functioning? *Adv Appl Microbiol* **75:** 33-70.

Bremner JM, Blackmer AM (1978). Nitrous oxice - emission from soils during nitrification of fertilizer nitrogen. *Science* **199:** 295-296.

Bremner JM, Blackmer AM, Waring SA (1980). Formation of nitrous oxide and dinitrogen by chemical decomposition of hydroxylamine in soils. *Soil Biology and Biochemistry* **12:** 263-269.

Breuninger C, Oswald R, Kesselmeier J, Meixner FX (2012). The dynamic chamber method: trace gas exchange fluxes (NO, NO_2, O_3) between plants and the atmosphere in the laboratory and in the field. *Atmos Meas Tech* **5:** 955-989.

Broske R, Kleffmann J, Wiesen P (2003). Heterogeneous conversion of NO_2 on secondary organic aerosol surfaces: A possible source of nitrous acid (HONO) in the atmosphere? *Atmospheric Chemistry and Physics* **3:** 469-474.

Burkholder JB, Mellouki A, Talukdar R, Ravishankara A (1992). Rate coefficients for the reaction of OH with HONO between 298 and 373 K. *Int J Chem Kinet* **24:** 711-725.

Cabail MZ, Pacheco AA (2003). Selective one-electron reduction of *Nitrosomonas europaea* hydroxylamine oxidoreductase with nitric oxide. *Inorg Chem* **42:** 270-272.

Camargo JA, Alonso A, Salamanca A (2005). Nitrate toxicity to aquatic animals: a review with new data for freshwater invertebrates. *Chemosphere* **58:** 1255-1267.

Camargo JA, Alonso Á (2006). Ecological and toxicological effects of inorganic nitrogen pollution in aquatic ecosystems: a global assessment. *Environ Int* **32:** 831-849.

Carstensen J, Andersen JH, Gustafsson BG, Conley DJ (2014). Deoxygenation of the Baltic Sea during the last century. *Proceedings of the National Academy of Sciences*.

Casciotti KL, Ward BB (2001). Dissimilatory Nitrite Reductase Genes from Autotrophic Ammonia-Oxidizing Bacteria. *Appl Environ Microbiol* **67:** 2213-2221.

Chain P, Lamerdin J, Larimer F, Regala W, Lao V, Land M *et al* (2003). Complete genome sequence of the ammonia-oxidizing bacterium and obligate chemolithoautotroph *Nitrosomonas europaea*. *J Bacteriol* **185:** 2759-2773.

Chan WH, Nordstrom RJ, Calvert JG, Shaw JH (1976). Kinetic study of nitrous acid formation and decay reactions in gaseous mixtures of nitrous acid, nitrogen oxide (NO), nitrogen oxide (NO_2), water, and nitrogen. *Environ Sci Technol* **10:** 674-682.

Conrad R (1994). Compensation concentration as critical variable for regulating the flux of trace gases between soil and atmosphere. *Biogeochemistry* **27:** 155-170.

Cox RA, Derwent RG (1975). Kinetics of the reaction of HO_2 with nitric oxide and nitrogen dioxide. *J Photochem* **4:** 139-153.

Crutzen PJ, Lelieveld J (2001). Human impacts on atmospheric chemisty. *Annu Rev Earth Pl Sc* **29:** 17-45.

Davidson EA (2009). The contribution of manure and fertilizer nitrogen to atmospheric nitrous oxide since 1860. *Nat Geosci* **2:** 659-662.

Donaldson MA, Berke AE, Raff JD (2014). Uptake of gas phase nitrous acid onto boundary layer soil surfaces. *Environ Sci Technol* **48:** 375-383.

Dransfield TJ, Donahue NM, Anderson JG (2000). High-Pressure Flow Reactor Product Study of the Reactions of $HO_x + NO_2$: The Role of Vibrationally Excited Intermediates†. *The Journal of Physical Chemistry A* **105:** 1507-1514.

Elshorbany Y, Steil B, Brühl C, Lelieveld J (2012). Impact of HONO on global atmospheric chemistry calculated with an empirical parameterization in the EMAC model. *Atmospheric Chemistry and Physics* **12:** 9977-10000.

Elshorbany YF, Crutzen PJ, Steil B, Pozzer A, Tost H, Lelieveld J (2014). Global and regional impacts of HONO on the chemical composition of clouds and aerosols. *Atmos Chem Phys* **14:** 1167-1184.

Erisman JW, Sutton MA, Galloway J, Klimont Z, Winiwarter W (2008). How a century of ammonia synthesis changed the world. *Nat Geosci* **1:** 636-639.

Erisman JW, Galloway JN, Seitzinger S, Bleeker A, Dise NB, Petrescu AMR *et al* (2013). Consequences of human modification of the global nitrogen cycle. *Philosophical Transactions of the Royal Society B: Biological Sciences* **368**.

Ermel M, Oswald R, Mayer JC, Moravek A, Song G, Beck M *et al* (2013). Preparation Methods to Optimize the Performance of Sensor Discs for Fast Chemiluminescence Ozone Analyzers. *Environ Sci Technol* **47:** 1930-1936.

Ermel M, Behrendt T, Oswald R, Derstroff B, Wu D, Hohlmann S *et al* (2014a). Hydroxylamine released by ammonia-oxidizing bacteria as precursor for HONO emission from soils *submitted to Proceedings of the National Academy of Sciences.*

Ermel M, Oswald R, Behrendt T, Wu D, Hohlmann S, Meixner FX *et al* (2014b). Bidirectional exchange of HONO between soil and air. *to be submitted to Biogeosciences*.

Fajersztajn L, Veras M, Barrozo LV, Saldiva P (2013). Air pollution: a potentially modifiable risk factor for lung cancer. *Nat Rev Cancer* **13:** 674-678.

Febo A, Perrino C (1991). Prediction and experimental evidence for high air concentration of nitrous acid in indoor environments. *Atmospheric Environment Part A General Topics* **25:** 1055-1061.

Febo A, Perrino C, Gherardi M, Sparapani R (1995). Evaluation of a high-purity and high-stability continuous generation system for nitrous acid. *Environ Sci Technol* **29:** 2390-2395.

Febo A, Perrino C, Allegrini I (1996). Measurement of nitrous acid in Milan, Italy, by DOAS and diffusion denuders. *Atmos Environ* **30:** 3599-3609.

Feig GT, Mamtimin B, Meixner FX (2008). Soil biogenic emissions of nitric oxide from a semi-arid savanna in South Africa. *Biogeosciences* **5:** 1723-1738.

Ferguson SJ (1998). Nitrogen cycle enzymology. *Curr Opin Chem Biol* **2:** 182-193.

Finlayson-Pitts B, Wingen L, Sumner A, Syomin D, Ramazan K (2003). The heterogeneous hydrolysis of NO_2 in laboratory systems and in outdoor and indoor atmospheres: An integrated mechanism. *Phys Chem Chem Phys* **5:** 223-242.

Fowler D, Coyle M, Skiba U, Sutton MA, Cape JN, Reis S *et al* (2013). The global nitrogen cycle in the twenty-first century. *Philosophical Transactions of the Royal Society B: Biological Sciences* **368**.

Freitag A, Bock E (1990). Energy conservation in *Nitrobacter*. *Fems Microbiology Letters* **66:** 157-162.

Freney JR, Randall PJ, Smith JWB, Hodgkin J, Harrington KJ, Morton TC (2000). Slow release sources of acetylene to inhibit nitrification in soil. *Nutr Cycl Agroecosys* **56:** 241-251.

Galbally I, Roy C (1978). Loss of fixed nitrogen from soils by nitric oxide exhalation.

Galloway JN, Aber JD, Erisman JW, Seitzinger SP, Howarth RW, Cowling EB *et al* (2003). The nitrogen cascade. *Bioscience* **53:** 341-356.

Galloway JN, Dentener FJ, Capone DG, Boyer EW, Howarth RW, Seitzinger SP *et al* (2004). Nitrogen Cycles: Past, Present, and Future. *Biogeochemistry* **70:** 153-226.

Galloway JN, Townsend AR, Erisman JW, Bekunda M, Cai Z, Freney JR *et al* (2008). Transformation of the Nitrogen Cycle: Recent Trends, Questions, and Potential Solutions. *Science* **320:** 889-892.

Galloway JN, Leach AM, Bleeker A, Erisman JW (2013). A chronology of human understanding of the nitrogen cycle. *Philosophical Transactions of the Royal Society B: Biological Sciences* **368**.

George C, Strekowski RS, Kleffmann J, Stemmler K, Ammann M (2005). Photoenhanced uptake of gaseous NO_2 on solid-organic compounds: a photochemical source of HONO? *Faraday Discuss* **130:** 195-210.

Gerecke A, Thielmann A, Gutzwiller L, Rossi MJ (1998). The chemical kinetics of HONO formation resulting from heterogeneous interaction of NO_2 with flame soot. *Geophysical Research Letters* **25:** 2453-2456.

Graham RA, Winer AM, Pitts Jr JN (1977). Temperature dependence of the unimolecular decomposition of pernitric acid and its atmospheric implications. *Chem Phys Lett* **51:** 215-220.

Harrison RM, Kitto A-MN (1994). Evidence for a surface source of atmospheric nitrous acid. *Atmos Environ* **28:** 1089-1094.

Harrison RM, Peak JD, Collins GM (1996). Tropospheric cycle of nitrous acid. *Journal of Geophysical Research: Atmospheres (1984–2012)* **101:** 14429-14439.

He Y, Zhou X, Hou J, Gao H, Bertman SB (2006). Importance of dew in controlling the air-surface exchange of HONO in rural forested environments. *Geophysical Research Letters* **33**.

Heland J, Kleffmann J, Kurtenbach R, Wiesen P (2001). A new instrument to measure gaseous nitrous acid (HONO) in the atmosphere. *Environ Sci Technol* **35:** 3207-3212.

Hendrich MP, Upadhyay AK, Riga J, Arciero DM, Hooper AB (2002). Spectroscopic characterization of the NO adduct of hydroxylamine oxidoreductase. *Biochemistry-Us* **41:** 4603-4611.

Henry W (1803). Experiments on the quantity of gases absorbed by water, at different temperatures, and under different pressures. *Philosophical Transactions of the Royal Society of London***:** 29-276.

Hicks B, Baldocchi D, Meyers T, Hosker Jr R, Matt D (1987). A preliminary multiple resistance routine for deriving dry deposition velocities from measured quantities. *Water, Air, and Soil Pollution* **36:** 311-330.

Hirokawa J, Kato T, Mafuné F (2008). Uptake of gas-phase nitrous acid by pH-controlled aqueous solution studied by a wetted wall flow tube. *The Journal of Physical Chemistry A* **112:** 12143-12150.

Hofman T, Lees H (1953). The Biochemistry of the Nitrifying Organisms .4. The Respiration and Intermediary Metabolism of *Nitrosomonas*. *Biochem J* **54:** 579-583.

Hollocher T, Tate M, Nicholas D (1981). Oxidation of ammonia by *Nitrosomonas europaea*. Definite ^{18}O-tracer evidence that hydroxylamine formation involves a monooxygenase. *J Biol Chem* **256:** 10834-10836.

Hollocher TC, Kumar S, Nicholas DJD (1982). Respiration-Dependent Proton Translocation in *Nitrosomonas europaea* and Its Apparent Absence in *Nitrobacter agilis* during Inorganic Oxidations. *J Bacteriol* **149:** 1013-1020.

Hooper AB, Terry KR (1979). Hydroxylamine oxidoreductase of *Nitrosomonas*: Production of nitric oxide from hydroxylamine. *Biochimica et Biophysica Acta (BBA) - Enzymology* **571:** 12-20.

Horst T, Weil J (1994). How far is far enough?: The fetch requirements for micrometeorological measurement of surface fluxes. *J Atmos Ocean Tech* **11:** 1018-1025.

Howard CJ (1977). Kinetics of the reaction of HO_2 with NO_2. *The Journal of Chemical Physics* **67:** 5258-5263.

Hughes MN, Nicklin HG (1971). Autoxidation of hydroxylamine in alkaline solutions. *Journal of the Chemical Society A: Inorganic, Physical, Theoretical* **0:** 164-168.

Hyman MR, Wood PM (1985). Suicidal Inactivation and Labeling of Ammonia Mono-Oxygenase by Acetylene. *Biochem J* **227:** 719-725.

Hynes RK, Knowles R (1984). Production of nitrous oxide by *Nitrosomonas europaea*: effects of acetylene, pH, and oxygen. *Can J Microbiol* **30:** 1397-1404.

Jia Z, Conrad R (2009). Bacteria rather than Archaea dominate microbial ammonia oxidation in an agricultural soil. *Environ Microbiol* **11:** 1658-1671.

Kalberer M, Ammann M, Arens F, Gäggeler H, Baltensperger U (1999). Heterogeneous formation of nitrous acid (HONO) on soot aerosol particles. *Journal of Geophysical Research: Atmospheres (1984–2012)* **104:** 13825-13832.

Kamboures MA, Raff JD, Miller Y, Phillips LF, Finlayson-Pitts BJ, Gerber RB (2008). Complexes of HNO_3 and NO_3^- with NO_2 and N_2O_4, and their potential role in atmospheric HONO formation. *Phys Chem Chem Phys* **10:** 6019-6032.

Kebede MA, Scharko NK, Appelt LE, Raff JD (2013). Formation of Nitrous Acid during Ammonia Photooxidation on TiO_2 under Atmospherically Relevant Conditions. *J Phys Chem Lett* **4:** 2618-2623.

Kleffmann J, Becker K, Wiesen P (1998). Heterogeneous NO_2 conversion processes on acid surfaces: possible atmospheric implications. *Atmos Environ* **32:** 2721-2729.

Kleffmann J, Heland J, Kurtenbach R, Lorzer J, Wiesen P (2002). A new instrument (LOPAP) for the detection of nitrous acid (HONO). *Environ Sci Pollut R***:** 48-54.

Kleffmann J, Kurtenbach R, Lorzer J, Wiesen P, Kalthoff N, Vogel B *et al* (2003). Measured and simulated vertical profiles of nitrous acid - Part I: Field measurements. *Atmos Environ* **37:** 2949-2955.

Kleffmann J, Gavriloaiei T, Hofzumahaus A, Holland F, Koppmann R, Rupp L *et al* (2005). Daytime formation of nitrous acid: A major source of OH radicals in a forest. *Geophysical Research Letters* **32**.

Kleffmann J, Lorzer JC, Wiesen P, Kern C, Trick S, Volkamer R *et al* (2006). Intercomparison of the DOAS and LOPAP techniques for the detection of nitrous acid (HONO). *Atmos Environ* **40:** 3640-3652.

Knowles R (1982). Denitrification. *Microbiology and Molecular Biology Reviews* **46:** 43-70.

Konneke M, Bernhard AE, de la Torre JR, Walker CB, Waterbury JB, Stahl DA (2005). Isolation of an autotrophic ammonia-oxidizing marine archaeon. *Nature* **437:** 543-546.

Koops H-P, Purkhold U, Pommerening-Röser A, Timmermann G, Wagner M (2006). The lithoautotrophic ammonia-oxidizing bacteria. *The prokaryotes* **5:** 778-811.

Koops HP, Pommerening-Roser A (2001). Distribution and ecophysiology of the nitrifying bacteria emphasizing cultured species. *FEMS Microbiology Ecology* **37:** 1-9.

Krümmel A, Harms H (1982). Effect of organic matter on growth and cell yield of ammonia-oxidizing bacteria. *Arch Microbiol* **133:** 50-54.

Kubota M, Asami T (1985a). Source of Nitrous-Acid Volatilized from Upland Soils. *Soil Sci Plant Nutr* **31:** 35-42.

Kubota M, Asami T (1985b). Volatilization of Nitrous Acid from Upland Soils. *Soil Sci Plant Nutr* **31:** 27-34.

Kumar S, Nicholas DJD (1983). Proton Electrochemical Gradients in Washed Cells of *Nitrosomonas europaea* and *Nitrobacter agilis*. *J Bacteriol* **154:** 65-71.

Lammel G, Cape JN (1996). Nitrous acid and nitrite in the atmosphere. *Chem Soc Rev* **25:** 361-+.

Lees H (1952). Hydroxylamine as an Intermediate in Nitrification. *Nature* **169:** 156-157.

Lehtovirta-Morley LE, Stoecker K, Vilcinskas A, Prosser JI, Nicol GW (2011). Cultivation of an obligate acidophilic ammonia oxidizer from a nitrifying acid soil. *Proceedings of the National Academy of Sciences* **108:** 15892-15897.

Leininger S, Urich T, Schloter M, Schwark L, Qi J, Nicol GW *et al* (2006). Archaea predominate among ammonia-oxidizing prokaryotes in soils. *Nature* **442:** 806-809.

Lelieveld J, Barlas C, Giannadaki D, Pozzer A (2013). Model calculated global, regional and megacity premature mortality due to air pollution. *Atmospheric Chemistry and Physics* **13:** 7023-7037.

Levine SZ, Uselman WM, Chan WH, Calvert JG, Shaw JH (1977). The kinetics and mechanisms of the HO_2-NO_2 reactions; the significance of peroxynitric acid formation in photochemical smog. *Chem Phys Lett* **48:** 528-535.

Levy JI, Chemerynski SM, Sarnat JA (2005). Ozone exposure and mortality - An empiric Bayes metaregression analysis. *Epidemiology* **16:** 458-468.

Levy M, Zhang R, Zheng J, Zhang AL, Xu W, Gomez-Hernandez M *et al* (2014). Measurements of nitrous acid (HONO) using ion drift-chemical ionization mass spectrometry during the 2009 SHARP field campaign. *Atmos Environ* **94:** 231-240.

Li S, Matthews J, Sinha A (2008). Atmospheric hydroxyl radical production from electronically excited NO_2 and H_2O. *Science* **319:** 1657-1660.

Li X, Brauers T, Haseler R, Bohn B, Fuchs H, Hofzumahaus A *et al* (2012). Exploring the atmospheric chemistry of nitrous acid (HONO) at a rural site in Southern China. *Atmospheric Chemistry and Physics* **12:** 1497-1513.

Li X, Rohrer F, Hofzumahaus A, Brauers T, Häseler R, Bohn B *et al* (2014). Missing Gas-Phase Source of HONO Inferred from Zeppelin Measurements in the Troposphere. *Science* **344:** 292-296.

Lide DR (2004). *CRC handbook of chemistry and physics*. CRC press.

Lipschultz F, Zafiriou OC, Wofsy SC, McElroy MB, Valois FW, Watson SW (1981). Production of NO and N_2O by soil nitrifying bacteria. *Nature* **294:** 641-643.

Loscher CR, Kock A, Konneke M, LaRoche J, Bange HW, Schmitz RA (2012). Production of oceanic nitrous oxide by ammonia-oxidizing archaea. *Biogeosciences* **9:** 2419-2429.

Meixner F, Yang W (2006). Biogenic Emissions of Nitric Oxide and Nitrous Oxide from Arid and Semi-arid Land. In: D'Odorico P, Porporato A (eds). *Dryland Ecohydrology*. Springer Netherlands. pp 233-255.

Meixner FX (1994). Surface Exchange of Odd Nitrogen Oxides. *Nova Acta Leopoldina* **70:** 299-348.

Meixner FX (1997). The surface exchange of nitric oxide. *Measurements and Modelling in Environmental Pollution***:** 325-334.

Meng Z, Dabdub D, Seinfeld JH (1997). Chemical Coupling Between Atmospheric Ozone and Particulate Matter. *Science* **277:** 116-119.

Mertes S, Wahner A (1995). Uptake of nitrogen dioxide and nitrous acid on aqueous surfaces. *The Journal of Physical Chemistry* **99:** 14000-14006.

Miller Y, Finlayson-Pitts BJ, Gerber RB (2009). Ionization of N_2O_4 in contact with water: mechanism, time scales and atmospheric implications. *J Am Chem Soc* **131:** 12180-12185.

Mochida M, Finlayson-Pitts BJ (2000). FTIR Studies of the Reaction of Gaseous NO with HNO_3 on Porous Glass: Implications for Conversion of HNO_3 to Photochemically Active NO_x in the Atmosphere. *The Journal of Physical Chemistry A* **104:** 9705-9711.

Müller JBA, Percival CJ, Gallagher MW, Fowler D, Coyle M, Nemitz E (2010). Sources of uncertainty in eddy covariance ozone flux measurements made by dry chemiluminescence fast response analysers. *Atmos Meas Tech* **3:** 163-176.

Ndour M, D'Anna B, George C, Ka O, Balkanski Y, Kleffmann J *et al* (2008). Photoenhanced uptake of NO_2 on mineral dust: Laboratory experiments and model simulations. *Geophysical Research Letters* **35**.

Nguyen MT, Sumathi R, Sengupta D, Peeters J (1998). Theoretical analysis of reactions related to the HNO_2 energy surface: OH + NO and H + NO_2. *Chem Phys* **230:** 1-11.

Niki H, Maker PD, Savage CM, Breitenbach LP (1977). Fourier transform IR spectroscopic observation of pernitric acid formed via HOO + NO_2 → $HOONO_2$. *Chem Phys Lett* **45:** 564-566.

Nishino N, Finlayson-Pitts BJ (2012). Thermal and photochemical reactions of NO_2 on chromium(III) oxide surfaces at atmospheric pressure. *Phys Chem Chem Phys* **14:** 15840-15848.

Oswald R, Behrendt T, Ermel M, Wu D, Su H, Cheng Y *et al* (2013a). HONO Emissions from Soil Bacteria as a Major Source of Atmospheric Reactive Nitrogen. *Science* **341:** 1233-1235.

Oswald R, Behrendt T, Ermel M, Wu D, Su H, Cheng Y *et al* (2013b). HONO emissions from soil bacteria as a major source of atmospheric reactive nitrogen. *Science* **341:** 1233-1235.

Oswald R, Ermel M, Hens K, Novelli A, Ouwersloot HG, Paasonen P *et al* (2014). Comparison of HONO budgets for two measurement heights at a field station within the boreal forest (SMEAR II - HUMPPA-COPEC 2010). *Atmos Chem Phys Discuss* **14:** 7823-7857.

Pagsberg P, Bjergbakke E, Ratajczak E, Sillesen A (1997). Kinetics of the gas phase reaction OH+ NO (+ M)→ HONO (+ M) and the determination of the UV absorption cross sections of HONO. *Chem Phys Lett* **272:** 383-390.

Paoletti E (2005). Ozone slows stomatal response to light and leaf wounding in a Mediterranean evergreen broadleaf, *Arbutus unedo*. *Environ Pollut* **134:** 439-445.

Pape L, Ammann C, Nyfeler-Brunner A, Spirig C, Hens K, Meixner F (2008). An automated dynamic chamber system for surface exchange measurement of non-reactive and reactive trace gases of grassland ecosystems. *Biogeosciences Discussions* **5**.

Perner D, Platt U (1979). Detection of Nitrous Acid in the Atmosphere by Differential Optical-Absorption. *Geophysical Research Letters* **6:** 917-920.

Pilegaard K (2013). Processes regulating nitric oxide emissions from soils. *Philosophical Transactions of the Royal Society B: Biological Sciences* **368**.

Placella SA, Firestone MK (2013). Transcriptional Response of Nitrifying Communities to Wetting of Dry Soil. *Appl Environ Microbiol* **79:** 3294-3302.

Platt U, Perner D, Harris GW, Winer AM, Pitts JN (1980). Observations of nitrous acid in an urban atmosphere by differential optical absorption. *Nature* **285:** 312-314.

Pommerening-Roser A, Koops HP (2005). Environmental pH as an important factor for the distribution of urease positive ammonia-oxidizing bacteria. *Microbiol Res* **160:** 27-35.

Prosser JI, Nicol GW (2012). Archaeal and bacterial ammonia-oxidisers in soil: the quest for niche specialisation and differentiation. *Trends Microbiol* **20:** 523-531.

Ramazan KA, Syomin D, Finlayson-Pitts BJ (2004). The photochemical production of HONO during the heterogeneous hydrolysis of NO_2. *Phys Chem Chem Phys* **6:** 3836-3843.

Rasche ME, Hicks RE, Hyman MR, Arp DJ (1990). Oxidation of Monohalogenated Ethanes and N-Chlorinated Alkanes by Whole Cells of *Nitrosomonas europaea*. *J Bacteriol* **172:** 5368-5373.

Ravishankara A, Daniel JS, Portmann RW (2009). Nitrous oxide (N_2O): the dominant ozone-depleting substance emitted in the 21st century. *Science* **326:** 123-125.

Reay DS, Davidson EA, Smith KA, Smith P, Melillo JM, Dentener F *et al* (2012). Global agriculture and nitrous oxide emissions. *Nature Clim Change* **2:** 410-416.

Remde A, Slemr F, Conrad R (1989). Microbial production and uptake of nitric oxide in soil. *Fems Microbiology Letters* **62:** 221-230.

Remde A, Conrad R (1990). Production of Nitric-Oxide in *Nitrosomonas europaea* by Reduction of Nitrite. *Arch Microbiol* **154:** 187-191.

Ren X, Harder H, Martinez M, Lesher RL, Oliger A, Simpas JB *et al* (2003). OH and HO_2 Chemistry in the urban atmosphere of New York City. *Atmos Environ* **37:** 3639-3651.

Roberts JM, Veres P, Warneke C, Neuman JA, Washenfelder RA, Brown SS *et al* (2010). Measurement of HONO, HNCO, and other inorganic acids by negative-ion proton-transfer chemical-ionization mass spectrometry (NI-PT-CIMS): application to biomass burning emissions. *Atmos Meas Tech* **3:** 981-990.

Rubio MA, Lissi E, Villena G, Elshorbany YF, Kleffmann J, Kurtenbach R *et al* (2009). Simultaneous measurements of formaldehyde and nitrous acid in dews and gas phase in the atmosphere of Santiago, Chile. *Atmos Environ* **43:** 6106-6109.

Rummel U, Ammann C, Gut A, Meixner FX, Andreae MO (2002). Eddy covariance measurements of nitric oxide flux within an Amazonian rain forest. *Journal of Geophysical Research: Atmospheres* **107:** 8050.

Russow R, Stange CF, Neue HU (2009). Role of nitrite and nitric oxide in the processes of nitrification and denitrification in soil: Results from ^{15}N tracer experiments. *Soil Biol Biochem* **41:** 785-795.

Sander SP, Golden D, Kurylo M, Moortgat G, Wine P, Ravishankara A *et al* (2006). Chemical kinetics and photochemical data for use in atmospheric studies evaluation number 15.

Schmidt I, Look C, Bock E, Jetten MSM (2004a). Ammonium and hydroxylamine uptake and accumulation in *Nitrosomonas*. *Microbiology+* **150:** 1405-1412.

Schmidt I, van Spanning RJM, Jetten MSM (2004b). Denitrification and ammonia oxidation by *Nitrosomonas europaea* wild-type, and NirK- and NorB-deficient mutants. *Microbiol-Sgm* **150:** 4107-4114.

Schütz H, Seiler W, Conrad R (1989). Processes involved in formation and emission of methane in rice paddies. *Biogeochemistry* **7:** 33-53.

Simonaitis R, Heicklen J (1974). Reaction of hydroperoxyl radicals with nitrogen monoxide and nitrogen dioxide. *The Journal of Physical Chemistry* **78:** 653-657.

Sleiman M, Gundel LA, Pankow JF, Jacob P, Singer BC, Destaillats H (2010). Formation of carcinogens indoors by surface-mediated reactions of nicotine with nitrous acid, leading to potential thirdhand smoke hazards. *Proceedings of the National Academy of Sciences* **107:** 6576-6581.

Smil V (2004). *Enriching the earth: Fritz Haber, Carl Bosch, and the transformation of world food production*. MIT press.

Smith BD (1995). *The emergence of agriculture*. Scientific American Library New York.

Smith FL, Harvey AH (2007). Avoid common pitfalls when using Henry's law. *Chem Eng Prog* **103:** 33-39.

Smith RA (1872). *Air and rain: the beginnings of a chemical climatology*. Longmans, Green, and Company.

Solomon S (2007). *Climate change 2007-the physical science basis: Working group I contribution to the fourth assessment report of the IPCC*, vol. 4. Cambridge University Press.

Sörgel M, Regelin E, Bozem H, Diesch JM, Drewnick F, Fischer H *et al* (2011a). Quantification of the unknown HONO daytime source and its relation to NO_2. *Atmospheric Chemistry and Physics* **11:** 10433-10447.

Sörgel M, Trebs I, Serafimovich A, Moravek A, Held A, Zetzsch C (2011b). Simultaneous HONO measurements in and above a forest canopy: influence of turbulent exchange on mixing ratio differences. *Atmospheric Chemistry and Physics* **11:** 841-855.

Spieck E, Lipski A (2011). Cultivation, Growth Physiology, and Chemotaxonomy of Nitrite-Oxidizing Bacteria. *Methods in Enzymology: Research on Nitrification and Related Processes, Vol 486, Part A* **486:** 109-130.

Stahl DA, de la Torre JR (2012). Physiology and Diversity of Ammonia-Oxidizing Archaea. *Annu Rev Microbiol* **66:** 83-101.

Stein LY, Yung YL (2003). Production, isotopic composition, and atmospheric fate of biologically produced nitrous oxide. *Annu Rev Earth Pl Sc* **31:** 329-356.

Stemmler K, Ammann M, Donders C, Kleffmann J, George C (2006). Photosensitized reduction of nitrogen dioxide on humic acid as a source of nitrous acid. *Nature* **440:** 195-198.

Stemmler K, Ndour M, Elshorbany Y, Kleffmann J, D'Anna B, George C *et al* (2007). Light induced conversion of nitrogen dioxide into nitrous acid on submicron humic acid aerosol. *Atmospheric Chemistry and Physics* **7:** 4237-4248.

Sterner RW, Elser JJ (2002). *Ecological stoichiometry: the biology of elements from molecules to the biosphere*. Princeton University Press.

Stockwell WR, Calvert JG (1978). The near ultraviolet absorption spectrum of gaseous HONO and N_2O_3. *J Photochem* **8:** 193-203.

Stromberger ME, Klose S, Ajwa H, Trout T, Fennimore S (2005). Microbial Populations and Enzyme Activities in Soils Fumigated with Methyl Bromide Alternatives. *Soil Sci Soc Am J* **69:** 1987-1999.

Stuhl F, Niki H (1972). Flash photochemical study of the reaction OH+ NO+ M using resonance fluorescent detection of OH. *The Journal of Chemical Physics* **57:** 3677-3679.

Stutz J, Kim ES, Platt U, Bruno P, Perrino C, Febo A (2000). UV-visible absorption cross sections of nitrous acid. *J Geophys Res-Atmos* **105:** 14585-14592.

Stutz J, Alicke B, Neftel A (2002). Nitrous acid formation in the urban atmosphere: Gradient measurements of NO_2 and HONO over grass in Milan, Italy. *J Geophys Res-Atmos* **107**.

Stutz JC, Wang SH, Hurlock SC (2004). Formation of nitrous acid in the urban nocturnal boundary layer. *Abstr Pap Am Chem S* **228:** U203-U203.

Su H, Cheng YF, Cheng P, Zhang YH, Dong S, Zeng LM *et al* (2008a). Observation of nighttime nitrous acid (HONO) formation at a non-urban site during PRIDE-PRD2004 in China. *Atmos Environ* **42:** 6219-6232.

Su H, Cheng YF, Shao M, Gao DF, Yu ZY, Zeng LM *et al* (2008b). Nitrous acid (HONO) and its daytime sources at a rural site during the 2004 PRIDE-PRD experiment in China. *Journal of Geophysical Research: Atmospheres (1984–2012)* **113**.

Su H, Cheng Y, Oswald R, Behrendt T, Trebs I, Meixner FX *et al* (2011). Soil nitrite as a source of atmospheric HONO and OH radicals. *Science* **333:** 1616-1618.

Takenaka N, Terada H, Oro Y, Hiroi M, Yoshikawa H, Okitsu K *et al* (2004). A new method for the measurement of trace amounts of HONO in the atmosphere using an air-dragged aqua-membrane-type denuder and fluorescence detection. *Analyst* **129:** 1130-1136.

Ten Brink HM, Spoelstra H (1998). The dark decay of HONO in environmental (SMOG) chambers. *Atmos Environ* **32:** 247-251.

Tie X, Zhang R, Brasseur G, Lei W (2002). Global NO_x production by lightning. *J Atmos Chem* **43:** 61-74.

Tourna M, Stieglmeier M, Spang A, Konneke M, Schintlmeister A, Urich T *et al* (2011). *Nitrososphaera viennensis*, an ammonia oxidizing archaeon from soil. *P Natl Acad Sci USA* **108:** 8420-8425.

Tyndall GS, Orlando JJ, Calvert JG (1995). Upper Limit for the Rate Coefficient for the Reaction $HO_2 + NO_2 \rightarrow HONO + O_2$. *Environ Sci Technol* **29:** 202-206.

Uysal N, Schapira RM (2003). Effects of ozone on lung function and lung diseases. *Curr Opin Pulm Med* **9:** 144-150.

Vajrala N, Martens-Habbena W, Sayavedra-Soto LA, Schauer A, Bottomley PJ, Stahl DA *et al* (2013). Hydroxylamine as an intermediate in ammonia oxidation by globally abundant marine archaea. *Proceedings of the National Academy of Sciences* **110:** 1006-1011.

van Dijk SM, Meixner FX (2001). Production and consumption of NO in forest and pasture soils from the Amazon basin. *Water, Air and Soil Pollution: Focus* **1:** 119-130.

VandenBoer TC, Brown SS, Murphy JG, Keene WC, Young CJ, Pszenny A *et al* (2013). Understanding the role of the ground surface in HONO vertical structure: High resolution vertical profiles during NACHTT-11. *Journal of Geophysical Research: Atmospheres* **118:** 10,155-110,171.

VandenBoer TC, Markovic MZ, Sanders JE, Ren X, Pusede SE, Browne EC *et al* (2014). Evidence for a nitrous acid (HONO) reservoir at the ground surface in Bakersfield, CA during CalNex 2010. *Journal of Geophysical Research: Atmospheres***:** n/a-n/a.

Villena G, Kleffmann J, Kurtenbach R, Wiesen P, Lissi E, Rubio MA *et al* (2011). Vertical gradients of HONO, NO_x and O_3 in Santiago de Chile. *Atmos Environ* **45:** 3867-3873.

Vitousek PM, Cassman K, Cleveland C, Crews T, Field CB, Grimm NB *et al* (2002). Towards an ecological understanding of biological nitrogen fixation. *Biogeochemistry* **57:** 1-45.

Vogel B, Vogel H, Kleffmann J, Kurtenbach R (2003). Measured and simulated vertical profiles of nitrous acid - Part II. Model simulations and indications for a photolytic source. *Atmos Environ* **37:** 2957-2966.

Wesely M, Hicks B (2000). A review of the current status of knowledge on dry deposition. *Atmos Environ* **34:** 2261-2282.

Wong KW, Oh HJ, Lefer BL, Rappengluck B, Stutz J (2011). Vertical profiles of nitrous acid in the nocturnal urban atmosphere of Houston, TX. *Atmospheric Chemistry and Physics* **11:** 3595-3609.

Wong KW, Tsai C, Lefer B, Haman C, Grossberg N, Brune WH *et al* (2012). Daytime HONO vertical gradients during SHARP 2009 in Houston, TX. *Atmospheric Chemistry and Physics* **12:** 635-652.

Wu D, Kampf CJ, Poschl U, Oswald R, Cui J, Ermel M *et al* (2014). Novel tracer method to measure isotopic labeled gas-phase nitrous acid (HO15NO) in biogeochemical studies. *Environ Sci Technol* **48:** 8021-8027.

Zakir HAKM, Subbarao GV, Pearse SJ, Gopalakrishnan S, Ito O, Ishikawa T *et al* (2008). Detection, isolation and characterization of a root-exuded compound, methyl 3-(4-hydroxyphenyl) propionate, responsible for biological nitrification inhibition by sorghum (*Sorghum bicolor*). *New Phytol* **180:** 442-451.

Zhang BQ, Tao FM (2010). Direct homogeneous nucleation of NO_2, H_2O, and NH_3 for the production of ammonium nitrate particles and HONO gas. *Chem Phys Lett* **489:** 143-147.

Zhang N, Zhou X, Shepson PB, Gao H, Alaghmand M, Stirm B (2009). Aircraft measurement of HONO vertical profiles over a forested region. *Geophysical Research Letters* **36**.

Zhang N, Zhou X, Bertman S, Tang D, Alaghmand M, Shepson PB *et al* (2012). Measurements of ambient HONO concentrations and vertical HONO flux above a northern Michigan forest canopy. *Atmospheric Chemistry and Physics* **12:** 8285-8296.

Zhou X, Zhang N, TerAvest M, Tang D, Hou J, Bertman S *et al* (2011). Nitric acid photolysis on forest canopy surface as a source for tropospheric nitrous acid. *Nat Geosci* **4:** 440-443.

Zhu T, Yarwood G, Chen J, Niki H (1993). Evidence for the heterogeneous formation of nitrous acid from peroxynitric acid in environmental chambers. *Environ Sci Technol* **27:** 982-983.

Appendix A

List of related publications

Oswald, R.*, Behrendt, T.*, Ermel, M.*, Wu, D., Su, H., Cheng, Y., Breuninger, C., Moravek, A., Mougin, E., Delon, C., Loubet, B., Pommerening-Röser, R., Sörgel, M., Pöschl, U., Hoffmann, T., Andreae, M. O., Meixner, F. X., Trebs, I., HONO emissions from soil bacteria as a major source of atmospheric reactive nitrogen, **Science**, 341, 1233 – 1235, 2014

Ermel, M., Behrendt, T., Oswald, R., Derstroff, B., Wu, D., Hohlmann, S., Stönner, C., Pommerening-Röser, A., Williams, J., Meixner, F. X., Andreae, M. O., Sörgel, M., Trebs, I., Hydroxylamine released by ammonia-oxidizing bacteria as precursor for HONO emission from soils, *to be submitted*, 2014

Wu, D., Kampf, C. J., Pöschl, U., Oswald, R., Cui, J., Ermel, M., Hu, C., Trebs, I., Sörgel, M., Novel Tracer Method To Measure Isotopic Labeled Gas-Phase Nitrous Acid ($HO^{15}NO$) in Biogeochemical Studies, **Environmental Science & Technology**, 48, 2021 – 2027, 2014

Ermel, M., Oswald, R., Behrendt, T., Wu, D., Hohlmann, S., Meixner, F. X., Trebs, I., Sörgel, M., Bidirectional exchange of HONO between soil and air, **Biogeosciences Discussion** *to be submitted*, 2014

Oswald, R., Ermel, M., Hens, K., Novelli, A., Ouwersloot, H. G., Paasonen, P., Petäjä, T., Sipilä, M., Keronen, P., Bäck, J., Königstedt, R., Hosaynali Beygi, Z., Fischer, H., Bohn, B., Kubistin, D., Harder, H., Martinez, M., Williams, J., Hoffmann, T., Trebs, I., Sörgel, M., Comparison of HONO budgets for two measurement heights at a field station within the boreal forest (SMEAR II - HUMPPA-COPEC 2010), **Atmospheric Chemistry and Physics Discussion**, 14, 7823 – 7857, 2014

Oswald, R., Behrendt, T., Ermel, M., Wu, D., Breuninger, C., Moravek, A., Loubet, B., Hoffmann, T., Andreae, M. O., Meixner, F. X., Sörgel, M., Trebs, I., Influence of soil properties and ambient mixing ratios on HONO emission, **Biogeosciences** *to be submitted*, 2014

Behrendt, B.*, Ermel, M.*, Mamtimin, B., Song, G., Voss, L., Bruse, M., Agam, N., Andreae, M. O., Meixner, F. X., A trace of water is enough - water vapour adsorption triggers nitric oxide emissions from deserts, *in preparation*, 2014

*: authors contributed equally

Wu, D., Horn, M., Behrendt, T., Ermel, M., Oswald, R., Trebs, I., Sörgel, M., HONO emissions from denitrification process and its potential mechanisms, *in preparation*, 2014

Song, W., Behrendt, T., Greule, M., Steinkamp, J., Ermel, M., Franz, M., Williams, J., Keppler, F., Strong emission of methyl chloride and methyl bromide from saline land at higher temperature, *in preparation*, 2014

Appendix B

Selected Publications

B1. Oswald, R.*, Behrendt, T.*, Ermel, M.*, Wu, D., Su, H., Cheng, Y., Breuninger, C., Moravek, A., Mougin, E., Delon, C., Loubet, B., Pommerening-Röser, R., Sörgel, M., Pöschl, U., Hoffmann, T., Andreae, M. O., Meixner, F. X., Trebs, I., HONO emissions from soil bacteria as a major source of atmospheric reactive nitrogen, **Science**, 341, 1233 – 1235, 2014

B2. Ermel, M., Behrendt, T., Oswald, R., Derstroff, B., Wu, D., Hohlmann, S., Stönner, C., Pommerening-Röser, A., Williams, J., Meixner, F. X., Andreae, M. O., Sörgel, M., Trebs, I., Hydroxylamine released by ammonia-oxidizing bacteria as precursor for HONO emission from soils, *to be submitted*, 2014

B3. Wu, D., Kampf, C. J., Pöschl, U., Oswald, R., Cui, J., Ermel, M., Hu, C., Trebs, I., Sörgel, M., Novel Tracer Method To Measure Isotopic Labeled Gas-Phase Nitrous Acid ($HO^{15}NO$) in Biogeochemical Studies, **Environmental Science & Technology**, 48, 2021 – 2027, 2014

B4. Ermel, M., Oswald, R., Behrendt, T., Wu, D., Hohlmann, S., Meixner, F. X., Trebs, I., Sörgel, M., Bidirectional exchange of HONO between soil and air, **Biogeosciences Discussion** *to be submitted*, 2014

B1. Oswald et al, Science, 2013

HONO emissions from soil bacteria as a major source of atmospheric reactive nitrogen

Authors: R. Oswald[1,2]†, T. Behrendt[1,3]†, M. Ermel[1,2]†, D. Wu[1,4], H. Su[5], Y. Cheng[5], C. Breuninger[1], A. Moravek[1,6], E. Mougin[7], C. Delon[8], B. Loubet[9], A. Pommerening-Röser[10], M. Sörgel[1], U. Pöschl[5], T. Hoffmann[2], M.O. Andreae[1], F.X. Meixner[1] and I. Trebs[1]

† These authors contributed equally to this work.

[1] Biogeochemistry Department, Max Planck Institute for Chemistry, P.O. Box 3060, 55020 Mainz, Germany

[2] Institute for Inorganic and Analytical Chemistry, Johannes Gutenberg University Mainz, 55128 Mainz, Germany

[3] Institute for Geography, Johannes Gutenberg University Mainz, 55128 Mainz, Germany

[4] Key Laboratory of Agricultural Water Research, Center for Agricultural Resources Research, Institute of Genetic and Developmental Biology, The Chinese Academy of Sciences, 050021 Shijiazhuang, China

[5] Multiphase Chemistry Department, Max Planck Institute for Chemistry, P. O. Box 3060, 55020 Mainz, Germany

[6] Department of Micrometeorology, University of Bayreuth, 95447 Bayreuth, Germany

[7] Géosciences Environnement Toulouse (GET), Observatoire Midi-Pyrénées, Université de Toulouse, CNRS, IRD, 14 avenue Edouard Belin, 31400, Toulouse, France

[8] Laboratoire d'Aérologie, Université de Toulouse, Toulouse, France

[9] INRA, Unité mixte de Recherche INRA-AgroParistech, Environnement et Grandes Cultures, 78850 Thiverval-Grignon, France

[10] Department of Microbiology and Biotechnology, University of Hamburg, Hamburg, Germany

HONO Emissions from Soil Bacteria as a Major Source of Atmospheric Reactive Nitrogen

R. Oswald,[1,2]*† T. Behrendt,[1,3]† M. Ermel,[1,2]† D. Wu,[1,4] H. Su,[5] Y. Cheng,[5] C. Breuninger,[1] A. Moravek,[1,6] E. Mougin,[7] C. Delon,[8] B. Loubet,[9] A. Pommerening-Röser,[10] M. Sörgel,[1] U. Pöschl,[5] T. Hoffmann,[2] M.O. Andreae,[1] F.X. Meixner,[1] I. Trebs[1]*

Abiotic release of nitrous acid (HONO) in equilibrium with soil nitrite (NO_2^-) was suggested as an important contributor to the missing source of atmospheric HONO and hydroxyl radicals (OH). The role of total soil-derived HONO in the biogeochemical and atmospheric nitrogen cycles, however, has remained unknown. In laboratory experiments, we found that for nonacidic soils from arid and arable areas, reactive nitrogen emitted as HONO is comparable with emissions of nitric oxide (NO). We show that ammonia-oxidizing bacteria can directly release HONO in quantities larger than expected from the acid-base and Henry's law equilibria of the aqueous phase in soil. This component of the nitrogen cycle constitutes an additional loss term for fixed nitrogen in soils and a source for reactive nitrogen in the atmosphere.

Soil biogenic NO emissions account for ~20% of the total NO sources to the atmosphere (*1*) and vary as a function of microbial activity and physicochemical soil properties. NO is produced during nitrification, in which soil microbes convert ammonium (NH_4^+) via NO_2^- to nitrate (NO_3^-), both of which can accumulate in soil (*2*, *3*). In addition, the reduction of NO_3^-, which is known as denitrification, can cause a release of NO. The two microbial processes are mainly influenced by temperature, soil water content, pH value, and mineral nitrogen availability in the soil (*4*–*6*). Previous studies have shown that HONO may also be emitted from soil; this release may originate from the transformation of soil NH_4^+ to NO_2^- (*7*) or from soil NO_2^- because of a chemical acid-base equilibrium (*8*).

To estimate the contribution of soil HONO emissions to the total reactive nitrogen flux (HONO + NO) from the soil to the atmosphere and to elucidate the major processes influencing HONO release from soil, we studied the relation of soil HONO emissions to biogenic soil NO emissions under controlled laboratory conditions using the dynamic chamber method (*9*, *10*). Earlier studies have shown that results from using this technique are consistent with those from field measurements (*9*, *11*, *12*). We investigated soils from various ecosystems around the world, covering a wide range of soil pH, organic matter, and soil nutrient contents (table S1). The soil samples were wetted in order to reach water holding capacity (WHC) (*10*) and placed into the chamber, which was then continuously flushed with purified air (free of HONO, NO_x, O_3, hydrocarbons, and water vapor), leading to a slow drying of the soil sample during the course of the experiment. The gas-phase mixing ratio of HONO released by the soil sample was measured at the chamber exit with a long path absorption photometer (LOPAP) (*13*). Mixing ratios of NO and water vapor were also measured (*14*).

The characteristic moisture dependency of HONO and NO fluxes that is known from previous studies of soil biogenic NO emissions is shown in Fig. 1 (*4*, *9*, *15*, *16*). We found that the maximal emission fluxes of HONO and NO [henceforth denoted as optimum fluxes; $F_{N,opt}$(HONO) and $F_{N,opt}$(NO)] are of comparable magnitude and occur at similar optimum soil water content (SWC) (*10*)—within 10% WHC of one another for all investigated samples.

Chemical acid-base equilibrium calculations predict that abiotic HONO emissions from soil nitrite should be largest for soils with low pH and high NO_2^- content (*8*). The soil pH reflects a sum parameter, which depends on the amount of acidic and basic species in soil, and regulates the solubility of soil constituents and the protonation equilibria. These variables, however, also influence nitrifier and denitrifier activity in soil. In general, abundance and diversity of bacteria are positively correlated with pH (*17*), and individuals mostly possess a maximum activity at a certain pH (*18*). In contrast to expectations based on the acid-base equilibrium, the results from different soil samples presented in Fig. 2 do not show a decrease of HONO fluxes with increasing pH. In fact, the neutral soil sample S12, taken from a wheat field in Germany, features extremely high values for HONO and NO emissions ($F_{N,opt}$: 257.5 ± 0.1 ng m^{-2} s^{-1} HONO, 134.8 ± 0.6 ng m^{-2} s^{-1} NO). The second highest emission of HONO and NO was found for the alkaline, sodic soil represented by sample S17. Comparison with soil NO_2^- and NH_4^+ concentrations (Fig. 2) clearly demonstrates that high HONO and NO emissions are favored for soils with high nutrient content.

The ratio of $F_{N,opt}$(HONO) to $F_{N,opt}$(NO) was found to be higher for arid and arable soils (on

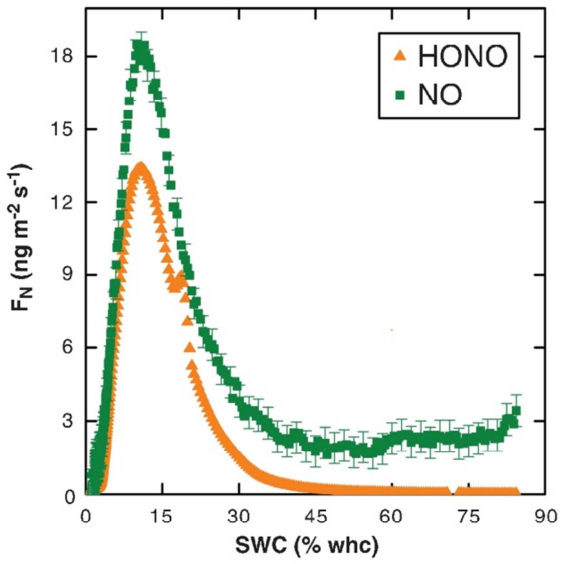

Fig. 1. Soil emissions of HONO and NO feature similar optimum curves. Characteristic HONO (triangles) and NO (squares) emission fluxes (F_N, in terms of nitrogen mass) from soil sample S15 (jujube field, semi-arid, fertilized, and irrigated; Mingfeng, Xinjiang, PR China) as a function of SWC expressed in percent of WHC. Experimental error bars (*10*) are shown for every fourth data point for NO. Error bars of HONO fluxes have the size of the symbols and were omitted.

[1]Biogeochemistry Department, Max Planck Institute for Chemistry, Post Office Box 3060, 55020 Mainz, Germany. [2]Institute for Inorganic and Analytical Chemistry, Johannes Gutenberg University Mainz, 55128 Mainz, Germany. [3]Institute for Geography, Johannes Gutenberg University Mainz, 55128 Mainz, Germany. [4]Key Laboratory of Agricultural Water Research, Center for Agricultural Resources Research, Institute of Genetic and Developmental Biology, Chinese Academy of Sciences, 050021 Shijiazhuang, China. [5]Multiphase Chemistry Department, Max Planck Institute for Chemistry, Post Office Box 3060, 55020 Mainz, Germany. [6]Department of Micrometeorology, University of Bayreuth, 95447 Bayreuth, Germany. [7]Géosciences Environnement Toulouse (GET), Observatoire Midi-Pyrénées, Université de Toulouse, CNRS, Institut pour la Recherche et le Développement, 14 Avenue Edouard Belin, 31400 Toulouse, France. [8]Laboratoire d'Aérologie, Université de Toulouse, Toulouse, France. [9]Institut National de la Recherche Agronomique (INRA), Unité mixte de Recherche INRA-AgroParistech, Environnement et Grandes Cultures, 78850 Thiverval-Grignon, France. [10]Department of Microbiology and Biotechnology, University of Hamburg, 22609 Hamburg, Germany.

*Corresponding author. E-mail: robert.oswald@mpic.de (R.O.); i.trebs@mpic.de (I.T.)
†These authors contributed equally to this work.

average 1.06 ± 0.44) than for nonarable soils of humid and temperate regions (on average 0.16 ± 0.12) (fig. S1). For soil pH values higher than 7, the optimum HONO emission fluxes always exceed 5 ng m^{-2} s^{-1} (in terms of N) and even reached ~258 ng m^{-2} s^{-1} (at 25°C). We anticipate that HONO emissions are particularly relevant for arid and arable areas with neutral or alkaline soil pH, where they may substantially influence tropospheric chemistry. Potential HONO soil emission hot spots comprise, for instance, large areas of northern Africa, central/southwestern Asia, and North America as well as some regions around the Mediterranean Sea (fig. S2), covering in total ~20% of the terrestrial surface (excluding Antarctica). Given the high spatial variability of soil properties (such as pH and nutrients) and our limited amount of soil samples, these hot spot areas may be even larger. This previously neglected ground source of reactive nitrogen may explain the unexpectedly high daytime HONO mixing ratios observed in many studies (*19*). In addition, NO is produced on a time scale of ~30 min from the photolysis of HONO during daytime. Hence, soil HONO emissions in the identified hot spot areas (fig. S2) may account for the observed discrepancies between soil emissions of reactive nitrogen estimated with global models by using the Yienger and Levy algorithm and those derived from "top-down" approaches by using nitrogen dioxide (NO_2) columns measured by satellites over arid ecosystems (*20*, *21*).

Biogenic NO emissions are known to depend strongly on soil temperature (*22*). We measured the temperature dependency of F_N(HONO) and

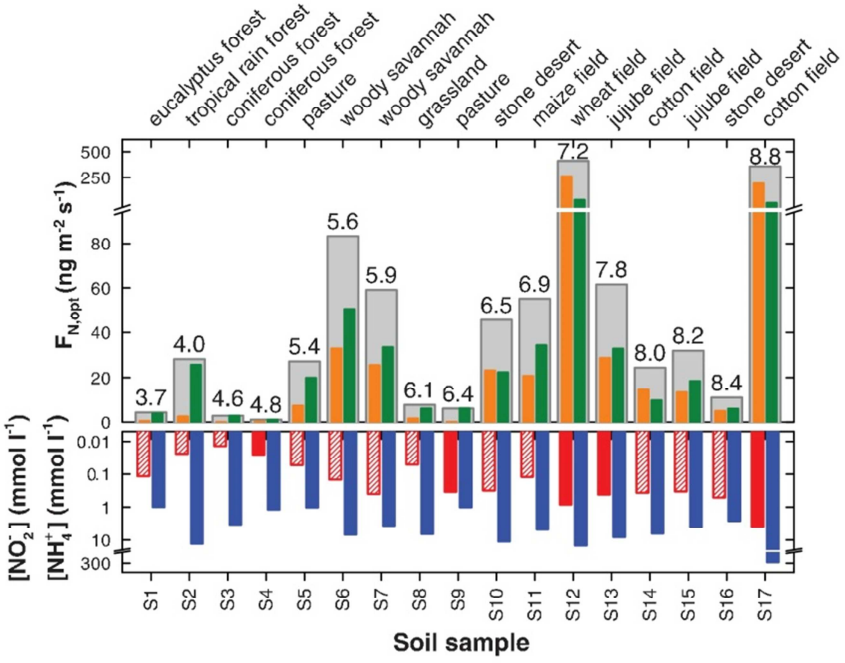

Fig. 2. Optimum emission fluxes of HONO are comparable with those of NO and are largest for NO_2^- rich, neutral-to-basic soils in arid and arable regions. (**Top**) Optimum emission fluxes of HONO (orange bars), NO (green bars), and their sum (gray bars) in terms of nitrogen for each soil sample (at 25°C), arranged by increasing pH. Numbers on top of gray bars represent the soil pH. Land use of soil samples is shown on the top axis. (**Bottom**) Calculated concentrations of NH_4^+ (blue bars) and NO_2^- (red bars) in the soil solution at $F_{N,opt}$(HONO) [striped bars refer to theoretical NO_2^- values at the limit of detection (*10*)].

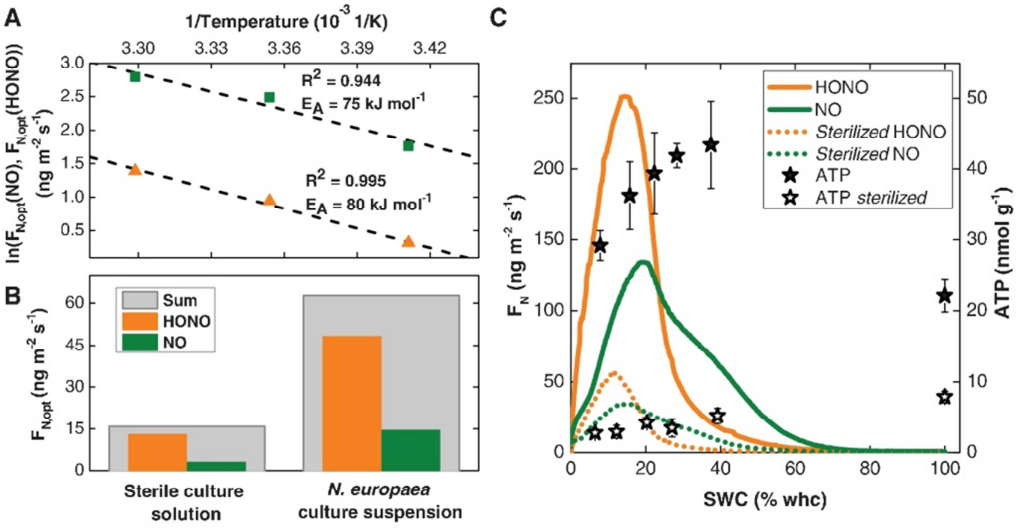

Fig. 3. Ammonia-oxidizing bacteria directly release HONO and cause high emissions from soil. (**A**) Arrhenius plot of the optimum fluxes of HONO (triangles) and NO (squares) for soil sample S8. (**B**) Optimum fluxes of HONO, NO, and their sum for a sterile AOB nutrient solution and a *N. europaea* culture suspension (activity equivalent to $1.1 \cdot 10^{-3}$ nmol ATP l^{-1}) applied to glass beads as a soil proxy. (**C**) Influence of bacterial activity on HONO and NO emissions for soil sample S12. Fluxes of HONO and NO for the untreated soil (solid orange and green line, respectively) and for a sterilized subsample (dotted orange and green line, respectively). ATP concentrations serve as indicators for bacterial activity during the dry-out of the untreated sample (black filled stars) and the sterilized sample (black open stars). Error bars denote SDs of three replicates.

F_N(NO) from soil sample S8 (an example for HONO is provided in fig. S3). A temperature increase from 20 to 30°C yielded Q_{10} values (averaged over the whole SWC range) of 3.7 (±1.4) for HONO and 2.1 (±0.2) for NO, which is typical for soil respiratory systems (*16*, *23*, *24*). From an Arrhenius plot (Fig. 3A), we obtained similar activation energies for HONO (80 kJ mol^{-1}) and for NO (75 kJ mol^{-1}). These values are much lower than the activation energies reported for denitrification (202 to 250 kJ mol^{-1}) (*25*) but are within the range reported for nitrification by ammonia-oxidizing bacteria (AOB) (25 to 149 kJ mol^{-1}) (*3*, *25*), suggesting that the latter process governs the observed co-emission of HONO and NO.

To test this hypothesis, we investigated a pure culture of *Nitrosomonas europaea*, a common and well-studied AOB (*26*). A suspension of the pure culture (buffered at pH = 8.2) was applied to glass beads serving as an inert soil-like matrix (*16*), and the model system was treated like a soil sample (*10*). $F_{N,opt}$(HONO) and $F_{N,opt}$(NO) of the *N. europaea* culture suspension are compared in Fig. 3B with the emissions by using a sterile AOB nutrient solution additionally containing 0.14 mmol l^{-1} NO_2^-, which equals 0.5 mg kg^{-1} of NO_2^- (in terms of N) in soil. The NO_2^- added to the sterile solution equals the NO_2^- that would have been produced by the bacteria during the experiment and reflects the chemical contribution to the HONO emission from the model system, whereas the observed difference in $F_{N,opt}$(HONO) between the sterile solution and the culture suspension can be attributed to the direct emissions by the AOB. The *N. europaea* culture emits four times more HONO than does the sterile reference, demonstrating that AOB can indeed act as a strong direct source of HONO.

Measured adenosine 5′-triphosphate (ATP) concentrations during the dry-out of S12 (Fig. 3C) show that soil microbes are active also under relatively dry conditions (% WHC < 20%), where $F_{N,opt}$(HONO) is observed. Because ATP is an indicator for microbial activity in general, the maximum activity of AOB might not coincide with the maximal ATP concentration. We applied methyl iodide—a strong sterilization agent for soil (*27*) also targeting nitrification (*28*)—to a subsample of S12 (Fig. 3C). Both HONO and NO emission fluxes were reduced by ~75%, revealing a strong microbial source. This demonstrates that the findings from the model system shown in Fig. 3B are transferable to a real soil sample. The residual emissions can largely be attributed to the chemical source because the ATP content and, hence, the microbial activity was reduced by ~92% at the HONO emission optimum. These results explain the high HONO emissions from nonacidic soil samples.

The conceptual model in Fig. 4 shows that $F_{N,opt}$(HONO) and $F_{N,opt}$(NO) occur in the lower SWC range (~0 to 40% WHC) (*16*, *29*), whereas at high SWC (~40 to 80% WHC), nitrogen is released from soil mainly as the greenhouse gas N_2O. In general, substrate diffusion is limited at low SWC, and gas diffusion is limited at higher SWC (*30*). HONO is produced and emitted during nitrification, which predominates at low SWC (*5*). Samples from different soil and land-use types show their maximal release of the respective nitrogen compound at different optimum SWC (*15*). The magnitude of the maximal emission of each compound varies depending on, for example, nutrient availability and abundance of soil bacteria.

HONO emissions by AOB and possibly other types of bacteria represent an additional component for gaseous losses from the soil nitrogen pool to the atmosphere. Our survey of soils from different ecosystems indicates that HONO emissions may account for up to 50% of the reactive nitrogen release from soil. This contribution of soil HONO emissions is currently not considered in model estimates of global soil reactive nitrogen emissions (*1*) and may constitute one of the major uncertainties in this budget. Furthermore, these HONO emissions contribute to atmospheric chemistry by enhancing the oxidation capacity of the lower atmosphere.

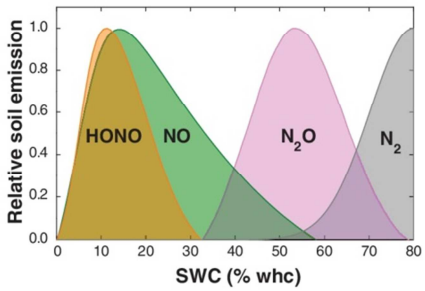

Fig. 4. HONO is a major component of nitrogen emissions from soil. The conceptual model of soil nitrogen emissions as a function of SWC was adopted from Firestone and Davidson (*31*). The curves are based on measurements of HONO, NO, and N_2O emissions from soil sample S12 [N_2 emissions were fitted from (*31*)].

References and Notes

1. IPCC, *Climate Change 2007: The Physical Science Basis. Contribution of Working Group I to the Fourth Assessment Report of the Intergovernmental Panel on Climate Change* (Cambridge, UK, 2007).
2. J. H. Quastel, *Annu. Rev. Plant Physiol.* **16**, 217–240 (1965).
3. Q. Q. Jiang, L. R. Bakken, *FEMS Microbiol. Ecol.* **30**, 171–186 (1999).
4. J. Ludwig, F. X. Meixner, B. Vogel, J. Forstner, *Biogeochemistry* **52**, 225–257 (2001).
5. M. Gödde, R. Conrad, *Soil Biol. Biochem.* **30**, 433–442 (1998).
6. W. Naegele, R. Conrad, *FEMS Microbiol. Ecol.* **74**, 49 (1990).
7. M. Kubota, T. Asami, *Soil Sci. Plant Nutr.* **31**, 35–42 (1985).
8. H. Su *et al.*, *Science* **333**, 1616–1618 (2011).
9. S. M. van Dijk *et al.*, *J. Geophys. Res. D Atmos.* **107**, 8058 (2002).
10. Materials and methods are available as supplementary materials on *Science* Online.
11. U. Rummel, C. Ammann, A. Gut, F. X. Meixner, M. O. Andreae, *J. Geophys. Res.* **107**, 8050 (2002).
12. A. Remde, J. Ludwig, F. X. Meixner, R. Conrad, *J. Atmos. Chem.* **17**, 249–275 (1993).
13. J. Kleffmann, J. Heland, R. Kurtenbach, J. Lörzer, P. Wiesen, *Environ. Sci. Pollut. Res. Int.* **9**, 48 (2002).
14. C. Breuninger, R. Oswald, J. Kesselmeier, F. X. Meixner, *Atmos. Meas. Tech.* **5**, 955–989 (2012).
15. K. Pilegaard, *Philos. Trans. R. Soc. Lond. B Biol. Sci.* **368**, 20130126 (2013).
16. G. T. Feig, B. Mamtimin, F. X. Meixner, *Biogeosciences* **5**, 1723–1738 (2008).
17. J. Rousk *et al.*, *ISME J.* **4**, 1340–1351 (2010).
18. S. Park, W. Bae, J. Chung, S.-C. Baek, *Process Biochem.* **42**, 1671–1676 (2007).
19. J. Kleffmann, *ChemPhysChem* **8**, 1137–1144 (2007).
20. J. J. Yienger, H. Levy II, *J. Geophys. Res. D Atmos.* **100**, 11447 (1995).
21. J. Steinkamp, M. G. Lawrence, *Atmos. Chem. Phys.* **11**, 6063–6082 (2011).
22. M. Gödde, R. Conrad, *Biol. Fertil. Soils* **30**, 33–40 (1999).
23. E. A. Davidson, I. A. Janssens, Y. Q. Luo, *Glob. Change Biol.* **12**, 154–164 (2006).
24. L. Breuer, R. Kiese, K. Butterbach-Bahl, *Soil Sci. Soc. Am. J.* **66**, 834 (2002).
25. O. Saad, R. Conrad, *Biol. Fertil. Soils* **15**, 21–27 (1993).
26. H. P. Koops, A. Pommerening-Röser, *FEMS Microbiol. Ecol.* **37**, 1 (2001).
27. M. E. Stromberger, S. Klose, H. Ajwa, T. Trout, S. Fennimore, *Soil Sci. Soc. Am. J.* **69**, 1987 (2005).
28. D. Yan *et al.*, *Soil Sci. Plant Nutr.* **59**, 142–148 (2013).
29. J. S. Levine *et al.*, *J. Geophys. Res. D Atmos.* **101**, 23689 (1996).
30. J. Skopp, M. D. Jawson, J. W. Doran, *Soil Sci. Soc. Am. J.* **54**, 1619 (1990).
31. M. K. Firestone, E. A. Davidson, in *Exchange of Trace Gases Between Terrestrial Ecosystems and the Atmosphere*, M. O. Andreae, D. S. Schimel, Eds. (Wiley, Chichester, UK, 1989), pp. 7–21.

Acknowledgments: This project was funded by the Max Planck Society. The work was supported by the Max Planck Graduate Center with the Johannes Gutenberg University Mainz (MPGC). We are grateful to S. Hohlmann, S. Müller, M. Welling, P. Stella, A. Held, B. L. Simmons, N. Mascher, C. Becker, A. C. Hertel, F. Hertel, and Z. Wu for supporting the experiments and helping to collect the soil samples and to S. Böhnke for assistance in creating the global map. We thank K. Emde and team as well as the company Envilytix for analyzing chemical and physical soil properties. Soil sample S7 was collected in Mali at the Agoufou site belonging to the African Multidisciplinary Monsoon Analysis–Couplage de l'Atmosphère Tropicale et du Cycle Hydrologique (AMMA-CATCH) observatory (www.amma-catch.org). The soil sample S11 from Grignon was collected within the framework of the European Commission project NitroEurope-IP (017841). The work of H.S. was supported by the European Commission within the framework of PEGASOS (265148). Supporting soil data are available in the supplementary materials.

Supplementary Material

www.sciencemag.org/cgi/content/full/341/6151/1233/DC1
Materials and Methods
Supplementary Text
Figs. S1 to S3
Table S1
References (*32*–*48*)

21 June 2013; accepted 7 August 2013
10.1126/science.1242266

www.sciencemag.org/cgi/content/full/341/6151/1233/DC1

Supplementary Material for

HONO Emissions from Soil Bacteria as a Major Source of Atmospheric Reactive Nitrogen

R. Oswald,* T. Behrendt, M. Ermel, D. Wu, H. Su, Y. Cheng, C. Breuninger, A. Moravek, E. Mougin, C. Delon, B. Loubet, A. Pommerening-Röser, M. Sörgel, U. Pöschl, T. Hoffmann, M.O. Andreae, F.X. Meixner, I. Trebs*

*Corresponding author. E-mail: robert.oswald@mpic.de (R.O.); i.trebs@mpic.de (I.T.)

Published 13 September 2013, *Science* **341**, 1233 (2013)
DOI: 10.1126/science.1242266

This PDF file includes:

Materials and Methods

Soil samples

All soil samples were taken from the uppermost layer of the soil (5 cm). Samples S1 (eucalyptus forest, Grose Valley, Australia, 33.61°S, 150.63°E), S5 (pasture, Hawkesbury River flood plain, Australia, 33.57°S, 150.77°E), S8 (grassland, Mainz-Finthen, Germany, 49.97°N, 8.16°E) (*32*), S11 (maize field, Grignon, France, 48.85°N, 1.97°E) (*33*) and S12 (wheat field, Mainz-Finthen, Germany, 49.97°N, 8.16°E) (*8*) were dried at 40 °C for 24 h, sieved to 2 mm and stored at 4 °C in open plastic bags before measurement.

Soil samples S2 (tropical rain forest, Suriname, 05.08°N, 55.00°W), S3 (coniferous forest, Hohenpeißenberg, Germany, 47.80°N, 11.01°E), S4 (coniferous forest, Fichtelgebirge, Germany, 50.09°N, 11.52°E) (*34*) and S9 (pasture, Hohenpeißenberg, Germany, 47.79°N, 11.00°E) (*35*) are characterized by high organic contents. These soils were sieved to 2 mm (S2) or 16 mm (S3, S4 and S9) (*36*) and measured directly after sampling.

All other soil samples, S6 (open woody savannah, Dahra, Senegal, 15.40°N, 15.43°W), S7 (open woody savannah, Agoufou, Mali, 15.34°N, 1.48°W) (*37*), S10 (stone desert, Ruta B 376, Chile, 23.48°S, 68.03°W), S13 (jujube field, Qiemo, China, 38.09°N, 85.55°E) (*38*), S14 (cotton field, Qiemo, China, 38.10°N, 85.55°E) (*38*), S15 (jujube field, Mingfeng, China, 37.05°N, 82.71°E) (*38*), S16 (stone desert, Sache, China, 37.69°N, 77.89°E) (*38*) and S17 (cotton field, Milan, China, 39.27°N, 88.91°E) (*38*) were already dry when sampled. They were sieved to 2 mm mesh size and stored at 4 °C in open plastic bags prior to measurement.

Physical and chemical properties of each soil sample were analyzed according to ISO or DIN standard procedures: bulk pH of soil according to ISO 10390, nitrite, nitrate and ammonium according to ISO/TS 14256-1, particle distribution according to ISO 11277, total C and N according to ISO 10649 and ISO 13878, loss on ignition according to DIN 19684-3 (*39*).

Measurements

The prepared soil samples were homogenously spread in a borosilicate glass dish to 5 mm thickness and wetted with purified water to water holding capacity (whc, Eq.4). After that, the glass dish was placed into the Teflon (PFE) chamber (volume 0.047 m^3) (*8*). Complete mixing of the chamber headspace volume was achieved by a fan. Dried and purified air was purged through the chamber at a flow rate of $1 \cdot 10^{-4}$ m^3 s^{-1} and mixing ratios of HONO, NO (NO_2), O_3 and H_2O were measured at the chamber outlet. The chamber was placed in a thermostatic cabinet to control the temperature of the experiment (accuracy ± 0.1 °C). All measurements were conducted in the dark to exclude photosensitized reactions found by Stemmler et. al (*40*). Additionally, potential interferences from background HONO formation can be excluded, as flushing the empty chamber with NO did not lead to HONO production. The inlet concentration of the purging air flow was measured regularly and was below the detection limits of the trace gas analyzers. A pure air generator (PAG 003, ECOPHYSICS, Switzerland) continuously provided dry air (dew point of about -30 °C).

HONO was measured by a long path absorption photometer (LOPAP) (QUMA Elektronik & Analytik GmbH, Wuppertal, Germany; limit of detection (LOD) ≈ 5 ppt) (*13*). NO (and NO_2) were detected by a gas phase chemiluminescence detector equipped with a blue light converter (Model 42C, Thermo Electron Corporation, USA; LOD_{NO} ≈ 120 ppt and LOD_{NO2} ≈ 300 ppt) (*14*). Additionally, the headspace concentration of O_3 was monitored using an UV-absorption analyzer (Model 49i, Thermo Electron Corporation, USA; LOD ≈ 0.5 ppb). The loss of soil water during the experiments was determined by measuring temperature and relative humidity at the outlet of the dynamic chamber (Model MP 103 A, Rotronic Messgeräte GmbH, Ettlingen, Germany).

For the measurement of the pure culture of *Nitrosomonas europaea*, the measurement of S2 and S12, including the ATP assays and the sterilization, the experimental setup was slightly modified. A smaller Teflon chamber (volume 0.008 m^3) was used and the Thermo NO_x instrument was replaced by a more sensitive chemiluminescence analyzer (CLD 780TR, ECOPHYSICS, Switzerland, LOD_{NO} ≈ 35 ppt and LOD_{NO2} ≈ 120 ppt). The water vapor difference between the inlet and outlet of the chamber was measured with an infrared gas analyzer (LI-7000, Li-Cor Biosciences GmbH, Germany). An intercomparison was performed using a constant source of NO_2, which yielded the same emission fluxes for both setups (not shown). During the experiment, a flow of $1 \cdot 10^{-4}$ m^3 s^{-1} was purged through the chamber containing the glass bead sample (0.25 – 0.50 mm diameter, Carl Roth, Germany) or the soil samples, respectively. To ensure sterile conditions, the chamber inlet was equipped with a sterile air filter (MILEX®-FG Vent Filter 0.2 µm, 50 mm diameter, Millipore, France). The glass beads and glass bowl were sterilized by washing with ethanol (70 %, absolute for analysis, Merck, Germany). Sterility of the setup was checked by an ATP assay for a sample of sterile AOB nutrient solution. For each experiment 50 g of glass beads were used and wetted either with sterile AOB nutrient solution (*41, 42*) or AOB culture suspension to reach whc. *Nitrosomonas europaea* was cultured as described by Krümmel and Harms (*41*) and the purity of the cultures was checked by microscopy. ATP was measured using a commercial ATP kit (BacTiterGlo, PROMEGA GmbH, Germany) combined with a luminometer (GloMax 20/20, PROMEGA GmbH, Germany). To sterilize sample S12 the soil was placed into a desiccator, along with 1 ml methyl iodide (99% Reagent Plus, SIGMA-ALDRICH Chemie GmbH, Germany) in a separate bowl. The desiccator was evacuated and the soil sample was exposed to a high partial pressure of methyl iodide for 24 hours. The sample was measured directly after this procedure.

Calculations

Fluxes of HONO, NO and NO_2 were calculated using the following formula:

$$F_N = \frac{Q}{A} \cdot (\chi_{out} - \chi_{in}) \cdot \frac{M_N}{V_m} \qquad (1)$$

with F_N the flux of trace gas in terms of N (ng m^{-2} s^{-1}), the purging flow rate Q (m^3 s^{-1}), the headspace mixing ratio at outlet and inlet of the chamber χ_{out} and χ_{in} (ppb), the area of soil A (m^2), the molar volume of air V_m (m^3 mol^{-1}) and the molar mass of nitrogen M_N (g mol^{-1}).

The uncertainties of the fluxes (ΔF_N) were calculated using Gaussian error propagation, neglecting the potential error of V_m. For the inlet and outlet mixing ratios (χ_{in} and χ_{out}) the errors are identical since $\Delta\chi$ was set to the noise of the instrument at the limit of detection (LOD):

$$\Delta F_N = \pm\sqrt{\left(\left[\left(\frac{\partial F_N}{\partial Q}\right)_{A,\chi_{in/out}} \cdot \Delta Q\right]^2 + \left[\left(\frac{\partial F_N}{\partial A}\right)_{Q,\chi_{in/out}} \cdot \Delta A\right]^2 + \left[2 \cdot \left(\frac{\partial F_N}{\partial \chi}\right)_{A,Q,\chi_{in}} \cdot \Delta\chi_{out}\right]^2\right)} \quad (2)$$

The area of the soil was calculated from the radius of the dish, which had an error of approximately 2 mm. The error of the purging air flow rate Q was calculated from the noise (3σ) of the measured flow rate. All measured values of χ_{out} that were not significantly different from χ_{in} were rejected.

We calculated the loss of water during the experiment from weighing the soil sample before and after the experiment and from the humidity measurements in the sample air, and subsequently derived the soil water content (normalized by the water holding capacity, see table S1):

$$SWC(t) = \left(1 - \frac{m(\text{loss of water})}{m(\text{dry soil})} \cdot \frac{\int_{t=0}^{t} RH(t) \cdot dt}{\int_{t=0}^{t_{max}} RH(t) \cdot dt} \cdot \frac{100}{whc}\right) \quad (3)$$

where SWC(t) is the soil water content (%) at time t (s), m(loss of water) is the mass of water (kg) evaporated from the soil during dry out, m(dry soil) is the mass of dry soil (kg), RH(t) is the relative humidity in the sample air (%) at time t and whc is the water holding capacity (%), defined as:

$$whc = \frac{m_{sat}(\text{water})}{m(\text{dry soil})}\% \quad (4)$$

where m_{sat}(water) is the mass of water in soil at field capacity (kg).

The NO_2^- and NH_4^+ concentrations at optimum SWC were calculated using the following equations:

$$\left[NO_2^-\right] = \frac{\rho(\text{water})}{SWC \cdot whc} \cdot \frac{\%m(NO_2^-)}{M(N)} \quad (5)$$

$$\left[NH_4^+\right] = \frac{\rho(\text{water})}{SWC \cdot whc} \cdot \frac{\%m(NH_4^+)}{M(N)} \quad (6)$$

where $[NO_2^-]$ and $[NH_4^+]$ are the concentrations (mmol l^{-1}), ρ(water) is the density of water (kg l^{-1}), M(N) is the molecular mass of nitrogen (g mol^{-1}) and %m(NO_2^-) and %m(NH_4^+) are the nutrient contents of dry soil (mg kg^{-1}) (see table S1).

Supplementary Text

All reported fluxes were calculated for χ_{in} equal to 0 ppb and, thus, represent fluxes prevailing under clean background conditions (very low atmospheric mixing ratios of trace gases) and may be considered as upper limit estimates. Typical daytime mixing ratios of HONO (50 – 500 ppt) (*43*) are much lower than those of NO (1-10 ppb) (*33, 44, 45*) in remote regions. Hence, the ratio of net HONO to NO fluxes should be even higher under these conditions.

$F_{N,opt}$(HONO) and $F_{N,opt}$(NO) were found to correlate only slightly with the calculated NO_2^- concentration at optimum SWC (R^2 = 0.52 and 0.51, respectively) and even less with NH_4^+ concentrations at optimum SWC (R^2 = 0.39 and 0.41, respectively).

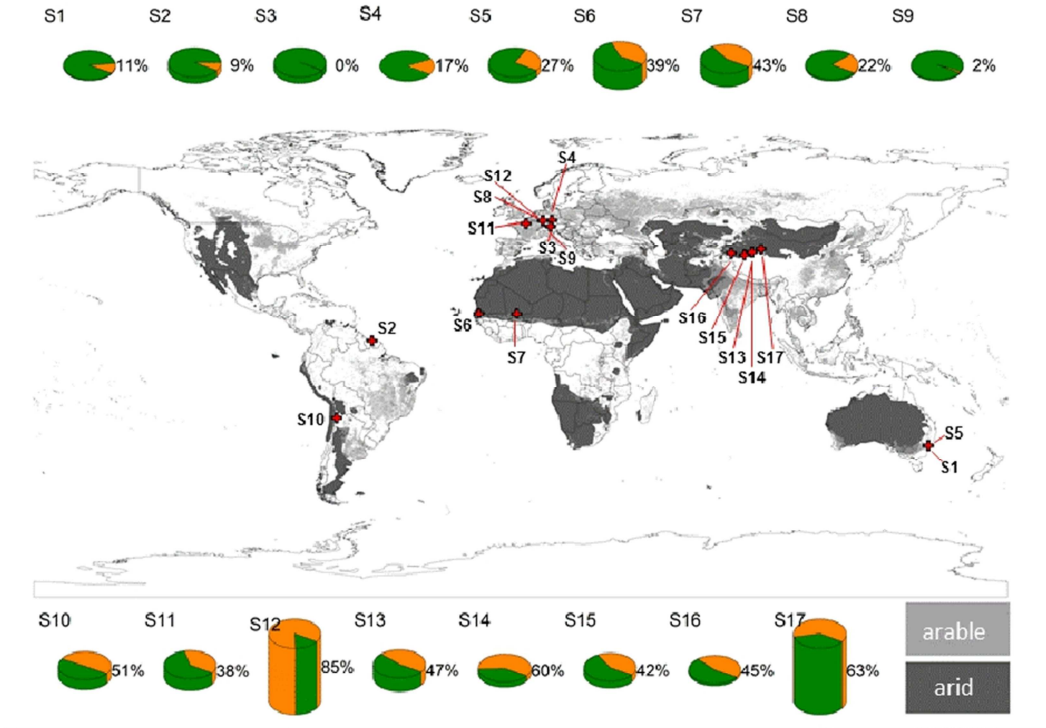

Fig. S1.

Global map (*46*) showing the contribution of $F_{N,opt}$(HONO) (orange) and $F_{N,opt}$(NO) (green) to their sum for the soil samples analyzed in this study. The height of the pie chart reflects the total emission flux (sum of $F_{N,opt}$(HONO) and $F_{N,opt}$(NO)). Light and dark grey shading of the map represent arable land use and arid climate according to Koeppen-Geiger climate zones (*47*). Black bordered red crosses mark the soil sampling sites (see Materials and Methods).

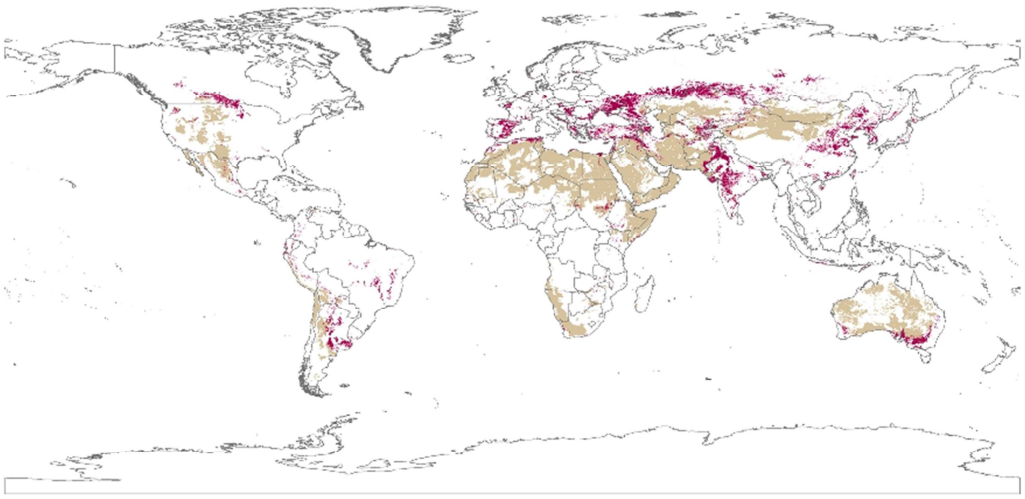

Fig. S2.

Global map (*46*) showing the potential HONO soil emission hot spots. The light brown color-code represents arid land with pH ≥ 7 and the dark red color-code refers to arable land with pH ≥ 7. The pH values were taken from (*48*).

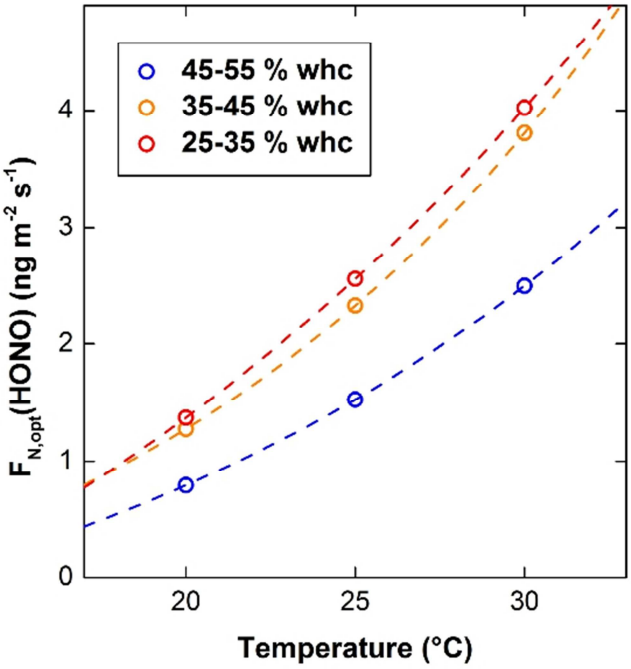

Fig. S3.

Temperature dependency of $F_{N,opt}$(HONO) measured for soil sample S8 for three different SWC ranges.

Table S1.
Physicochemical soil properties (nutrient content is shown in terms of N; n.a. = not analyzed, LOD of NO_2^- is 0.15 mg kg^{-1}).

soil sample	pH	nitrite	nitrate	ammonium	loss on ignition	C/N	sand	clay	gravimetric soil water content at whc
	1	mg kg^{-1}	mg kg^{-1}	mg kg^{-1}	%	1	%	%	%
S1	3.7	<LOD	12.3	1.3	4.4	39.2	77.4	8.7	68.8
S2	4.0	<LOD	4.9	83.4	18.2	13.8	n.a.	n.a.	143.3
S3	4.6	<LOD	3.5	36.6	37.1	18.9	n.a.	n.a.	188.8
S4	4.8	1.0	5.7	48.4	85.3	20.1	n.a.	n.a.	577.1
S5	5.4	<LOD	17.5	2.9	3.5	12.8	79.2	8.3	62.7
S6	5.6	<LOD	6.4	7.1	0.8	5.4	89.7	7.2	36.0
S7	5.9	0.3	5.6	2.7	0.7	10.0	90.3	8.7	37.1
S8	6.1	<LOD	0.7	19.4	10.0	14.6	38.4	25.6	74.9
S9	6.4	1.6	14.6	4.6	18.3	10.6	17.2	32.9	116.1
S10	6.5	<LOD	0.1	5.3	n.a.	n.a.	n.a.	n.a.	35.0
S11	6.9	<LOD	25.3	6.0	5.3	11.7	5.0	25.3	54.9
S12	7.2	1.0	77.7	18.1	5.2	10.5	21.7	27.8	63.5
S13	7.8	0.2	37.8	4.2	2.7	42.2	29.9	11.7	28.9
S14	8.0	<LOD	41.5	2.6	4.0	41.5	21.0	17.0	33.1
S15	8.2	<LOD	14.2	1.8	1.9	98.0	29.9	5.2	29.7
S16	8.4	<LOD	4.2	0.8	2.1	82.0	55.3	3.4	24.0
S17	8.8	1.1	691.7	83.0	7.4	40.6	21.4	11.2	30.6

References and Notes

1. IPCC, *Climate Change 2007: The Physical Science Basis. Contribution of Working Group I to the Fourth Assessment Report of the Intergovernmental Panel on Climate Change* (Cambridge, UK, 2007).

2. J. H. Quastel, soil metabolism. *Annu. Rev. Plant Physiol.* **16**, 217–240 (1965). doi:10.1146/annurev.pp.16.060165.001245

3. Q. Q. Jiang, L. R. Bakken, Comparison of Nitrosospira strains isolated from terrestrial environments. *FEMS Microbiol. Ecol.* **30**, 171–186 (1999). doi:10.1111/j.1574-6941.1999.tb00646.x Medline

4. J. Ludwig, F. X. Meixner, B. Vogel, J. Forstner, Soil-air exchange of nitric oxide: An overview of processes, environmental factors, and modeling studies. *Biogeochemistry* **52**, 225–257 (2001). doi:10.1023/A:1006424330555

5. M. Gödde, R. Conrad, Simultaneous measurement of nitric oxide production and consumption in soil using a simple static incubation system, and the effect of soil water content on the contribution of nitrification. *Soil Biol. Biochem.* **30**, 433–442 (1998). doi:10.1016/S0038-0717(97)00197-1

6. W. Naegele, R. Conrad, Influence of soil pH on the nitrate-reducing microbial population and their potential to reduce nitrate tor nitric oxide and nitrous oxide. *FEMS Microbiol. Ecol.* **74**, 49 (1990). doi:10.1111/j.1574-6968.1990.tb04051.x

7. M. Kubota, T. Asami, Source of nitrous-acid volatilized from upland soils. *Soil Sci. Plant Nutr.* **31**, 35–42 (1985). doi:10.1080/17470765.1985.10555215

8. H. Su, Y. Cheng, R. Oswald, T. Behrendt, I. Trebs, F. X. Meixner, M. O. Andreae, P. Cheng, Y. Zhang, U. Pöschl, Soil nitrite as a source of atmospheric HONO and OH radicals. *Science* **333**, 1616–1618 (2011). doi:10.1126/science.1207687 Medline

9. S. M. van Dijk *et al.*, Biogenic NO emissions from forest and pasture soils: Relating laboratory studies to field measurements. *J. Geophys. Res. D Atmos.* **107**, 8058 (2002). doi:10.1029/2001JD000358

10. Materials and methods are available as supplementary materials on *Science* Online.

11. U. Rummel, C. Ammann, A. Gut, F. X. Meixner, M. O. Andreae, Eddy covariance measurements of nitric oxide flux within an Amazonian rain forest. *J. Geophys. Res.* **107**, 8050 (2002). doi:10.1029/2001JD000520

12. A. Remde, J. Ludwig, F. X. Meixner, R. Conrad, A study to explain the emission of nitric-oxide from a marsh soil. *J. Atmos. Chem.* **17**, 249–275 (1993). doi:10.1007/BF00694400

13. J. Kleffmann, J. Heland, R. Kurtenbach, J. Lörzer, P. Wiesen, A new instrument (LOPAP) for the detection of nitrous acid (HONO). *Environ. Sci. Pollut. Res. Int.* **9**, 48 (2002). Medline

14. C. Breuninger, R. Oswald, J. Kesselmeier, F. X. Meixner, The dynamic chamber method: trace gas exchange fluxes (NO, NO_2, O_3) between plants and the atmosphere in the laboratory and in the field. *Atmos. Meas. Tech.* **5**, 955–989 (2012). doi:10.5194/amt-5-955-2012

15. K. Pilegaard, Processes regulating nitric oxide emissions from soils. *Philos. Trans. R. Soc. Lond. B Biol. Sci.* **368**, 20130126 (2013). doi:10.1098/rstb.2013.0126 Medline

16. G. T. Feig, B. Mamtimin, F. X. Meixner, Soil biogenic emissions of nitric oxide from a semi-arid savanna in South Africa. *Biogeosciences* **5**, 1723–1738 (2008). doi:10.5194/bg-5-1723-2008

17. J. Rousk, E. Bååth, P. C. Brookes, C. L. Lauber, C. Lozupone, J. G. Caporaso, R. Knight, N. Fierer, Soil bacterial and fungal communities across a pH gradient in an arable soil. *ISME J.* **4**, 1340–1351 (2010). doi:10.1038/ismej.2010.58 Medline

18. S. Park, W. Bae, J. Chung, S.-C. Baek, Empirical model of the pH dependence of the maximum specific nitrification rate. *Process Biochem.* **42**, 1671–1676 (2007). doi:10.1016/j.procbio.2007.09.010

19. J. Kleffmann, Daytime sources of nitrous acid (HONO) in the atmospheric boundary layer. *ChemPhysChem* **8**, 1137–1144 (2007). doi:10.1002/cphc.200700016 Medline

20. J. J. Yienger, H. Levy, II, Empirical-model of global soil-biogenic NO_x emissions. *J. Geophys. Res. D Atmos.* **100**, 11447 (1995). doi:10.1029/95JD00370

21. J. Steinkamp, M. G. Lawrence, Improvement and evaluation of simulated global biogenic soil NO emissions in an AC-GCM. *Atmos. Chem. Phys.* **11**, 6063–6082 (2011). doi:10.5194/acp-11-6063-2011

22. M. Gödde, R. Conrad, Immediate and adaptational temperature effects on nitric oxide production and nitrous oxide release from nitrification and denitrification in two soils. *Biol. Fertil. Soils* **30**, 33–40 (1999). doi:10.1007/s003740050584

23. E. A. Davidson, I. A. Janssens, Y. Q. Luo, On the variability of respiration in terrestrial ecosystems: Moving beyond Q(10). *Glob. Change Biol.* **12**, 154–164 (2006). doi:10.1111/j.1365-2486.2005.01065.x

24. L. Breuer, R. Kiese, K. Butterbach-Bahl, Temperature and moisture effects on nitrification rates in tropical rain-forest soils. *Soil Sci. Soc. Am. J.* **66**, 834 (2002). doi:10.2136/sssaj2002.0834

25. O. Saad, R. Conrad, Temperature-dependence of nitrification, denitrification, and turnover of nitric-oxide in different soils. *Biol. Fertil. Soils* **15**, 21–27 (1993). doi:10.1007/BF00336283

26. H. P. Koops, A. Pommerening-Röser, Distribution and ecophysiology of the nitrifying bacteria emphasizing cultured species. *FEMS Microbiol. Ecol.* **37**, 1 (2001). doi:10.1111/j.1574-6941.2001.tb00847.x

27. M. E. Stromberger, S. Klose, H. Ajwa, T. Trout, S. Fennimore, Microbial populations and enzyme activities in soils fumigated with methyl bromide alternatives. *Soil Sci. Soc. Am. J.* **69**, 1987 (2005). doi:10.2136/sssaj2005.0076

28. D. Yan, Q. Wang, L. Mao, T. Ma, Y. Li, M. Guo, A. Cao, Nitrification dynamics in a soil after addition of different fumigants. *Soil Sci. Plant Nutr.* **59**, 142–148 (2013). doi:10.1080/00380768.2012.754727

29. J. S. Levine, E. L. Winstead, D. A. B. Parsons, M. C. Scholes, R. J. Scholes, W. R. Cofer, III, D. R. Cahoon, Jr., D. I. Sebacher, Biogenic soil emissions of nitric oxide (NO) and nitrous oxide (N_2O) from savannas in South Africa: The impact of wetting and burning. *J. Geophys. Res. D Atmos.* **101**, 23689 (1996). doi:10.1029/96JD01661

30. J. Skopp, M. D. Jawson, J. W. Doran, Steady-state aerobic microbial activity as a function of soil-water content. *Soil Sci. Soc. Am. J.* **54**, 1619 (1990). doi:10.2136/sssaj1990.03615995005400060018x

31. M. K. Firestone, E. A. Davidson, in *Exchange of Trace Gases Between Terrestrial Ecosystems and the Atmosphere*, M. O. Andreae, D. S. Schimel, Eds. (Wiley, Chichester, UK, 1989), pp. 7–21.

32. D. Plake, I. Trebs, An automated system for selective and continuous measurements of vertical thoron profiles for the determination of transport times near the ground. *Atmos. Meas. Tech.* **6**, 1017–1030 (2013). doi:10.5194/amt-6-1017-2013

33. P. Stella, B. Loubet, P. Laville, E. Lamaud, M. Cazaunau, S. Laufs, F. Bernard, B. Grosselin, N. Mascher, R. Kurtenbach, A. Mellouki, J. Kleffmann, P. Cellier, Comparison of methods for the determination of NO-O_3-NO_2 fluxes and chemical interactions over a bare soil. *Atmos. Meas. Tech.* **5**, 1241–1257 (2012). doi:10.5194/amt-5-1241-2012

34. M. Sörgel, I. Trebs, A. Serafimovich, A. Moravek, A. Held, C. Zetzsch, Simultaneous HONO measurements in and above a forest canopy: Influence of turbulent exchange on mixing ratio differences. *Atmos. Chem. Phys.* **11**, 841–855 (2011). doi:10.5194/acp-11-841-2011

35. K. Acker, D. Möller, W. Wieprecht, F. X. Meixner, B. Bohn, S. Gilge, C. Plass-Dülmer, H. Berresheim, Strong daytime production of OH from HNO_2 at a rural mountain site. *Geophys. Res. Lett.* **33**, L02809 (2006). doi:10.1029/2005GL024643

36. A. Bargsten, E. Falge, K. Pritsch, B. Huwe, F. X. Meixner, Laboratory measurements of nitric oxide release from forest soil with a thick organic layer under different understory types. *Biogeosciences* **7**, 1425–1441 (2010). doi:10.5194/bg-7-1425-2010

37. E. Mougin *et al.*, The AMMA-CATCH Gourma observatory site in Mali: Relating climatic variations to changes in vegetation, surface hydrology, fluxes and natural resources. *J. Hydrol. (Amst.)* **14**, 12 (2009).

38. B. Mamtimin *et al.*, "The project 'Desert encroachment in central Asia – Quantification of soil biogenic nitric oxide emissions by ground- and satellite-based methodologies (DEQNO)'—An overview," presented at EGU General Assembly (2011).

39. H.-P. Blume *et al.*, *Handbuch der Bodenuntersuchung* (Wiley-VCH, Weinheim, ed. 1, 2000), vol. 11.

40. K. Stemmler, M. Ammann, C. Donders, J. Kleffmann, C. George, Photosensitized reduction of nitrogen dioxide on humic acid as a source of nitrous acid. *Nature* **440**, 195–198 (2006). doi:10.1038/nature04603 Medline

41. A. Krümmel, H. Harms, Effect of organic matter on growth and cell yield of ammonia oxidizing bacteria. *Arch. Microbiol.* **133**, 50 (1982). doi:10.1007/BF00943769

42. H.-P. Koops, U. Purkhold, A. Pommerening-Röser, G. Timmermann, M. Wagner, *The Lithoautotrophic Ammonia-Oxidizing Bacteria*. M. Dworkin, S. Falkow, E. Rosenberg, K. H. Schleifer, E. Stackebrandt, Eds. (Springer, New York, 2006), pp. 778-811.

43. F. Rohrer, B. Bohn, T. Brauers, D. Brüning, F.-J. Johnen, A. Wahner, J. Kleffmann, Characterisation of the photolytic HONO-source in the atmosphere simulation chamber SAPHIR. *Atmos. Chem. Phys.* **5**, 2189–2201 (2005). doi:10.5194/acp-5-2189-2005

44. I. Gelfand, G. Feig, F. X. Meixner, D. Yakir, Afforestation of semi-arid shrubland reduces biogenic NO emission from soil. *Soil Biol. Biochem.* **41**, 1561–1570 (2009). doi:10.1016/j.soilbio.2009.04.018

45. U. Rummel, C. Ammann, A. Gut, F. X. Meixner, M. O. Andreae, Eddy covariance measurements of nitric oxide flux within an Amazonian rain forest. *J. Geophys. Res.* **107**, (D20), 8050 (2002). doi:10.1029/2001JD000520

46. VDS Technologies, World Data. (2000-2013).

47. M. Kottek, J. Grieser, C. Beck, B. Rudolf, F. Rubel, World Map of the Koppen-Geiger climate classification updated. *Meteorologische Zeitschrift* **15**, 259–263 (2006). doi:10.1127/0941-2948/2006/0130

48. Data from IGBP-Dros. Inf. Serv. SoilData: A program for creating global soil-property databases., (1998).

B2. Ermel et al, to be submitted, 2014

Hydroxylamine released by ammonia-oxidizing bacteria as precursor for HONO emission from soils

Authors: M. Ermel[1,2], T. Behrendt[1,3], R. Oswald[1], B. Derstroff[4], D. Wu[1,5], S. Hohlmann[1], C. Stönner[4], A. Pommerening-Röser[6], J. Williams[4], F. X. Meixner[1], M. O. Andreae[1], M. Sörgel[1] and I. Trebs[1#]

[1] Biogeochemistry Department, Max Planck Institute for Chemistry, P.O. Box 3060, 55020 Mainz, Germany
2 Institute for Inorganic and Analytical Chemistry, Johannes Gutenberg University Mainz, 55128 Mainz, Germany
3 Multiphase Chemistry Department, Max Planck Institute for Chemistry, P.O. Box 3060, 55020 Mainz, Germany
4 Atmospheric Chemistry Department, Max Planck Institute for Chemistry, P.O. Box 3060, 55020 Mainz, Germany
5 Key Laboratory of Agricultural Water Research, Center for Agricultural Resources Research, Institute of Genetic and Developmental Biology, The Chinese Academy of Sciences, 050021 Shijiazhuang, China
6 Department of Microbiology and Biotechnology, University of Hamburg, Hamburg, Germany
now at: Centre de Recherche Public - Gabriel Lippmann, Department Environment and Agro-biotechnologies, 41 rue du Brill, L-4422 Belvaux, Luxembourg

Fehler! Textmarke nicht definiert.

Abstract

Nitrous acid (HONO) is a major precursor of the hydroxyl radical (OH) in the atmosphere, contributing up to 60 % to the total OH production during daytime. Consequently, HONO has a strong influence on atmospheric oxidative capacity, but is also an important source of nitric oxide (NO), a key catalyst for tropospheric ozone production. It was recently shown that soil can emit HONO at amounts similar to NO, and that nitrification by soil bacteria is responsible for a large fraction of these HONO emissions. Here, we investigate the microbial formation process of HONO. Laboratory experiments with pure cultures show that HONO emission is restricted to ammonia-oxidizing bacteria (AOB), whereas nitrite-oxidizing bacteria (NOB) do not emit HONO. These findings are confirmed by inhibition experiments with these groups of nitrifying soil bacteria. Hydroxylamine (NH_2OH), which is released as a result of cell membrane damage by drying stress, is identified as precursor of HONO emissions by AOB, whereas nitrite production is of minor importance. Using a glass bead matrix, we observed that HONO is formed by a surface reaction of gaseous NH_2OH with water vapor with an uptake coefficient $\gamma = (9.3 \pm 3.1) \cdot 10^{-7}$, which is comparable to other heterogeneous reactions forming HONO. This explains why HONO emissions are mainly found at low soil water contents, as only then the soil particle surface is available for the heterogeneous reaction. Our results suggest that NH_2OH is an important precursor in HONO formation from ammonia-oxidizing bacteria in soil.

Significance Statement

The hydroxyl radical (OH), the main oxidant or “detergent” of the atmosphere, is produced to a significant extent by the photolysis of nitrous acid (HONO), and therefore HONO has a strong influence on the atmospheric oxidative self-cleansing mechanism. It was recently shown that ammonia-oxidizing bacteria in soil emit HONO at the same order of magnitude as the previously well-studied nitric oxide (NO). In this study we investigate the mechanisms driving this microbial emission of HONO. From pure culture experiments we find that a bacterial metabolite, hydroxylamine, is a precursor for HONO, and we identified a heterogeneous reaction explaining this formation process.

Introduction

The release of reactive nitrogen (N_r) from soil has been studied for more than 50 years (1, 2), mainly focusing on nitric oxide (NO) and nitrous oxide (N_2O). In general, NO can be emitted

by soil microbes during nitrification (3) and denitrification (4). During the latter process nitrate (NO_3^-) is mostly anaerobically reduced to nitrogen (N_2) via nitrite (NO_2^-), releasing NO and the greenhouse gas N_2O as intermediates (5). Nitrification can be separated into two steps: the oxidation of ammonia (NH_4^+) via hydroxylamine (NH_2OH) to NO_2^- by ammonia-oxidizing bacteria (AOB)(6) and ammonia-oxidizing archaea (AOA)(7), followed by the transformation of NO_2^- to NO_3^- by nitrite-oxidizing bacteria (NOB) (8). The soil water content (SWC), which affects gas permeability, and hence the oxygen availability, determines which of the two processes dominates (9). Furthermore, SWC has a strong influence on the composition of the microbial communities (10). During these microbial transformations, NO can be released by either AOB (11) or NOB (12).

Recently, Oswald et al. (13) demonstrated that, in addition to its abiotic formation from NO_2^- and protons in the aqueous phase of soil (14), nitrous acid (HONO) can also be emitted by the AOB *Nitrosomonas europaea*, particularly at low SWC. This is an important finding for atmospheric chemistry, because HONO significantly influences the oxidative capacity of the atmosphere due to its photolysis during daytime, which yields the OH radical. Furthermore, the resulting NO has adverse effects on tropospheric ozone formation and hence, on air quality (15, 16). While the work of Oswald et al. (13) showed that soil HONO emissions are closely linked to NO emissions, the biological processes underlying the release of HONO from bacteria have not been investigated in detail.

The NO release by AOB can occur at different steps of the ammonia oxidation chain. In the first step, the ammonium monooxygenase (AMO) produces NH_2OH (17). The intermediate, NH_2OH, is known to easily autoxidize in solution to NO_2^- releasing the trace gases NO, N_2O and N_2 (18). In a second step, NH_2OH is oxidized to NO_2^- by hydroxylamine oxidoreductase (HAO) (19). This reaction is thought to form NO as a byproduct (20). During denitrification by nitrifiers, NO_2^- is reduced stepwise to N_2, which mostly proceeds analogously to the denitrification by denitrifiers (21, 22). However, the structure of the enzymes of the AOB differs from that of the denitrifiers, which reduce NO_2^- by nitrite reductase (NIR) to NO (23). This is subsequently converted to N_2O by nitric oxide reductase (NOR) (24). During these processes all intermediate gases can be emitted to the atmosphere (24). While the emission pathways of NO and N_2O are relatively well studied, detailed investigations of the processes underlying soil HONO emissions are still lacking.

To close the gap of knowledge about this important pathway in the biogeochemical nitrogen cycle, we investigated several strains of AOB and NOB with the following goals: (a) identification of groups of nitrifying bacteria that are involved in soil HONO emission and (b) investigation of the different enzymatic reactions of bacterial nitrification and intermediates that are potentially responsible for HONO formation. Our aim is to provide an experimental basis to explain and quantify the role of soil HONO emissions and their impact on atmospheric chemistry.

Results and Discussion

We performed our experiments under controlled laboratory conditions using the dynamic chamber method (25). The soil samples were placed in Petri dishes and were wetted initially to reach field capacity (fc) (26). The bacterial cultures were grown in a liquid medium (27), which was applied to a layer of glass beads in a Petri dish to reach the fc of the glass beads. The Petri dishes containing the samples were placed into the chamber, which was then continuously flushed with dry purified air leading to a slow drying, during which the trace gases (HONO, NO, H_2O, O_3) in the air leaving the chamber were measured by commercial analyzers (for details see material and methods). Typically, a maximal emission of HONO and NO is observed at an optimal gravimetric water content during this drying-out process. These maximal emissions will be henceforth denoted as F_{opt}(HONO) and F_{opt}(NO). We will mainly use these optima to characterize and discuss the results. As an example, the results from a complete experiment are displayed in Fig S1. The cell density of the cultures was quantified by measuring the concentration of adenosine 5´-triphosphate (ATP) in µmol l^{-1}, which correlates well with the microscopically derived cell density (Fig. S2). The cell density of the AOB cultures was typically determined just before the experiment, and was in the range of 2 to 20 µmol l^{-1} ATP. Since one experiment lasted about seven hours and the reproduction rate of AOB ranges between 12 and 20 hours (28), we neglect any significant growth of the cultures during the experiments.

Overview of Bacteria Emitting HONO

We investigated the ability of the NOB species, *Nitrobacter winogradskyi*, *Nitrospira defluvii,* and *Nitrospira moscoviensis*, and the AOB species, *Nitrosmonas communis*, *Nitrosmonas europaea*, *Nitrsosomonas nitrosa*, *Nitrosomonas ureae*, and *Nitrosolobus multiformis*, which represent all phylogenetic lineages comprising terrestrial and limnic AOB species (29), to

emit HONO and NO at a temperature of 25°C (Fig. 1). Our experiments showed that HONO emissions from AOB substantially exceed those of NO. In contrast, the NOB only emit very small amounts of NO and no detectable HONO. Our findings are in agreement with Oswald et al. (13), who found F_{opt}(HONO) to be four times larger than F_{opt}(NO) at low bacterial activity of the culture.

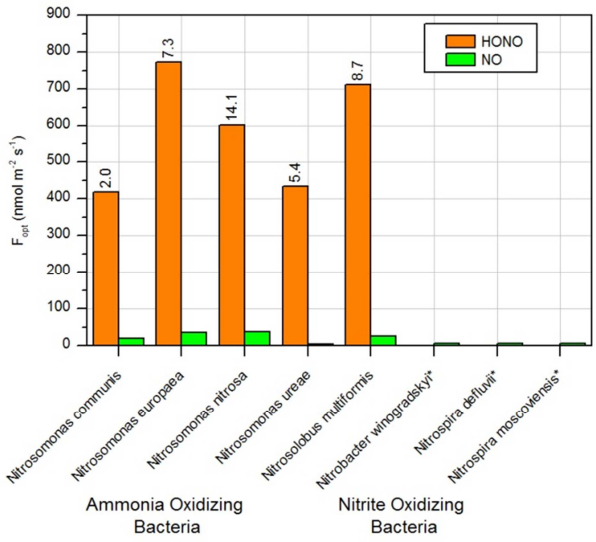

Figure 1: HONO and NO are emitted by AOB, while NOB only emit very small amounts of NO. The cell density of the culture expressed as ATP concentration in µmol l^{-1} is shown above the corresponding bars. For the NOB no density data is available. All experiments were carried out at 25°C.

Inhibition of Microbial Activity in Soil

A soil sample taken from a wheat field was treated with the inhibitors methyl 3-(4-hydroxyphenyl) propionate (MHPP) (30) and potassium chlorate ($KClO_3$) (31) before performing a dry-out experiment in the dynamic chamber.

The comparison between the inhibited and the untreated samples in Figs. 2a and 2b shows that F_{opt}(HONO) was reduced by 73 % and F_{opt}(NO), was reduced by 78 % by the MHPP inhibition. This result is comparable to the sterilization experiment with methyl iodide performed by Oswald et al. (13), reaching 75 % reduction of HONO and NO emissions for the same batch of wheat field soil. In contrast to the MHPP inhibition, the inhibition with $KClO_3$ showed a reduction of only 41 % in F_{opt}(NO), whereas F_{opt}(HONO) increased by 29 % compared to the untreated sample. These results from the inhibition of microbial activity in

soil samples are consistent with pure culture experiments, as MHPP, an inhibitor of AMO (30) and hence of AOB activity, has an analogous effect as the sterilization agent methyl iodide (32) that was applied by Oswald et al. (13).

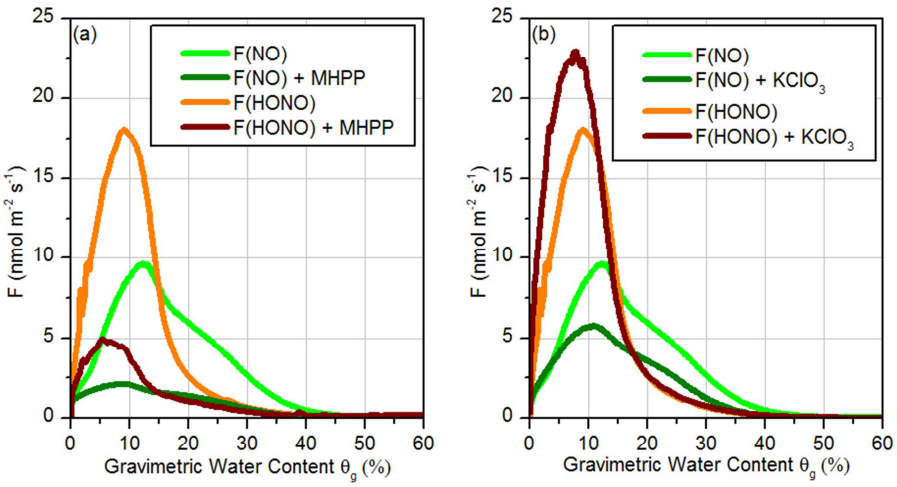

Figure 2: The inhibitors MHPP and ($KClO_3$) have opposite effects on soil HONO emissions from a wheat field soil (T = 25°C). The emissions are shown in light colors for the untreated sample and in dark colors for the inhibited sample. ((a) 1.0 µg g^{-1} soil MHPP and (b) 819 µg g^{-1} soil potassium chlorate was used to inhibit the microbial activity from the wheat field soil).

The NOB inhibitor chlorate (31) reduces only the emissions of NO while it increases HONO release, which is likely due to the accumulation of NO_2^-, increasing abiotic HONO emission (14). This confirms that bacterial HONO emission during the bacterial nitrification process is restricted to the ammonia oxidizing step and to AOB. In the following sections, we will focus on the HONO formation process by AOB.

HONO Emission vs Cell Density

HONO emissions from cultures of *N. europaea* (type strain) were measured during their growth at different cell densities (Fig. 3). Over the range of cell density of 0 to 5 µmol l^{-1} ATP, F_{opt}(HONO) rises linearly, followed by a slower increase between 7 and 12 µmol l^{-1} l ATP. Beyond 12 µmol l^{-1} ATP, F_{opt}(HONO) decreases quickly and drops to nearly zero at a cell density of 20 µmol l^{-1} ATP. *N. communis*, *N. nitrosa*, *N. ureae* and *N. multiformis* follow the same pattern. The oligotrophic *N. ureae* shows lower emissions than the eutrophic strains.

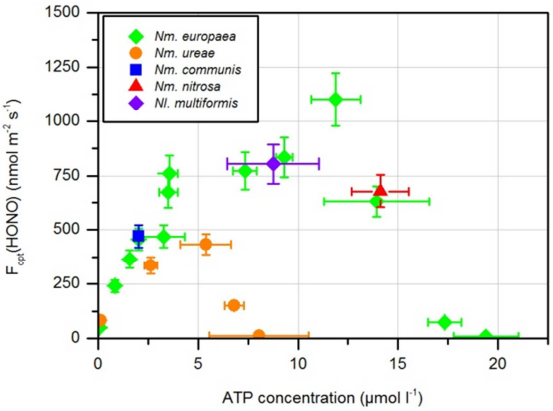

Figure 3: Optimum emission F_{opt}(HONO) of *N. europaea* (green diamonds), *N. communis* (blue square), *N. nitrosa* (red triangle), *N. ureae* (orange circles) and *N. multiformis* (violet diamond) at different cell densities shown as ATP concentration. The cultures were grown on a suspension containing 10 mmol l^{-1} NH_4^+. Error bars of F_{opt} represent the uncertainty of the results derived from Gaussian error propagation calculation (ΔF_{opt}). Error bars of ATP measurements denote standard deviations (n=3).

The lack of a linear relationship between F_{opt}(HONO) and cell number (Fig. 3) is in contrast to the results from previous studies on NO emissions from AOB, which had shown a linear relationship (21). This linear relationship for NO release was mainly attributed to the enzymatic pathway of nitrifier denitrification. Hence, HONO emissions might not be directly correlated with enzyme activity, a parameter related to the number of cells, but with the different metabolic intermediates and products, whose concentration in the medium changes due to their production or consumption during the growth of the culture. We also investigated the behavior of the knockout mutants, *nirK* (33) and *norB* (34), of *N. europaea*, which are each lacking nitrite reductase (NIR) and NO reductase (NOR), respectively. Both emitted HONO at rates similar to the type strain (data not shown). Since these enzymes are both known to be involved in the nitrifier denitrification pathway, this mechanism can be excluded for HONO formation.

The Effect of Nitrite and Hydroxylamine

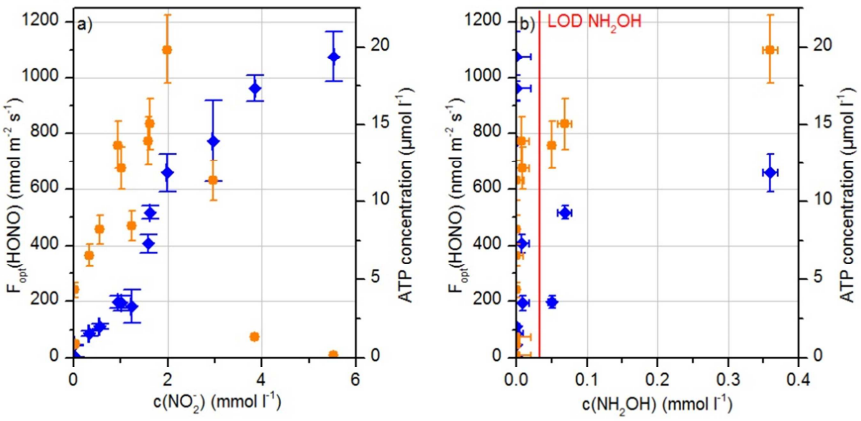

Figure 4: (a) Optimum emission fluxes, F_{opt}(HONO) (orange circles), and ATP concentration (blue diamonds) for *N. europaea* as a function of NO_2^- concentration in the culture. The NO_2^- concentration in the culture suspension is positively correlated with the cell density of the culture measured as ATP concentration. b) Optimum emissions F_{opt}(HONO) (orange circles) and ATP concentration (blue diamonds) for *N. europaea* as a function of NH_2OH concentration in the culture. For *N. europaea*, accumulation of NH_2OH appears at cell densities between 7 and 12 µmol l^{-1} ATP. Error bars of F_{opt} represent results from the Gaussian error propagation calculation (ΔF_{opt}). Error bars of ATP concentrations denote standard deviations (n=3). Error bars of c(NO_2^-) and c(NH_2OH) represent 1σ of the background.

Figure 4a shows that F_{opt}(HONO) is positively correlated with NO_2^- at concentrations below 2 mmol l^{-1}. However, above this threshold HONO emissions decline and approach zero at 5.5 mmol l^{-1}. This is in contrast to the linear correlation with c(NO_2^-) that would be expected for abiotic HONO emission from NO_2^- according to Henry's law. Furthermore, the pH of 6.8 – 7.2 inside *N. europaea* cells (35, 36) is too high for an effective protonation of NO_2^- and, hence, a strong abiotic HONO emission. On the other hand, a nearly exponential correlation exists between the cell density and the NO_2^- concentration (Fig. 4a), consistent with NO_2^- being a metabolism product of *N. europaea*. This close linkage between c(NO_2^-) and the number of cells explains the observed NO_2^- dependency of F_{opt}(HONO). The cell density (Fig. 3) also shows the pattern of a strong decrease in F_{opt}(HONO) after reaching a maximum, similar to the behavior of c(NO_2^-) (Fig. 4a).

Figure 4b shows that F_{opt}(HONO) is positively correlated with the concentration of NH_2OH in the culture suspension (for details on determination see material and methods). NH_2OH as an intermediate is only observed at low concentrations of 0 – 0.35 mmol l^{-1}, in contrast to NO_2^-, which accumulates. Unfortunately, c(NH_2OH) data are not available for all measurements, and due to the high limit of detection (LOD) of 0.033 mmol l^{-1} for NH_2OH only three data points are valid. Higher values of c(NH_2OH) result in stronger HONO emission. However, only some of the investigated cultures show NH_2OH accumulation in the culture suspension (Fig. 4b). For *N. europaea*, accumulation of NH_2OH appears at cell densities between 7 and 12 µmol l^{-1} ATP, just before the observed collapse of HONO production shown in Fig. 2. The positive correlation of the HONO emission flux and c(NH_2OH) may suggest that NH_2OH is a precursor for HONO. The known hydrolysis of NH_2OH to NO_2^- in aqueous solution supports this theory (37). However, the number of data points is too low for robust conclusions.

Effect of Ammonia Limitation on HONO Emission

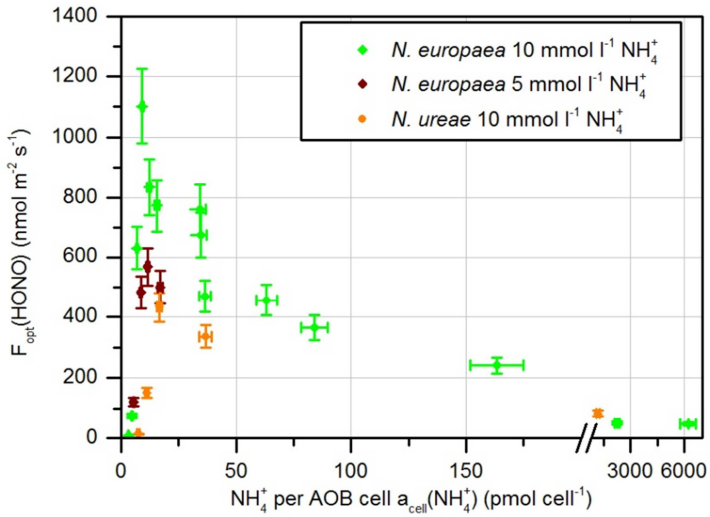

Figure 5: Optimum emissions, F_{opt}(HONO), for *N. europaea* and *N. ureae* cultures as a function of the ammonia availability per AOB cell $a_{cell}(NH_4^+)$expressed as pmol $cell^{-1}$. Green diamonds show *N. europaea* cultured in a 10 mmol l^{-1} NH_4^+ culture suspension, brown diamonds show the results from cultivation in a 5 mmol l^{-1} NH_4^+ culture suspension. Results from *N. ureae* cultured in 10 mmol l^{-1} NH_4^+ culture suspension are represented by orange dots. Error bars of F_{opt} represent results from Gaussian error propagation calculation (ΔF_{opt}).

The strong decrease in F_{opt}(HONO) shown in Figs. 3 and 4a could be related to the ammonia concentration in the medium. Although NO_2^- is still produced at higher cell densities, which indicates that sufficient ammonia is present for the culture to grow, a threshold in the availability of ammonia might limit F_{opt}(HONO). Therefore we calculated the ammonia availability per AOB cell, $a_{cell}(NH_4^+)$, expressed as pmol $cell^{-1}$, from the NH_4^+ concentration and the cell density at the start of the experiment. For *N. europaea* a maximum of F_{opt}(HONO) was observed at 10-12 pmol $cell^{-1}$, followed by a strong decrease of F_{opt}(HONO) with increasing $a_{cell}(NH_4^+)$ (Fig. 5). This pattern was found for *N. europaea* cultivated in suspensions containing 10 mmol l^{-1} NH_4^+ or 5 mmol l^{-1} NH_4^+. In addition, the oligotrophic species, *N. ureae*, followed the same pattern, although it showed a different F_{opt}(HONO) at different cell densities (Fig. 3). These findings indicate that the ammonia availability has a strong influence on HONO emission. Schmidt et al. (38) have shown that several AOB, including *N. europaea*, are able to accumulate ammonium and NH_2OH up to an internal concentration of 1 mol l^{-1} and 0.8 mol l^{-1}, respectively. At a low ammonium availability, below about 10 pmol $cell^{-1}$, where F_{opt}(HONO) decreases strongly, the AOB might not be able to maintain their high internal stocks. The strongest emission F_{opt}(HONO) occurs at a low gravimetric water content θ_g of ~1.5% in each experiment. Thus the culture suspension becomes highly concentrated, as the volume of the suspension is reduced by ~94%. Hence AOBs are exposed to a strong osmotic pressure, which might lead to cell lysis and the release of accumulated NH_4^+ and NH_2OH. Reactions of NH_3 and NH_4^+ have been widely studied and it seems unlikely that they are a precursor of HONO. Instead, our results suggest that NH_2OH, a molecule that has not been extensively studied in the gas phase under atmospherically relevant conditions, might be involved in the formation of HONO.

Relation of F(HONO) and F(NH_2OH) to Damaged Cells

To confirm a link between F_{opt}(HONO) and the internally accumulated NH_2OH, we applied formaldehyde (CH_2O) to a culture suspension (Fig. 6). CH_2O increases the permeability of the cell membranes, which should trigger the release of NH_2OH and thereby initiate the HONO emission. Indeed, we found the onset of the release of HONO and NO to occur directly after the application of CH_2O. The large peak at the end of the experiment, which is the discussed F_{opt}(HONO), can be attributed to the progressive drying-out process, which is indicated by the drop of H_2O evaporated from the soil.

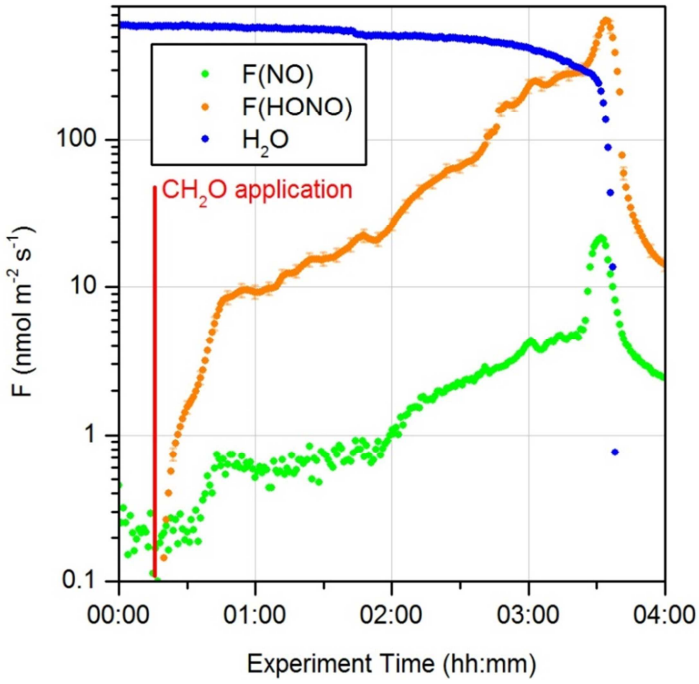

Figure 6: Disruption of the cell membrane by formaldehyde (CH_2O) causes instantaneous emission of HONO and NO. The H_2O release from soil in the chamber is represented in arbitrary units.

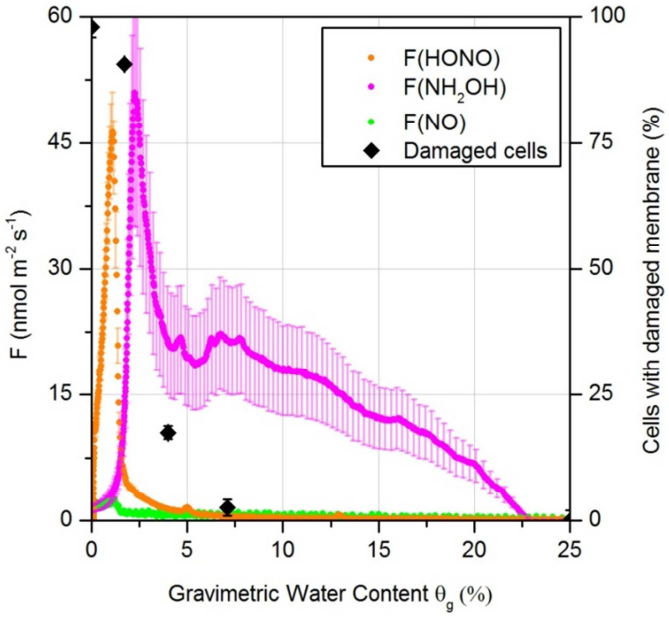

Figure 7: NH_2OH is emitted by *N. europaea* at the same order of magnitude as HONO, but is released at higher gravimetric water content, θ_g, compared to HONO. The number of cells with damaged membranes rises with decreasing θ_g. Error bars of damaged cell numbers denote standard deviations (n=3).

We used a Proton Transfer Reaction Time of Flight Mass Spectrometer (PTR-TOF-MS) to investigate the potential release of NH_2OH during the drying out of a culture suspension applied to glass beads. Additionally, the number of cells with damaged membranes was determined using fluorescence microscopy. Our results show that *N. europaea* is capable of emitting NH_2OH (Fig. 7). The release starts at higher values of θ_g compared to the release of HONO and increases further during the drying out. Shortly before F(HONO) starts to rise strongly (at θ_g= 6 %), the F(NH_2OH) maximum is reached and followed by a sharp decline. The rise in cells with damaged membranes follows the same pattern as F(HONO) from the *N. europaea* culture. This can be explained by the loss of membrane integrity caused by dehydration stress at low θ_g. F_{opt}(HONO) and F_{opt}(NH_2OH) correspond to the strongest cell damage and support our theory of cellular NH_2OH being released during the drying out of the cultures as precursor for gaseous HONO emissions.

Surface Reaction of Gaseous NH2OH with Water Vapor

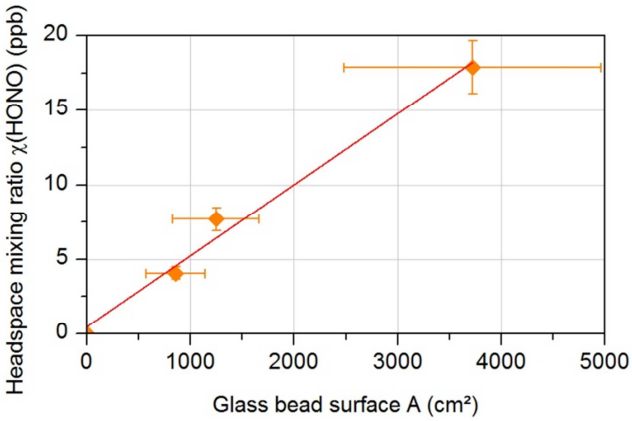

Figure 8: Dependency of HONO formation on the glass bead surface during the surface reaction of NH_2OH (207 ppb) with water vapor (12.5 mmol mol^{-1}).

To investigate the process of HONO emission further, we used a source of gaseous NH_2OH that we flowed together with humidified air through a cartridge filled with different amounts of glass beads. We observed that the following reaction yields HONO (R1) in this setup:

$$NH_2OH + H_2O + \text{surface} \rightarrow HONO + \text{unknown products} \qquad \text{R1}$$

A linear relationship between the glass bead surface and the produced HONO was found (Fig. 8). For the very short contact time of only 3 s between air and glass beads, the maximal conversion of NH_2OH to HONO was found to be 8.6 %. We calculated the uptake coefficient,

γ, for the largest amount of glass beads to be $\gamma = (9.3 \pm 3.1) \cdot 10^{-7}$, which is of the same order of magnitude as other heterogeneous reactions forming HONO (39, 40). Formation of HONO was not observed under completely dry conditions. Furthermore, a gas phase reaction of NH_2OH with water vapor was not found (data not shown). Our results show that NH_2OH can react to HONO on moist surfaces, which explains the observation of highest HONO emissions at low θ_g, as only in this case the full surface of the glass beads is available for the heterogeneous reaction R1.

Finally, we investigated four different soil samples for their NH_2OH release; however, no NH_2OH emission could be detected, because an isotopomer of methanol ($^{13}CH_3OH$) apparently masks the very small expected NH_2OH signal. Since soils have a substantially higher specific surface area (~ 10^3 - 10^6 $cm^2\ g^{-1}$) compared to glass beads (59.6 $cm^2\ g^{-1}$), the heterogeneous reaction forming HONO is expected to be much more efficient. Hence, NH_2OH cannot accumulate and its fluxes from soil samples are likely to be negligible, being replaced by HONO emissions.

Conclusions

In this study, we have discovered and explained a previously unknown process within the biogeochemical nitrogen cycle, which causes HONO emission from soils and is thus vitally important for atmospheric chemistry. Our results show that within the bacterial nitrification process the emission of HONO is restricted to AOB, and that NOB are not able to produce or emit this compound. F_{opt}(HONO) is not linearly correlated with the cell density of AOB cultures , but shows a maximum at intermediate cell densities followed by a strong decrease at higher cell densities. This indicates that HONO emission is not directly linked to enzyme activity in cells. Instead, the HONO emission strength depends on the ammonia availability per cell and hence also on the NH_2OH concentration. We find that NH_2OH, until now only known as an intermediate of the ammonia oxidation in cells, is released by AOB at all gravimetric water contents. This release is strongest during the drying-out phase of a culture suspension, which causes cell membrane damage and the release of internally accumulated NH_2OH. In the presence of water vapor, NH_2OH can react on surfaces to yield HONO. This heterogeneous reaction explains why HONO release occurs only at low soil water contents (<40 %), as only then sufficient particle surface is available. Although we cannot fully exclude soil as a source for NH_2OH, its flux from the soil into the atmosphere is likely to be of minor importance due to the efficient conversion of NH_2OH to HONO.

Materials and methods

Experimental details on the dynamic chamber setup, NH_2OH measurements, cultivation of bacteria, soil sampling and analysis, measurement of bacteria cultures and soil samples, as well as flux calculations can be found in the SI.

Acknowledgements

This project was funded by the Max Planck Society and the Max Planck Graduate Center with the Johannes Gutenberg-Universität Mainz (MPGC). We are grateful to M. Welling, T. Klüpfel, P. Stella and E. Fries for supporting the experiments. We thank E. Spieck from the University of Hamburg for providing the cultures of nitrite-oxidizing bacteria and R. van Spanning for providing the mutant strains of *N. europaea*.

References

1. Galbally I & Roy C (1978) Loss of fixed nitrogen from soils by nitric oxide exhalation.
2. Arnold P (1954) Losses of nitrous oxide from soil. *J Soil Sci* 5(1):116-128.
3. Meixner F & Yang W (2006) Biogenic Emissions of Nitric Oxide and Nitrous Oxide from Arid and Semi-arid Land. *Dryland Ecohydrology*, eds D'Odorico P & Porporato A (Springer Netherlands), pp 233-255.
4. Knowles R (1982) Denitrification. *Microbiology and Molecular Biology Reviews* 46(1):43-70.
5. Braker G & Conrad R (2011) Diversity, Structure, and Size of N_2O-Producing Microbial Communities in Soils-What Matters for Their Functioning? *Adv Appl Microbiol* 75:33-70.
6. Koops H-P, Purkhold U, Pommerening-Röser A, Timmermann G, & Wagner M (2006) The lithoautotrophic ammonia-oxidizing bacteria. *The prokaryotes* 5:778-811.
7. Stahl DA & de la Torre JR (2012) Physiology and Diversity of Ammonia-Oxidizing Archaea. *Annu Rev Microbiol* 66:83-101.
8. Spieck E & Lipski A (2011) Cultivation, Growth Physiology, and Chemotaxonomy of Nitrite-Oxidizing Bacteria. *Methods in Enzymology: Research on Nitrification and Related Processes, Vol 486, Part A* 486:109-130.
9. Bollmann A & Conrad R (1998) Influence of O_2 availability on NO and N_2O release by nitrification and denitrification in soils. *Global Change Biology* 4(4):387-396.
10. Placella SA & Firestone MK (2013) Transcriptional Response of Nitrifying Communities to Wetting of Dry Soil. *Appl. Environ. Microbiol.* 79(10):3294-3302.
11. Lipschultz F, *et al.* (1981) Production of NO and N_2O by soil nitrifying bacteria. *Nature* 294(5842):641-643.
12. Freitag A & Bock E (1990) Energy conservation in *Nitrobacter*. *Fems Microbiology Letters* 66(1-3):157-162.
13. Oswald R, *et al.* (2013) HONO Emissions from Soil Bacteria as a Major Source of Atmospheric Reactive Nitrogen. *Science* 341(6151):1233-1235.

14. Su H, *et al.* (2011) Soil nitrite as a source of atmospheric HONO and OH radicals. *Science* 333(6049):1616-1618.
15. Crutzen PJ & Lelieveld J (2001) Human impacts on atmospheric chemisty. *Annu Rev Earth Pl Sc* 29:17-45.
16. Solomon S (2007) *Climate change 2007-the physical science basis: Working group I contribution to the fourth assessment report of the IPCC* (Cambridge University Press).
17. Lees H (1952) Hydroxylamine as an Intermediate in Nitrification. *Nature* 169(4291):156-157.
18. Bremner JM, Blackmer AM, & Waring SA (1980) Formation of nitrous oxide and dinitrogen by chemical decomposition of hydroxylamine in soils. *Soil Biology and Biochemistry* 12(3):263-269.
19. Andersson KK & Hooper AB (1983) O_2 and H_2O are each the source of one O in NO_2^- produced from NH_3 by Nitrosomonas: ^{15}N-NMR evidence. *Febs Lett* 164(2):236-240.
20. Hooper AB & Terry KR (1979) Hydroxylamine oxidoreductase of *Nitrosomonas*: Production of nitric oxide from hydroxylamine. *Biochimica et Biophysica Acta (BBA) - Enzymology* 571(1):12-20.
21. Remde A & Conrad R (1990) Production of Nitric-Oxide in *Nitrosomonas europaea* by Reduction of Nitrite. *Arch Microbiol* 154(2):187-191.
22. Abeliovich A & Vonshak A (1992) Anaerobic Metabolism of *Nitrosomonas Europaea*. *Arch Microbiol* 158(4):267-270.
23. Casciotti KL & Ward BB (2001) Dissimilatory Nitrite Reductase Genes from Autotrophic Ammonia-Oxidizing Bacteria. *Appl. Environ. Microbiol.* 67(5):2213-2221.
24. Schmidt I, van Spanning RJM, & Jetten MSM (2004) Denitrification and ammonia oxidation by *Nitrosomonas europaea* wild-type, and NirK- and NorB-deficient mutants. *Microbiol-Sgm* 150:4107-4114.
25. Breuninger C, Oswald R, Kesselmeier J, & Meixner FX (2012) The dynamic chamber method: trace gas exchange fluxes (NO, NO_2, O_3) between plants and the atmosphere in the laboratory and in the field. *Atmos Meas Tech* 5(5):955-989.
26. Behrendt T, *et al.* (2014) Characterisation of NO production and consumption: new insights by an improved laboratory dynamic chamber technique. *Biogeosciences Discuss.* 11(1):1187-1275.
27. Krümmel A & Harms H (1982) Effect of organic matter on growth and cell yield of ammonia-oxidizing bacteria. *Arch Microbiol* 133(1):50-54.
28. Belser LW & Schmidt EL (1980) Growth and Oxidation-Kinetics of 3 Genera of Ammonia Oxidizing Nitrifiers. *Fems Microbiology Letters* 7(3):213-216.
29. Koops HP & Pommerening-Roser A (2001) Distribution and ecophysiology of the nitrifying bacteria emphasizing cultured species. *FEMS Microbiology Ecology* 37(1):1-9.
30. Zakir HAKM, *et al.* (2008) Detection, isolation and characterization of a root-exuded compound, methyl 3-(4-hydroxyphenyl) propionate, responsible for biological nitrification inhibition by sorghum (*Sorghum bicolor*). *New Phytol* 180(2):442-451.
31. Belser LW & Mays EL (1980) Specific-Inhibition of Nitrite Oxidation by Chlorate and Its Use in Assessing Nitrification in Soils and Sediments. *Appl. Environ. Microbiol.* 39(3):505-510.
32. Stromberger ME, Klose S, Ajwa H, Trout T, & Fennimore S (2005) Microbial Populations and Enzyme Activities in Soils Fumigated with Methyl Bromide Alternatives. *Soil Sci. Soc. Am. J.* 69(6):1987-1999.

33. Beaumont HJE, *et al.* (2002) Nitrite reductase of *Nitrosomonas europaea* is not essential for production of gaseous nitrogen oxides and confers tolerance to nitrite. *J Bacteriol* 184(9):2557-+.
34. Beaumont HJE, van Schooten B, Lens SI, Westerhoff HV, & van Spanning RJM (2004) *Nitrosomonas europaea* expresses a nitric oxide reductase during nitrification. *J Bacteriol* 186(13):4417-4421.
35. Hollocher TC, Kumar S, & Nicholas DJD (1982) Respiration-Dependent Proton Translocation in *Nitrosomonas europaea* and Its Apparent Absence in *Nitrobacter agilis* during Inorganic Oxidations. *J Bacteriol* 149(3):1013-1020.
36. Kumar S & Nicholas DJD (1983) Proton Electrochemical Gradients in Washed Cells of *Nitrosomonas europaea* and *Nitrobacter agilis*. *J Bacteriol* 154(1):65-71.
37. Hughes MN & Nicklin HG (1971) Autoxidation of hydroxylamine in alkaline solutions. *Journal of the Chemical Society A: Inorganic, Physical, Theoretical* 0(0):164-168.
38. Schmidt I, Look C, Bock E, & Jetten MSM (2004) Ammonium and hydroxylamine uptake and accumulation in *Nitrosomonas*. *Microbiology+* 150(5):1405-1412.
39. Ndour M, *et al.* (2008) Photoenhanced uptake of NO_2 on mineral dust: Laboratory experiments and model simulations. *Geophysical Research Letters* 35(5).
40. Kebede MA, Scharko NK, Appelt LE, & Raff JD (2013) Formation of Nitrous Acid during Ammonia Photooxidation on TiO_2 under Atmospherically Relevant Conditions. *J Phys Chem Lett* 4(16):2618-2623.

Supporting Information

Title: Hydroxylamine released by ammonia-oxidizing bacteria as precursor for HONO emission from soils

Authors: M. Ermel[1,2], T. Behrendt[1,3], R. Oswald[1], B. Derstroff[4], D. Wu[1,5], S. Hohlmann[1], C. Stönner[4], A. Pommerening-Röser[6], J. Williams[4], F. X. Meixner[1], M. O. Andreae[1], M. Sörgel[1]* and I. Trebs[1#]

Author Affiliations:

[1] Biogeochemistry Department, Max Planck Institute for Chemistry, P.O. Box 3060, 55020 Mainz, Germany

[2] Institute for Inorganic and Analytical Chemistry, Johannes Gutenberg University Mainz, 55128 Mainz, Germany

[3] Multiphase Chemistry Department, Max Planck Institute for Chemistry, P.O. Box 3060, 55020 Mainz, Germany

[4] Atmospheric Chemistry Department, Max Planck Institute for Chemistry, P.O. Box 3060, 55020 Mainz, Germany

[5] Key Laboratory of Agricultural Water Research, Center for Agricultural Resources Research, Institute of Genetic and Developmental Biology, The Chinese Academy of Sciences, 050021 Shijiazhuang, China

[6] Department of Microbiology and Biotechnology, University of Hamburg, Hamburg, Germany

[#]now at: Centre de Recherche Public - Gabriel Lippmann, Department Environment and Agro-biotechnologies, 41 rue du Brill, L-4422 Belvaux, Luxembourg

Corresponding Author: Matthias Sörgel (Max Planck Institute for Chemistry, P.O. Box 3060, 55020 Mainz, m.soergel@mpic.de, +4961313056401)

Materials and methods

Dynamic chamber setup. A chamber made of Teflon (FEP) foil with a volume of 0.008 m^3 was flushed with purified dry air at a flow rate of $1 \cdot 10^{-4}$ m^3 s^{-1} (Figure S1). The air supplied to the chamber first passed through a membrane dryer combined with a filter for compressed air (Clearpoint and Drypoint M from BEKO Deutschland GmbH, Germany). In the second step, any HONO present was photolyzed to NO and OH with a UV lamp (OG-1, Ultra-Violet Products Ltd, USA). A pure air generator (PAG 003, ECOPHYSICS, Switzerland) further purified the air of HONO, nitrogen oxides (NO_x = NO + NO_2), ozone (O_3), hydrocarbons and water vapor. To prevent any reactive nitrogen trace gases from entering the system, a cartridge filled with Purafill (Headline Filters, Germany) completed the purification. To ensure sterile conditions, the chamber inlet was equipped with a sterile air filter (MILEX®-FG Vent Filter 0.2 µm, 50 mm diameter, Millipore, France). NO_x was measured at the outlet of the chamber by a chemiluminescence analyzer (CLD 780TR, ECOPHYSICS, Switzerland, $LOD_{NO} \approx 35$ ppt and $LOD_{NO2} \approx 120$ ppt). A UV-absorption analyzer (Model 49i, Thermo Electron Corporation, USA; LOD ≈ 0.5 pbb) was used to measure O_3. The water vapor difference between the inlet and outlet of the chamber was determined with an infrared gas analyzer (LI-7000, Li-Cor Biosciences GmbH, Germany). A long path absorption photometer (LOPAP) (QUMA Elektronik & Analytik GmbH, Germany; limit of detection (LOD) ≈ 5 ppt) (1) was connected directly to the chamber to measure HONO. The chamber and the LOPAP sampling unit were placed in a temperature controlled cabinet. Data were acquired by a CR3000 Datalogger (Campbell Scientific, Inc., USA) every 60 s.

NH_2OH measurements. Gaseous hydroxylamine (NH_2OH) was measured using a commercial PTR-TOF-MS (Proton Transfer Reaction Time of Flight Mass Spectrometer, Ionicon Analytik GmbH, Innsbruck, Austria) (2). The measurement technique is based on the protonation of molecules with a proton affinity higher than water by H_3O^+ ions that are generated in a hollow cathode discharge. NH_2OH has a proton affinity of 803 kJ mol^{-1} (3), while the value for water is 691 kJ mol^{-1} (4). All protonated molecular ions are accelerated by an electrical field to the same kinetic energy such that the resultant velocity of the ions depends on the mass-to-charge ratio. Hence, the time-of-flight is used to measure the velocity, from which the mass-to-charge ratio can be determined (5). The mass resolution was approximately 3700 m/Δm and NH_2OH was measured at mass 34.029. It should be noted that the ^{13}C isotope of methanol at mass 34.037, which represents 1 % of the methanol signal, can

potentially interfere ambient measurements. For the pure culture experiments, NH_2OH was in large excess over methanol. The instrument was operated with a drift pressure of 2.20 hPa (E/N 140 Td) and a drift voltage of 600 V. For mass calibration, 1,3,5- trichlorobenzene was used as internal standard. Data post-processing and analysis was performed by using the program "PTR-TOF DATA ANALYZER", which is described elsewhere (6). NH_2OH measurements were made with the chamber system described by Behrendt, *et al.* (7). The same inlet tube length was used for calibration and measurement in order to minimize the effect of wall losses. The instrument was calibrated for gas phase NH_2OH using a custom sublimation unit with NH_2OH purified by the method of Chang et al.(8). NH_2OH was exposed to a nitrogen gas flow and the concentration was determined gravimetrically. The PTR-TOF-MS was calibrated with a NH_2OH mixing ratio of 893.8 ppb. Since the measured mixing ratios of NH_2OH were lower (0-230 ppb) than the single-point calibration value, we assume a systematic error of 30 %, in contrast to compounds calibrated with pressurized gas standards, which typically have an overall uncertainty of about 10 %. The calculated detection limit (3σ of the noise) was about 15 ppt. For the surface reaction experiment with glass beads, the gas flow from the NH_2OH source (745 ppb) was diluted with humidified air (12.5 mmol mol^{-1} H_2O) to a mixing ratio of 207 ppb NH_2OH and directly passed through a cartridge with the glass beads. HONO produced from other wall reactions was subtracted as background signal.

The measurement of NH_2OH by any technique that requires tubing connections is challenging, because this molecule has a high affinity to adsorb on tubing walls due to its polarity. The possibility that the maximum $F(NH_2OH)$ observed in Fig. 7 might have been related to a desorption of NH_2OH from the tubing, caused by the decreasing humidity, could be ruled out, since similarly soluble molecules, e.g., methanol, did not show such effects.

Cultivation of bacteria. Ammonia-oxidizing bacteria were cultivated according to Krümmel and Harms (9) in a culture suspension containing 10 mM NH_4^+. The purity of the cultures was checked microscopically and by the use of a nutrient broth test (Standard 1 nutrient broth, Merck KGaA, Germany) to ensure that the cultures were free of heterotrophic contaminants (10). The AOB *Nitrosomonas communis* (Nm2) (11), *Nitrosomonas europaea* (Nm50, ATCC 25978) (12) , *Nitrosomonas nitrosa* (Nm90) (11), *Nitrosomonas ureae* (Nm10) (11), and *Nitrosolobus multiformis* (Nl13) (13), and the NOB *Nitrobacter winogradskyi* (« Engel »), *Nitrospira defluvii* (A17), and *Nitrospira moscoviensis* (M) were used in this study.

Soil sampling and analysis. The soil sample from the wheat field (Mainz-Finthen, Germany, 49.97°N, 8.16°E) (14) was taken from the uppermost soil layer (5 cm). The sample was dried at 40 °C for 24 hours, sieved to 2 mm, and stored at 4 °C in open plastic bags before measurement.

Measurement of bacteria and soil samples. All samples were prepared in petri dishes (100 x 20 mm, Duran Group, Germany) with 50 g of either soil sample or glass beads (0.25 – 0.50 mm diameter, Carl Roth, Germany) (14). For NH_2OH measurements a smaller petri dish (50 x 20 mm, Duran Group, Germany) with 12 g of glass beads and soil, respectively, was used. The soil samples were wetted with purified water to reach water holding capacity (WHC), see Behrendt et al. (7). The sample was subsequently placed into the dynamic chamber. For the inhibition experiments either potassium chlorate (1.3 g l^{-1}; ≥ 99%, Carl Roth, Germany) or methyl 3-(4-hydroxyphenyl) propionate (2.0 mg l^{-1}, 97%, Sigma-Aldrich, Germany) were added to the purified water.

For bacteria culture samples, the glass beads and glass bowl were sterilized by washing with 70 % ethanol (absolute for analysis, Merck, Germany). Sterility of the setup was checked by an ATP assay on a sample of sterile AOB nutrient solution. Bacteria culture suspension or sterile culture solution was added to the glass beads to reach whc and the sample was subsequently placed into the dynamic chamber. Prior to the measurement, the cell density of the culture was measured using an ATP kit (BacTiterGlo, PROMEGA GmbH, Germany) and a luminometer (GloMax 20/20, PROMEGA GmbH, Germany). The NO_2^- concentration in the culture suspension was measured according to ISO/TS 14256-1. NH_2OH in the culture suspension was oxidized with iodate to NO_2^- by the method of Afkhami, Madrakian and Maleki (15). NO_2^- from this reaction was also determined according to ISO/TS 14256-1. The difference between the NO_2^- concentration before and after the iodate addition equals the NH_2OH concentration. The ammonium availability per AOB cell $a_{cell}(NH_4^+)$ was calculated as follows:

$$a_{hyp,cell}(NH_4^+) = \frac{c_{init}(NH_4^+) - c_{meas}(NO_2^-)}{c(Bact) \cdot V_{cult}} \quad (1)$$

with the initial NH_4^+ concentration of the culture suspension, $c_{init}(NH_4^+)$ in mmol l^{-1}, the measured NO_2^- concentration, $c_{meas}(NO_2^-)$, in mmol l^{-1}, the volume of the culture suspension, V_{cult}, in l^{-1}, the number of bacteria per volume, c(Bact) in cells l^{-1}. The error was calculated according to Gaussian error propagation.

Flux calculations. HONO, NH_2OH and NO fluxes were calculated according to the following formula:

$$F = \frac{Q}{A \cdot V_m} \cdot (\chi_{out} - \chi_{in}) \quad (2)$$

where F is the flux of trace gas in nmol m^{-2} s^{-1}, Q is the purging flow rate in m^3 s^{-1}, A is the area of soil in m^2, V_m is the molar volume of air in m^3 mol^{-1}, and χ_{out} and χ_{in} are the headspace mixing ratios at the outlet and inlet of the chamber, respectively, in ppb.

The error of F was calculated as follows:

$$\Delta F = \pm \sqrt{\left(\left[\left(\frac{\partial F}{\partial Q} \right)_{A,\chi_{in/out}} \cdot \Delta Q \right]^2 + \left[\left(\frac{\partial F}{\partial A} \right)_{Q,\chi_{in/out}} \cdot \Delta A \right]^2 + \left[\left(\frac{\partial F}{\partial \chi} \right)_{A,Q,\chi_{in}} \cdot \Delta \chi_{out} \right]^2 + \left[\left(\frac{\partial F}{\partial \chi} \right)_{A,Q,\chi_{out}} \cdot \Delta \chi_{in} \right]^2 \right)} \quad (3)$$

The error of V_m was neglected. The error of A was assumed to result from a 1 mm uncertainty of the dish radius. The noise (3σ) of the measured flow rate was used to estimate ΔQ. The error of χ_{in} was set to the limit of detection of the instruments. For the error of χ_{out} of HONO, an additional uncertainty of 10 % of the absolute value was added to the limit of detection. For the other species the error of χ_{out} was derived as for χ_{in}.

Supporting Figures

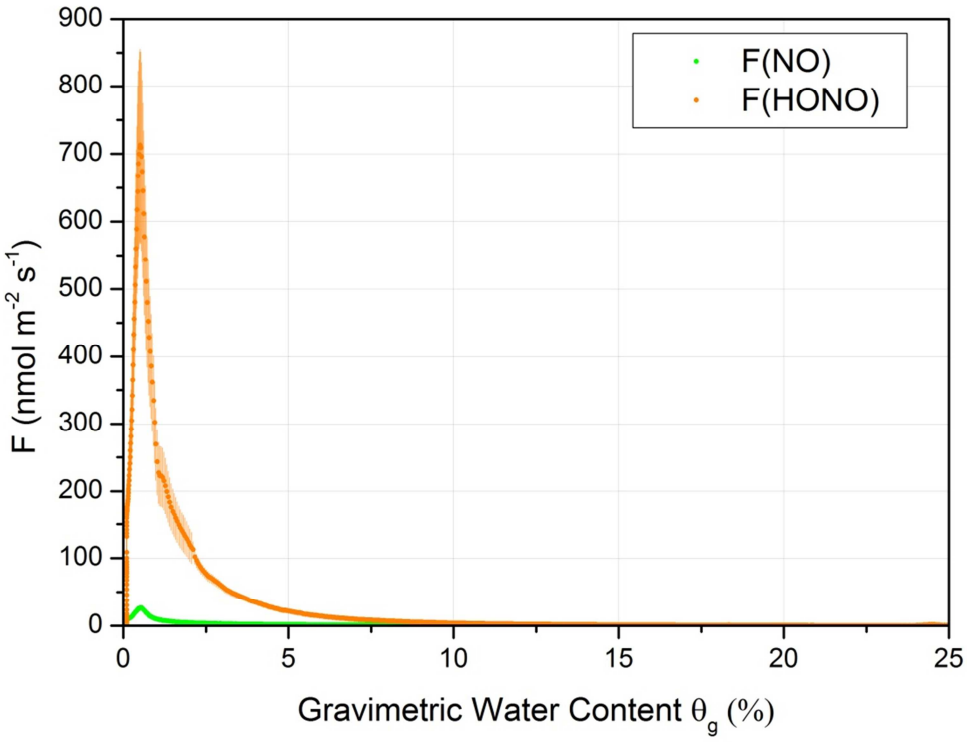

Figure S1: F(HONO) and F(NO) of a pure culture experiment as a function of the gravimetric water content θ_g. The experiment starts under wet conditions at high Θ on the right hand side and proceeds to low θ_g during the drying out on the left hand side.

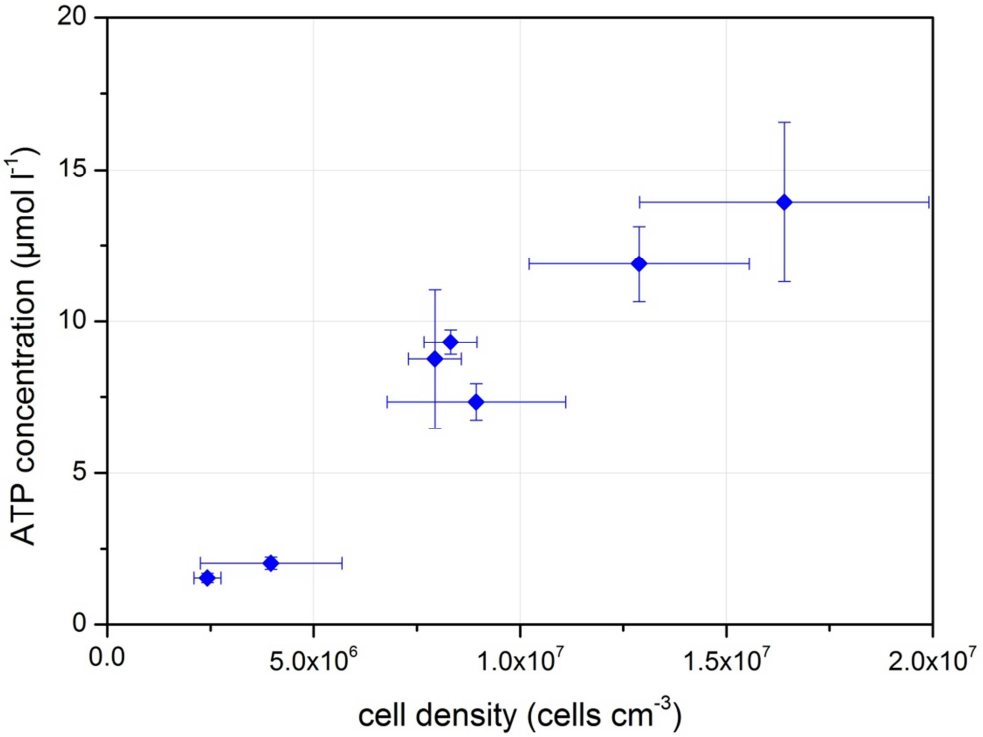

Figure S2: The ATP concentration of a culture as a function of the microscopically determined cell density. Error bars denote standard deviations (n=3).

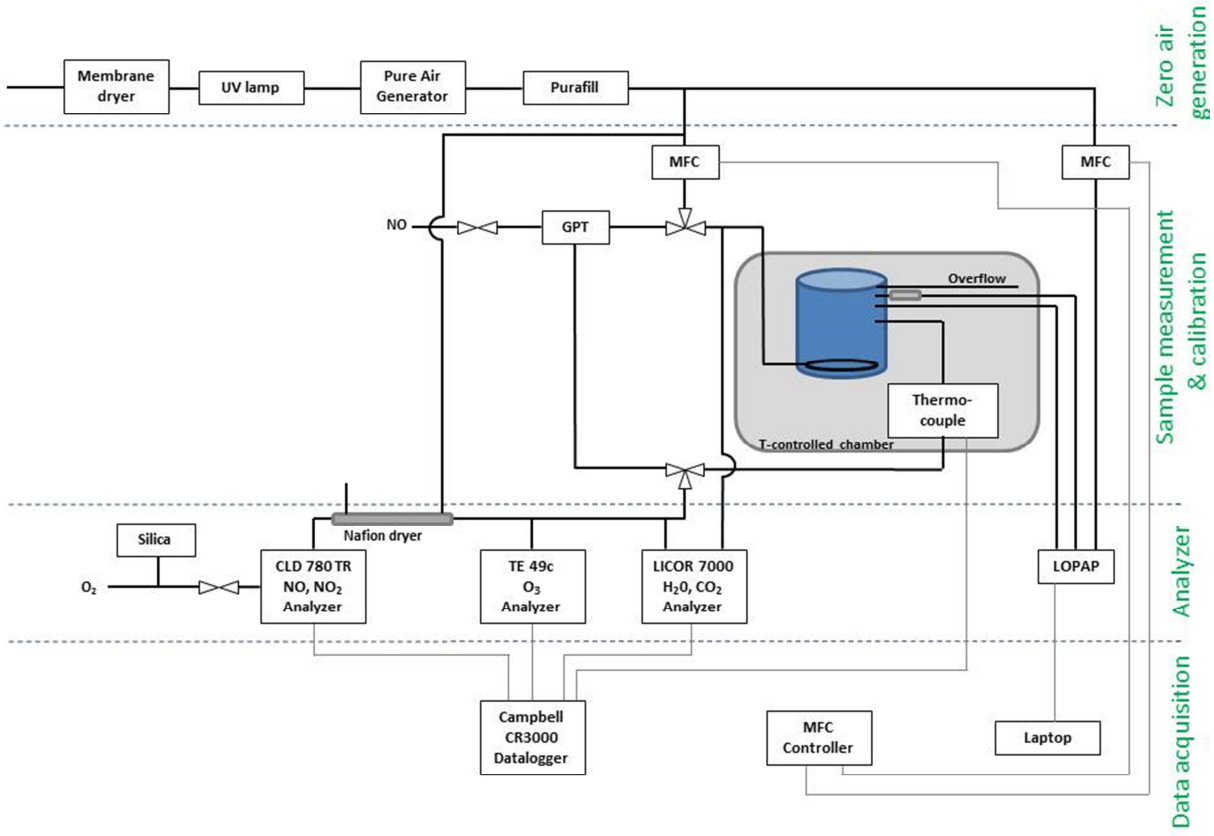

Figure S3: Schematic overview of the setup used to measure F(HONO) and F(NO). It can be separated into zero air generation, measurement and calibration, analyzer and data acquisition.

References

1. Kleffmann J, Heland J, Kurtenbach R, Lorzer J, & Wiesen P (2002) A new instrument (LOPAP) for the detection of nitrous acid (HONO). *Environ Sci Pollut R*:48-54.
2. Graus M, Müller M, & Hansel A (2010) High resolution PTR-TOF: quantification and formula confirmation of VOC in real time. *J Am Soc Mass Spectr* 21(6):1037-1044.
3. Jolly WL (1991) *Modern inorganic chemistry* (McGraw-Hill New York).
4. Linstrom PJM, W.G. (2009) NIST Chemistry WebBook, Linstrom, NIST Standard Reference Database Number 69. ed Linstrom PJM, W.G. (National Institute of Standards and Technology, Gaithersburg MD, 20899, http://webbook.nist.gov).
5. Williams J (2006) Mass spectrometric methods for atmospheric trace gases. *Analytical Techniques for Atmospheric Measurement*:229.
6. Müller M, Mikoviny T, Jud W, D'Anna B, & Wisthaler A (2013) A new software tool for the analysis of high resolution PTR-TOF mass spectra. *Chemometrics and Intelligent Laboratory Systems* 127:158-165.
7. Behrendt T*, et al.* (2014) Characterisation of NO production and consumption: new insights by an improved laboratory dynamic chamber technique. *Biogeosciences Discuss.* 11(1):1187-1275.

8. Chang Y*, et al.* (2014) Paper-like N-doped graphene films prepared by hydroxylamine diffusion induced assembly and their ultrahigh-rate capacitive properties. *Electrochim Acta* 115(0):461-470.
9. Krümmel A & Harms H (1982) Effect of organic matter on growth and cell yield of ammonia-oxidizing bacteria. *Arch Microbiol* 133(1):50-54.
10. Koops HP, Harms H, & Wehrmann H (1976) Isolation of a Moderate Halophilic Ammonia-Oxidizing Bacterium, *Nitrosococcus mobilis Nov Sp*. *Arch Microbiol* 107(3):277-282.
11. Koops HP, Bottcher B, Moller UC, Pommerening-Röser A, & Stehr G (1991) Classification of 8 New Species of Ammonia-Oxidizing Bacteria - *Nitrosomonas communis Sp nov*, *Nitrosomonas ureae Sp nov*, *Nitrosomonas aestuarii Sp nov*, *Nitrosomonas marina Sp nov*, *Nitrosomonas nitrosa Sp nov*, *Nitrosomonas eutropha Sp nov*, *Nitrosomonas oligotropha Sp nov* and *Nitrosomonas halophila Sp nov*. *J Gen Microbiol* 137:1689-1699.
12. Watson SW (1971) Taxonomic considerations of the family Nitrobacteraceae Buchanan requests for opinions. *Int J Syst Bacteriol* 21(3):254-270.
13. Watson SW, Graham LB, Remsen CC, & Valois FW (1971) Lobular, Ammonia-Oxidizing Bacterium, *Nitrosolobus multiformis Nov Gen Nov Sp*. *Arch Mikrobiol* 76(3):183-&.
14. Oswald R*, et al.* (2013) HONO Emissions from Soil Bacteria as a Major Source of Atmospheric Reactive Nitrogen. *Science* 341(6151):1233-1235.
15. Afkhami A, Madrakian T, & Maleki A (2006) Indirect Kinetic Spectrophotometric Determination of Hydroxylamine Based on Its Reaction with Iodate. *Anal Sci* 22(2):329-331.

B3. Wu et al, ES&T, 2014

A novel method to measure isotopic labeled gas-phase nitrous acid (HO15NO) in biogeochemical studies

Authors: D. Wu,[†,‡,@] C. J. Kampf,[§] U. Pöschl,[§] R. Oswald,[†,X] J. Cui,[∥,⊥] M. Ermel,[†,X] C. Hu,[‡] I. Trebs,[†,#] M. Sörgel[†]

† Biogeochemistry Department, Max Plank Institute for Chemistry, P. O. Box 3060, 55020 Mainz, Germany
‡ Key Laboratory of Agricultural Water Research, Center for Agricultural Resources Research, Institute of Genetic and Developmental Biology, The Chinese Academy of Sciences, 050021 Shijiazhuang, China
§ Multiphase Chemistry Department, Max Plank Institute for Chemistry, P. O. Box 3060, 55020 Mainz, Germany
∥ UCD School of Biosystems Engineering, University College Dublin, Dublin 4, Ireland
⊥ Institute of Mountain Hazards and Environment, The Chinese Academy of Sciences, 610041 Chengdu, China
@ University of the Chinese Academy of Sciences, 100049 Beijing, China
X Institute for Inorganic and Analytical Chemistry, Johannes Gutenberg University Mainz, 55128 Mainz, Germany
Now at: Centre de Recherche Public - Gabriel Lippmann, Department Environment and Agro-biotechnologies, 41 rue du Brill, L-4422 Belvaux, Luxembourg

Environmental Science & Technology

Article

pubs.acs.org/est

Novel Tracer Method To Measure Isotopic Labeled Gas-Phase Nitrous Acid ($HO^{15}NO$) in Biogeochemical Studies

Dianming Wu,*[,†,‡,▲] Christopher J. Kampf,*[,§] Ulrich Pöschl,[§] Robert Oswald,[†,△] Junfang Cui,[∥,⊥] Michael Ermel,[†,△] Chunsheng Hu,[‡] Ivonne Trebs,[†,#] and Matthias Sörgel[†]

[†]Biogeochemistry Department, Max Plank Institute for Chemistry, P.O. Box 3060, 55020 Mainz, Germany

[‡]Key Laboratory of Agricultural Water Research, Center for Agricultural Resources Research, Institute of Genetic and Developmental Biology, The Chinese Academy of Sciences, 050021 Shijiazhuang, Hebei, China

[§]Multiphase Chemistry Department, Max Plank Institute for Chemistry, P.O. Box 3060, 55020 Mainz, Germany

[∥]UCD School of Biosystems Engineering, University College Dublin, Belfield, Dublin 4, Ireland

[⊥]Institute of Mountain Hazards and Environment, The Chinese Academy of Sciences, 610041 Chengdu, Sichuan, China

[▲]University of the Chinese Academy of Sciences, 100049 Beijing, China

[△]Institute for Inorganic and Analytical Chemistry, Johannes Gutenberg University Mainz, 55128 Mainz, Germany

Supporting Information

ABSTRACT: Gaseous nitrous acid (HONO), the protonated form of nitrite, contributes up to ~60% to the primary formation of hydroxyl radical (OH), which is a key oxidant in the degradation of most air pollutants. Field measurements and modeling studies indicate a large unknown source of HONO during daytime. Here, we developed a new tracer method based on gas-phase stripping-derivatization coupled to liquid chromatography–mass spectrometry (LC-MS) to measure the ^{15}N relative exceedance, $\psi(^{15}N)$, of HONO in the gas-phase. Gaseous HONO is quantitatively collected and transferred to an azo dye, purified by solid phase extraction (SPE), and analyzed using high performance liquid chromatography coupled to mass spectrometry (HPLC-MS). In the optimal working range of $\psi(^{15}N) = 0.2–0.5$, the relative standard deviation of $\psi(^{15}N)$ is <4%. The optimum pH and solvents for extraction by SPE and potential interferences are discussed. The method was applied to measure $HO^{15}NO$ emissions from soil in a dynamic chamber with and without spiking ^{15}N labeled urea. The identification of $HO^{15}NO$ from soil with ^{15}N urea addition confirmed biogenic emissions of HONO from soil. The method enables a new approach of studying the formation pathways of HONO and its role for atmospheric chemistry (e.g., ozone formation) and environmental tracer studies on the formation and conversion of gaseous HONO or aqueous NO_2^- as part of the biogeochemical nitrogen cycle, e.g., in the investigation of fertilization effects on soil HONO emissions and microbiological conversion of NO_2^- in the hydrosphere.

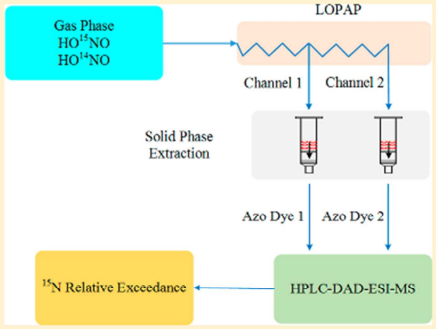

INTRODUCTION

In the lower atmosphere, nitrous acid (HONO) contributes up to ~60% to the primary formation of hydroxyl radical (OH), which is a key oxidant in the degradation of most air pollutants.[1−3] Upon reaction with tobacco smoke, HONO can also form carcinogens and is thus linked to health risks of indoor air pollution.[4]

During daytime, HONO undergoes rapid photolysis, and most field measurement and modeling studies indicate a large unknown source of HONO.[5−9] This unknown source has been tentatively attributed to photosensitized reduction of nitrogen dioxide on humic acid,[10] nitric acid photolysis on surfaces,[11] photolytically enhanced nitrogen dioxide (NO_2) conversion on the ground,[6] anion catalyzed NO_2 conversion,[12] or the photolysis of ortho-nitrophenols.[13] Another potential explanation is the release of HONO from biogenic soil nitrite.[14,15] Large quantities of HONO may be released from a chemical equilibrium of acid–base reaction and gas–liquid partitioning controlled by the temperature, water content, nitrite concentration, and pH of soil,[14] and soil ammonia-oxidizing bacteria (AOB) may release even more HONO than the chemical equilibrium.[16] Soil samples from arid and arable areas as well as peatlands were found to emit HONO in quantities comparable to the emissions of nitric oxide (NO).[16,17]

Several instruments based on spectroscopic methods, (e.g., refs 18–21) and wet chemistry methods have been developed to determine HONO mixing ratios in the atmosphere (e.g., refs

Received: March 19, 2014
Revised: June 16, 2014
Accepted: June 22, 2014
Published: June 23, 2014

   dx.doi.org/10.1021/es501353x | Environ. Sci. Technol. 2014, 48, 8021−8027

22−25). A very sensitive and reliable technique is the so-called Long Path Absorption Photometer (LOPAP).[26,27] HONO is sampled quantitatively by two stripping coils in series with an efficiency of about 98% in the first coil due to a fast reaction forming the diazonium ion which is the precursor of the azo dye. Hence, potential interferences by species that are not quantitatively removed in the first coil can be detected by the signal from the second coil, and measured values are subsequently corrected for. The instrument measures the light absorption by the azo dye which is formed through the derivatization of HONO by sulfanilamide (SA) and N-(1-naphthyl)-ethylenediamine dihydrochloride (NED), which are Griess type reagents previously used in the analysis of nitrogen dioxide.[28] A similar technique of coil sampling is used to detect the derivated HONO by high performance liquid chromatography (HPLC).[25,29]

The stable nitrogen isotope ^{15}N has been widely used to study biogeochemical N transformation processes in ecosystems.[30−32] ^{15}N labeled nitrite and nitrate were measured by different methods and instruments, e.g., in biological fluids by gas chromatography−mass spectrometry (GC-MS),[33] in seawater by continuous flow isotope ratio mass spectrometry (CF-IRMS),[34] and in various aqueous samples by the sample preparation unit for inorganic nitrogen and mass spectrometer (SPINMAS) technique.[35] The ^{15}N in nitrogen gases, like NO, NO_2, nitrous oxide (N_2O), and nitrogen (N_2), were also determined in a number of studies (e.g., refs 36−39).

However, due to the reactivity, solubility, and low mixing ratios of HONO in the atmosphere, up to now a method to measure the ^{15}N isotope ratio of HONO ([$HO^{15}NO$]/[$HO^{14}NO$]) is lacking. In this work, we present a new method (gas-phase stripping-derivatization coupled to liquid chromatography−mass spectrometry (LC-MS), LOPAP-HPLC-MS) to determine the ^{15}N relative exceedance ($\psi(^{15}N)$, see ref 40) of the HONO in the gas-phase. The principle of this method is to convert $HO^{15}NO$ to the corresponding ^{15}N azo dye through a Griess reaction during LOPAP analysis and subsequent isotope ratio measurement by HPLC-MS.

EXPERIMENTAL SECTION

Gas Sampling. Gaseous HONO was sampled and analyzed using a commercial LOPAP instrument (LOPAP-03, QUMA Elektronik & Analytik, Germany), which was described in detail previously (see ref 23). Briefly, the HONO from the sample gas flow was quantitatively and continuously sampled into the acidic SA solution and immediately converted to a diazonium ion inside a two channel stripping coil (channel 1: HONO absorption channel; and channel 2: reference channel). The SA solution (58 mM SA in 1 M hydrochloric acid) was pumped continuously to the stripping coil and, after stripping HONO, flushed back to the instrument where it was mixed with 0.39 mM NED to form the azo dye (see the following reaction of the $HO^{15}NO$ derivatization):

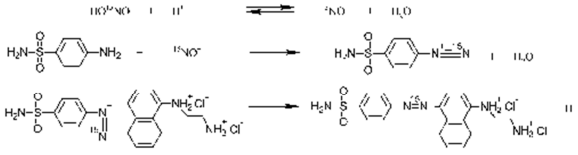

To determine the HONO gas-phase concentrations the dye solutions are passed through a 2−3 m long Teflon AF tubing, a so-called liquid core waveguide, which acts as an absorption cell. The solutions from channels 1 and 2 were collected separately in 5 mL volumetric flasks after the photometric measurement and used for the subsequent analysis of the $\psi(^{15}N)$ of the HONO produced by the experiments.

Sample Purification. The azo dye solution, which was collected from the LOPAP instrument, was purified by reversed-phase solid phase extraction (SPE, DSC-18, Sigma-Aldrich, USA). The following procedure was applied: 1) the pH of the azo dye solution was adjusted to ∼5.5 (the color of the solution changed from red to pink) using 1 M NaOH (VWR International, Germany); 2) the solution was diluted to 20 mL using ultrapure water (18.2 MΩ·cm water, PURELAB Option-Q, ELGA LabWater, UK); 3) preconditioning of the SPE column with 2 mL of acetonitrile (HPLC gradient grade, Carl Roth, Germany) and 2 mL of ultrapure water; 4) extraction of the sample solution (one drop per 2 to 3 s); 5) washing of the extracted sample material using 2 mL of ultrapure water (removal of inorganic ions); and 6) elution of the azo dye from the SPE column using 35/65 (v/v) of acetonitrile (ACN)/0.1% (v/v) trifluoroacetic acid in water (TFA, for liquid chromatography, Merck, Germany) into a 2 mL volumetric flask.

HPLC-MS Analysis. The extracted azo dye samples were analyzed by HPLC-DAD-ESI-MS (Agilent Technologies 1200 series, Agilent technologies, USA). The system consisted of a binary pump (G1379B), autosampler with thermostat (G1330B), column thermostat (G1316B), photodiode array detector (DAD; G1315C), and electrospray ionization quadrupole mass spectrometer (ESI-MS, G6130B). Chemstation software (Rev. B.03.02, Agilent technologies, USA) was used for system control and data analysis. A reversed-phase analytical column (Agilent XDB-C18, 50 mm × 4.6 mm inner diameter, 1.8 μm particle size, Agilent Technologies, USA) was used for chromatographic separation. Eluents were 0.1% TFA in water (Eluent A) and ACN (Eluent B). Gradient elution was applied at a flow rate of 500 μL min^{-1}. For each chromatographic run, the solvent gradient started with 25% B for 1 min followed by a linear gradient to 90% B within 3.5 min, holding this composition for another 3.5 min, flushing back to 3% B within 1 min, and column re-equilibration for 6 min before the next run. The injection volume was 20−80 μL during the method development, and 80 μL was used for soil experiment sample analysis. Each chromatographic run was repeated three times. The acquired wavelength range was 200−800 nm for DAD detection. Detection and reference wavelengths for azo dye analysis were 540 and 700 nm with bandwidths of 10 and 60 nm, respectively. The ESI-MS instrument was operated in the positive ionization mode (ESI+) with an ionization voltage of 1750 V and a fragmentor voltage of 175 V at a dry gas temperature of 300 °C. MS spectra were recorded in scan mode (m/z 50−500) and single ion monitoring mode (m/z 370.1, 371.1, 372.1, and 373.1).

Calibration. The azo dye concentration and the $\psi(^{15}N)$ in the azo dye samples were calibrated using the DAD and MS detectors, respectively. Aqueous sodium nitrite standard solution (Carl Roth, Germany) was used to prepare the azo dye concentration calibration curve. A series of nitrite working standard solutions containing 0 to 18.1 μM sodium nitrite were prepared before use from a 14.5 mM sodium nitrite standard, which was stored at 4 °C. Five mL of the working solutions were mixed with equal amounts of 58 mM SA in 1 M hydrochloric acid and additional 5 mL of 0.39 mM NED to form the azo dye calibration solutions. Unlabeled and ^{15}N labeled sodium nitrite (98%+, Cambridge Isotope Laboratories,

dx.doi.org/10.1021/es501353x | Environ. Sci. Technol. 2014, 48, 8021−8027

USA) solutions of the same concentration were mixed together in varying ratios and processed as mentioned before to obtain the $\psi(^{15}N)$ calibration standards. The sample purification and analysis were carried out as described above.

^{15}N Relative Exceedance Calculation. The $\psi(^{15}N)$ of the azo dye was calculated according to refs 33 and 41. Due to the natural isotope distribution of the unlabeled azo dye (M ($C_{18}H_{19}O_2N_5S$) = 369.1 g mol^{-1}), the ESI+ mass spectra include the protonated molecular ions ($[M + H]^+$, *M*) *M + 0*, *M + 1*, *M + 2*, and *M + 3*. Unlabeled azo dye working standards were used to analyze the isotope distributions at different azo dye concentrations. The ratio of the *M + 1*, *M + 2*, and *M + 3* ions for a given azo dye concentration was found to show slight daily variations, likely due to small fluctuations of the conditions in the ion source. Peak areas (mAU) of the extracted ion chromatograms (EIC) for *m/z* 370, *m/z* 371, *m/z* 372, and *m/z* 373 were used to calculate the normalized signal ratios of unlabeled azo dye standards shown in Table 1.

Table 1. Normalized Isotope Distribution of the Unlabeled Azo Dye

parameter	value			
ion monitored (*m/z*)	370	371	372	373
mass	*M*	*M + 1*	*M + 2*	*M + 3*
intensity	1.00	0.244[a]	0.072[a]	0.011[a]

[a]Average data obtained from different azo dye concentrations.

Since the liquid-chromatographic separation represents an isotope fractionation process, it is important to take into account the whole peak area of the EICs of interest for the analysis of isotope distributions by HPLC-MS.[42]

Using the values from Table 1, the $\psi(^{15}N)$ is calculated according to Green et al. (1982)[33] as

$$\psi(^{15}N) = \frac{^{371}AD - 0.244\,^{370}AD}{^{370}AD + {}^{371}AD - 0.244\,^{370}AD + 0.072\,^{370}AD + 0.011\,^{370}AD} \quad (1)$$

where ^{370}AD and ^{371}AD are the peak areas of the EICs for *m/z* 370 and *m/z* 371, respectively.

This is simplified to

$$\psi(^{15}N) = \frac{R - 0.244}{R + 0.839} \quad (2)$$

where $R = (^{371}AD)/(^{370}AD)$, and ^{370}AD and ^{371}AD are the peak areas of the EICs for *m/z* 370 and *m/z* 371, respectively.

Soil Experiments. The method was applied for the $\psi(^{15}N)$ analysis of HONO emissions from soil samples spiked with ^{15}N labeled urea ($CO(^{15}NH_2)_2$, 98%+, Cambridge Isotope Laboratories, USA). Soil samples were collected from a long-term tillage field (winter wheat and summer corn rotation) in Lyons Estate (53°18′32.85″N, 60°32′31.62″W), Co. Kildare, Ireland. The soil was a clay loam (sand 30.4%, silt 39.7%, clay 29.9%; bulk density 1.47 g cm^{-3}; total porosity 44.3%; pH (H_2O) 7.2; organic carbon 2.06%; total nitrogen 0.31%; NH_4^+-N 1.4 mg kg^{-1}; NO_2^--N 0.27 mg kg^{-1}; NO_3^--N 6.8 mg kg^{-1}) and was classified as Gray Brown Podzolic soil (Haplic Luvisol soil unit and Luvisol major soil grouping in FAO/UNESCO system, belongs to Alfisol soil order in the USDA system).[43] After being air-dried and passed through a 2 mm sieve, the soil was stored at 4 °C before being used for an experiment. Fifty grams of a homogeneously mixed soil sample were placed in a Petri dish (inner diameter = 88 mm) and wetted with ultrapure water to water holding capacity (WHC, see ref 16). The Petri dish was placed into a dynamic chamber made of Teflon (volume 47 L), which was located in a temperature controlled (25 °C) climate cabinet, and flushed with purified dry air at a flow rate 8 L min^{-1}. Mixing ratios of HONO, NO, NO_2, O_3, CO_2, and H_2O were monitored in the chamber headspace by the LOPAP, a NO_x chemiluminescence analyzer (Model 42i-TL, Thermo Scientific, USA), an Ozone analyzer (Model 49i, Thermo Scientific, USA), and a LI-COR (Model 840A, LI-COR, USA), respectively. This setup was described in detail elsewhere.[16] The limit of detection was ∼5 ppt for HONO, ∼80 ppt for NO, and ∼280 ppt for NO_2, respectively. Fluxes of HONO and NO were calculated based on the following formula (see ref 16)

$$F = \frac{Q}{A} * \frac{1}{V_m} * (\chi_{out} - \chi_{in}) \quad (3)$$

where *F* is the flux of HONO and NO (nmol m^{-2} s^{-1}), *Q* is the purging flow rate (m^3 s^{-1}), χ_{out} and χ_{in} are the headspace mixing ratio at outlet and inlet of the chamber (ppb), *A* is the area of soil (m^2), and V_m is the molar volume of air (m^3 mol^{-1}).

The corresponding errors of the fluxes were calculated using Gaussian error propagation.[16] Soil gravimetric water content (SWC) was calculated from the loss of water during the experiment and then normalized to the WHC.[16] For the experiment with ^{15}N labeled urea, 8.62 mL of $CO(^{15}NH_2)_2$ solution with a concentration of 16.4 mM was added to the soil sample before the addition of ultrapure water and continuing the experiment as described above. The addition of urea corresponds to 150 kg ha^{-1} (in terms of N) fertilizer applied in the field. The azo dye solutions from channels 1 and 2 of the LOPAP instrument were collected, and $\psi(^{15}N)$ of the emitted HONO was analyzed according to the presented procedure. The $\psi(^{15}N)$ of HONO caused by fertilizing was calculated using the $\psi(^{15}N)$ of HONO from the fertilized soil experiment and subtracting the values obtained from the unfertilized soil experiment. Before and after the soil measurements, soil nutrient (ammonium, nitrite, and nitrate) contents were analyzed according to the ISO/TS 14256-1 standard procedure.

■ RESULTS AND DISCUSSION

A detailed characterization of the collection efficiency, potential interferences (NO_2, O_3, PAN, HNO_3, etc.), and instrument parameters of the LOPAP were presented by Kleffmann and co-workers.[23,26,27] Here, we discuss the analytical method development of $\psi(^{15}N)$ determination of HONO by HPLC-MS.

Azo Dye Extraction and Chromatography. Azo dye recovery was found to be affected by solution pH and extraction solvent composition. Too high or too low pH of the sample solution decreased the azo dye recovery, e.g. by protonation, which prevented or strongly reduced azo dye retention on the SPE column. Hence, the pH of the azo dye sample was adjusted to ∼5.5 before SPE extraction, which is the value of the change of color of the azo dye. Results of recovery experiments showed that the best extraction efficiency was obtained using 35/65 (v/v) of ACN/0.1% TFA (Figure S1) as extraction solvent.

Typical chromatograms of the ^{15}N labeled azo dye are shown in Figure S2. The eluent gradient for chromatographic

dx.doi.org/10.1021/es501353x | Environ. Sci. Technol. 2014, 48, 8021−8027

separation was optimized to ensure a chromatographic resolution of the azo dye signal that allows for a reliable use of the automatic integration tool provided in the Chemstation software, while maintaining short overall run times (<20 min). The retention time of the azo dye was 2.8 min.

Method Blanks and Calibration. Method blanks for calibration purposes were obtained by applying the derivatization and SPE procedure as discussed in the Experimental Section without adding sodium nitrite. The method blanks therefore include all relevant factors that could affect the azo dye concentrations, e.g. exposure to ambient air, impurities in water and reagents, SPE column, matrix effects, measurement artifacts, and HPLC-MS background signal. The average (n = 3) concentrations of the method blanks detected during the method development were 0.11 μM (corresponding to ~0.4 ppb HONO in the gas-phase for the experimental setup described above). The detection limit was found to be 0.078 μM (3σ method).

A calibration curve for unlabeled aqueous sodium nitrite solution with concentrations ranging from 0 to 19 μM is shown in Figure 1. The error bars represent the standard deviation of

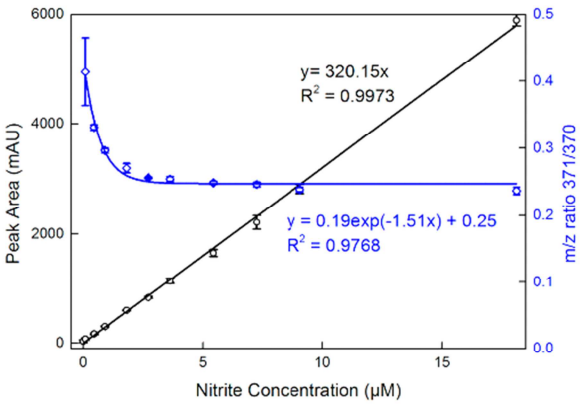

Figure 1. Calibration curve for unlabeled nitrous acid and concentration dependence of m/z ratio 371/370. Open circles (black) represent the 540 nm signal peak area (mAU) of azo dye for different nitrite concentrations. Open diamonds (blue) correspond to the m/z ratio of 371/370. Error bars denote the standard deviation (n = 3).

three calibration curves obtained on a monthly basis. The values agree within 5% of the peak area, thus proving the reproducibility of sample preparation and analysis. The nitrite calibration range corresponds to a HONO gas-phase mixing ratios range of 0–200 ppb measured with the LOPAP.

Despite the good linearity of the concentration calibration, a dependence of the ratio of the signal areas of the EICs of m/z 371 and m/z 370 (termed m/z ratio 371/370 hereafter, which is used to calculate $\psi(^{15}N)$ in eq 2) from the azo dye concentration was observed (Figure 1). The m/z ratio 371/370 decreased from 0.41 to 0.27 with nitrite concentrations increasing from 0.09 μM to 1.81 μM and remained nearly stable at higher concentrations. The lowest observed ratio was 0.23, which is close to the theoretical value of 0.22. A similar behavior was observed for the determination of ^{15}N abundance in ammonium, nitrite, and nitrate by the SPINMAS method, which was attributed to contaminations by atmospheric N_2 for low total N-amounts.[35] In our method, a positive linear relationship (R^2 = 0.97) was found between the m/z ratio 371/370 and the percentage of blank concentration in total nitrite concentration (Figure S3). This suggests that the overestimation of the m/z ratio 371/370 was caused by the method blank at low nitrite concentrations (<1.81 μM). However, as long as the nitrite concentration was above this threshold value, the observed ratio was close to the theoretical value (Figure S3). Hence, the threshold amount of N injected was found to be 2.03 ng (in 80 μL injection volume). This value corresponds to ~5 ppb HONO in the gas-phase measured by the LOPAP.

Figure 2 shows the average $\psi(^{15}N)$ of the calibration curve for four different dye concentrations above the threshold (1.81,

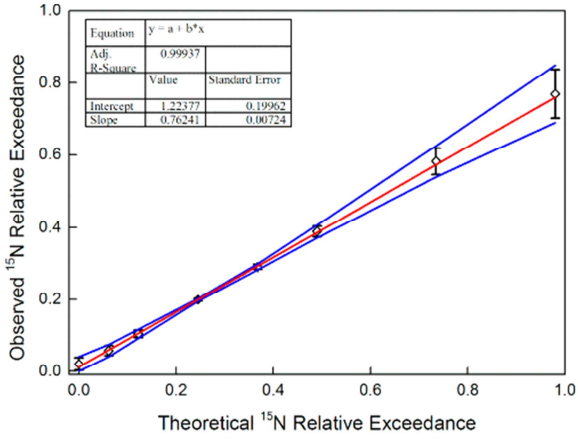

Figure 2. Correlation (y = 0.7624x + 1.2238) between $\psi(^{15}N)$ of calibration standards and measurements by HPLC-MS. Shown are mean values and standard deviations for the analysis of four isotope ratio calibration curves at different dye concentrations (see text). The blue lines show the upper and lower confidence bands (±95%).

4.53, 9.06, and 18.1 μM). The calibration curve of the $\psi(^{15}N)$ is linear (R^2 = 0.9994) but has an optimum range as can be seen from the ±95% confidence bands. The relative standard deviation of the $\psi(^{15}N)$ is <4% between $\psi(^{15}N)$ = 0.2 and 0.5, while it increases to ~10% and ~100% with the $\psi(^{15}N)$ increasing to 0.98 or decreasing to 0, respectively. Therefore, the highest accuracy for deriving the $\psi(^{15}N)$ is obtained within the range of 0.2–0.5.

Notably, the slope of the calibration curve is <1 (0.76). This could be caused by the observed background signal at m/z 370, e.g., in the method blanks. A similar deviation from the 1:1 line was observed in a study of ^{13}C labeled fatty acids analyzed by HPLC-API-MS.[44] To test for the influence of the mass resolution of the instrument on the $\psi(^{15}N)$ analysis, a series of ^{15}N labeled calibration standards ($\psi(^{15}N)$ range from 0–0.49 with a concentration of 0.91 μM) was analyzed using a nano high performance liquid chromatography coupled to quadruple Time-of-Flight mass spectrometry (nanoHPLC-nanoESI-QToF) instrument (mass resolution ~20,000, see the Supporting Information for more details). Using this instrument, the slope of the $\psi(^{15}N)$ calibration curve was found to be 0.8855 (Figure S4). Apparently, less background signal intensity due to higher mass resolution could partly eliminate the cause for the low slope. However, for the proposed application to soil experiments, the results from the low resolution HPLC-MS system were found to be sufficient.

dx.doi.org/10.1021/es501353x | Environ. Sci. Technol. 2014, 48, 8021–8027

Potential Interferences. Due to the concentration dependency of m/z ratio 371/370, factors that might influence nitrite or dye concentration will affect analysis of the $\psi(^{15}N)$. It was reported previously that the absorbance of the azo dye at 540 nm attained its maximum intensity within 2 min.[45,46] We investigated the influence of storage time and temperature on azo dye concentration and its m/z ratio 371/370. The azo dye concentration was found to decrease linearly with time independent of its concentration (Figure S5). Sample storage at 4 °C reduced the concentration decrease over time by a factor ~2 compared to storage at room temperature (RT). For this study, samples were analyzed on the same or the following day of the soil experiments. More importantly, the m/z ratio 371/370 of the dye was found to be unaffected by its decomposition (Figure S5).

Potential interferences from matrix effects were also investigated. The LOPAP reaction solution contains considerably high concentration of SA (58 mM) and NED (0.39 mM). While SA is supposed to be relatively stable, NED is subject to decomposition under irradiated conditions. Hence, samples of 2 mL of 0.39 mM NED solution were exposed to sunlight for 0, 1, 5, 10, 30, and 60 min, respectively, and then analyzed by HPLC-MS with and without addition of 2 mL of 0.91 μM azo dye solution. The results showed that neither the azo dye signal area nor its $\psi(^{15}N)$ was affected by the NED matrix (Table S1).

Application to Soil Experiments. Figure 3 shows calculated HONO and NO fluxes as well as $\psi(^{15}N)$ of HONO emitted during soil measurements conducted with and without fertilizing with ^{15}N labeled urea. The corresponding HONO mixing ratios in the gas-phase were ~7 and ~10 ppb for unfertilized and fertilized soil, respectively, and thus higher than the threshold value of ~5 ppb. The $\psi(^{15}N)$ values in Figure 3 were corrected for the $\psi(^{15}N)$ values of the unfertilized sample. Compared to the unfertilized soil sample, the optimum fluxes of HONO and NO increased from ~15 and ~19 nmol m^{-2} s^{-1} to ~20 and ~24 nmol m^{-2} s^{-1} for the fertilized soil sample, respectively. The hydrolysis of urea to ammonia or ammonium by ammonia-oxidizing bacteria or archaea[47−49] and the subsequent emission of HONO and NO through nitrification[16,50,51] are potentially responsible for the increased fluxes. This finding is supported by measurements of soil nutrients (ammonium, nitrite, and nitrate), which increased by a factor of 12 for ammonium, a factor of 2 for nitrite, while not significantly for nitrate after the soil measurement with the addition of labeled urea (Table S2). This conversion is indicative for microbial processes.[52] The $\psi(^{15}N)$ of HONO caused by fertilizing was in the range of 0.41−0.5 during the soil measurements. Statistical analysis showed that the $\psi(^{15}N)$ values of the emitted HONO, that were measured at SWC below the optimum emission (labeled with b), were significantly higher than the $\psi(^{15}N)$ values close to the optimum emission flux (labeled with a). However, from the AVONA t test no significant difference among the $\psi(^{15}N)$ values labeled with b was found. The change of the $\psi(^{15}N)$ of the emitted HONO during the dry-out of the soil samples can be explained by the depletion of natural nutrient pools over time, increasing microbial activity, or by various sources of HONO emission from soils (AOB combined with chemical equilibrium). The $\psi(^{15}N)$ of the optimum HONO flux caused by fertilizing was ~0.42 and, thus, comparable to the increase of the optimum HONO flux from unfertilized to fertilized soil samples (~38%). These results confirm biogenic HONO emissions from soil,[16] which significantly influence the oxidation capacity of the atmosphere.

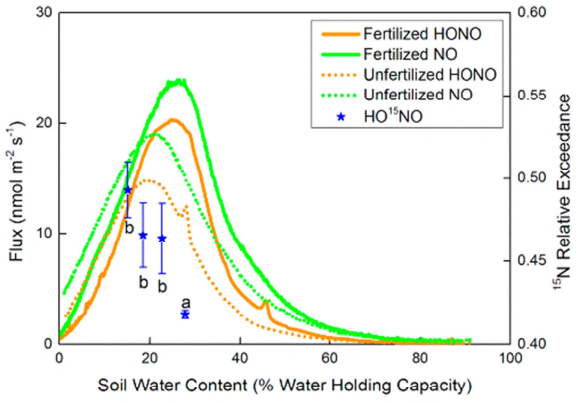

Figure 3. Application of the method to soil measurements. Fluxes of HONO and NO with spiking of ^{15}N labeled urea (solid orange and green line, respectively) and without spiking of ^{15}N labeled urea (dotted orange and green line, respectively). Error bars of HONO and NO fluxes were omitted for clarity, but in general the relative errors determined by error propagation were within 10% of the flux. The $\psi(^{15}N)$ of HONO caused by fertilizing (blue filled stars, difference between the $\psi(^{15}N)$ of fertilized and unfertilized sample) were measured during the dry-out of the soil samples. Error bars are ±95% confidence intervals of the $\psi(^{15}N)$ based on the calibration curve in Figure 3. Means marked by different lowercase letters (a and b, see text) are significantly different from each other at $P < 0.05$ according to the ANOVA t test ($n = 3$).

In conclusion, the presented ^{15}N tracer method provides a new opportunity to study the processes of HONO emission from soils. In the optimal working range of $\psi(^{15}N) = 0.2-0.5$, the relative standard deviation of $\psi(^{15}N)$ is <4%, which is comparable to other ^{15}N tracer studies.[31,53,54] Future investigations should focus on the improvement of the precision of the method, which includes decreasing the injection threshold to detect the $\psi(^{15}N)$ by HPLC-MS. Due to the limitations of our method, the measurement of natural ^{15}N isotope abundances of atmospheric HONO is not possible up to now. Future developments may use nitrogen-free derivatization agents, a high resolution mass spectrometer, or laser techniques to investigate the natural ^{15}N distribution of HONO. The method could potentially be applied for tracer studies in other research fields, such as atmospheric chemistry (e.g., ozone formation from HONO and photolysis of labeled HNO_3), ecohydrology (e.g., refs 55 and 56), and wastewater treatment studies (e.g., potential HONO release during nitrogen and phosphorus removal from ammonium-rich wastewater).

■ ASSOCIATED CONTENT

Supporting Information

Information on the nanoHPLC-nanoESI-QToF setup, typical HPLC-MS chromatograms, the $\psi(^{15}N)$ of calibration curve measured by nanoHPLC-nanoESI-QToF, the effects of solvents, blank concentrations, storage time and temperature, and matrix on the azo dye concentration and its $\psi(^{15}N)$, and the nutrient content before and after measurements; Figures S1−S5 and Tables S1 and S2. This material is available free of charge via the Internet at http://pubs.acs.org.

dx.doi.org/10.1021/es501353x | Environ. Sci. Technol. 2014, 48, 8021−8027

AUTHOR INFORMATION

Corresponding Authors

*Phone: 49 61313056404. Fax: 49 61313056405. E-mail: dianming.wu@mpic.de.

*Phone: 49 61313056206. Fax: 49 61313056405. E-mail: c.kampf@mpic.de.

Present Address

#Centre de Recherche Public - Gabriel Lippmann, Department Environment and Agro-biotechnologies, 41 rue du Brill, L-4422 Belvaux, Luxembourg.

Notes

The authors declare no competing financial interest.

ACKNOWLEDGMENTS

This project was funded by the Max Planck Society and the Max Planck Graduate Center with the Johannes Gutenberg-Universität Mainz (MPGC). We are grateful to Drs. Oliver Spott, Hang Su, and Yafang Cheng for their comments during the method development. We also thank Prof. Dr. Jürgen Kesselmeier, Michael Welling, Nina-Maria Knothe, and Dr. Daniel Plake for supporting our experiments.

REFERENCES

(1) Alicke, B.; Geyer, A.; Hofzumahaus, A.; Holland, F.; Konrad, S.; Pätz, H. W.; Schäfer, J.; Stutz, J.; Volz-Thomas, A.; Platt, U. OH formation by HONO photolysis during the BERLIOZ experiment. *J. Geophys. Res.: Atmos.* **2003**, *108* (D4), 8247.

(2) Volkamer, R.; Sheehy, P.; Molina, L. T.; Molina, M. J. Oxidative capacity of the Mexico City atmosphere − Part 1: A radical source perspective. *Atmos. Chem. Phys.* **2010**, *10* (14), 6969−6991.

(3) Ren, X.; Harder, H.; Martinez, M.; Lesher, R. L.; Oliger, A.; Simpas, J. B.; Brune, W. H.; Schwab, J. J.; Demerjian, K. L.; He, Y.; Zhou, X.; Gao, H. OH and HO_2 Chemistry in the urban atmosphere of New York City. *Atmos. Environ.* **2003**, *37* (26), 3639−3651.

(4) Sleiman, M.; Gundel, L. A.; Pankow, J. F.; Jacob, P.; Singer, B. C.; Destaillats, H. Formation of carcinogens indoors by surface-mediated reactions of nicotine with nitrous acid, leading to potential thirdhand smoke hazards. *Proc. Natl. Acad. Sci. U. S. A.* **2010**, *107* (15), 6576−6581.

(5) Sörgel, M.; Regelin, E.; Bozem, H.; Diesch, J. M.; Drewnick, F.; Fischer, H.; Harder, H.; Held, A.; Hosaynali-Beygi, Z.; Martinez, M.; Zetzsch, C. Quantification of the unknown HONO daytime source and its relation to NO_2. *Atmos. Chem. Phys.* **2011**, *11* (20), 10433−10447.

(6) Wong, K. W.; Tsai, C.; Lefer, B.; Haman, C.; Grossberg, N.; Brune, W. H.; Ren, X.; Luke, W.; Stutz, J. Daytime HONO vertical gradients during SHARP 2009 in Houston, TX. *Atmos. Chem. Phys.* **2012**, *12* (2), 635−652.

(7) Kleffmann, J. Daytime sources of nitrous acid (HONO) in the atmospheric boundary layer. *ChemPhysChem* **2007**, *8* (8), 1137−1144.

(8) Su, H.; Cheng, Y. F.; Shao, M.; Gao, D. F.; Yu, Z. Y.; Zeng, L. M.; Slanina, J.; Zhang, Y. H.; Wiedensohler, A. Nitrous acid (HONO) and its daytime sources at a rural site during the 2004 PRIDE-PRD experiment in China. *J. Geophys. Res.: Atmos.* **2008**, *113* (D14), D14312.

(9) Li, X.; Brauers, T.; Häseler, R.; Bohn, B.; Fuchs, H.; Hofzumahaus, A.; Holland, F.; Lou, S.; Lu, K. D.; Rohrer, F.; Hu, M.; Zeng, L. M.; Zhang, Y. H.; Garland, R. M.; Su, H.; Nowak, A.; Wiedensohler, A.; Takegawa, N.; Shao, M.; Wahner, A. Exploring the atmospheric chemistry of nitrous acid (HONO) at a rural site in Southern China. *Atmos. Chem. Phys.* **2012**, *12* (3), 1497−1513.

(10) Stemmler, K.; Ammann, M.; Donders, C.; Kleffmann, J.; George, C. Photosensitized reduction of nitrogen dioxide on humic acid as a source of nitrous acid. *Nature* **2006**, *440* (7081), 195−198.

(11) Zhou, X.; Zhang, N.; TerAvest, M.; Tang, D.; Hou, J.; Bertman, S.; Alaghmand, M.; Shepson, P. B.; Carroll, M. A.; Griffith, S.; Dusanter, S.; Stevens, P. S. Nitric acid photolysis on forest canopy surface as a source for tropospheric nitrous acid. *Nat. Geosci.* **2011**, *4* (7), 440−443.

(12) Yabushita, A.; Enami, S.; Sakamoto, Y.; Kawasaki, M.; Hoffmann, M. R.; Colussi, A. J. Anion-catalyzed dissolution of NO_2 on aqueous microdroplets. *J. Phys. Chem. C* **2009**, *113* (17), 4844−4848.

(13) Bejan, I.; Abd-el-Aal, Y.; Barnes, I.; Benter, T.; Bohn, B.; Wiesen, P.; Kleffmann, J. The photolysis of ortho-nitrophenols: a new gas phase source of HONO. *Phys. Chem. Chem. Phys.* **2006**, *8* (17), 2028−2035.

(14) Su, H.; Cheng, Y.; Oswald, R.; Behrendt, T.; Trebs, I.; Meixner, F. X.; Andreae, M. O.; Cheng, P.; Zhang, Y.; Pöschl, U. Soil nitrite as a source of atmospheric HONO and OH radicals. *Science* **2011**, *333* (6049), 1616−1618.

(15) Kubota, M.; Asami, T. Source of nitrous acid volatilized from upland soils. *Soil Sci. Plant Nutr.* **1985**, *31* (1), 35−42.

(16) Oswald, R.; Behrendt, T.; Ermel, M.; Wu, D.; Su, H.; Cheng, Y.; Breuninger, C.; Moravek, A.; Mougin, E.; Delon, C.; Loubet, B.; Pommerening-Röser, A.; Sörgel, M.; Pöschl, U.; Hoffmann, T.; Andreae, M. O.; Meixner, F. X.; Trebs, I. HONO emissions from soil bacteria as a major source of atmospheric reactive nitrogen. *Science* **2013**, *341* (6151), 1233−1235.

(17) Maljanen, M.; Yli-Pirilä, P.; Hytönen, J.; Joutsensaari, J.; Martikainen, P. J. Acidic northern soils as sources of atmospheric nitrous acid (HONO). *Soil Biol. Biochem.* **2013**, *67* (0), 94−97.

(18) Perner, D.; Platt, U. Detection of nitrous acid in the atmosphere by differential optical absorption. *Geophys. Res. Lett.* **1979**, *6* (12), 917−920.

(19) Winer, A. M.; Biermann, H. W. Long pathlength differential optical absorption spectroscopy (DOAS) measurements of gaseous HONO, NO_2 and HCNO in the California South Coast Air Basin. *Res. Chem. Intermed.* **1994**, *20* (3−5), 423−445.

(20) Alicke, B.; Platt, U.; Stutz, J. Impact of nitrous acid photolysis on the total hydroxyl radical budget during the Limitation of Oxidant Production/Pianura Padana Produzione di Ozono study in Milan. *J. Geophys. Res.: Atmos.* **2002**, *107* (D22), 8196.

(21) Roberts, J. M.; Veres, P.; Warneke, C.; Neuman, J. A.; Washenfelder, R. A.; Brown, S. S.; Baasandorj, M.; Burkholder, J. B.; Burling, I. R.; Johnson, T. J.; Yokelson, R. J.; de Gouw, J. Measurement of HONO, HNCO, and other inorganic acids by negative-ion proton-transfer chemical-ionization mass spectrometry (NI-PT-CIMS): application to biomass burning emissions. *Atmos. Meas. Tech.* **2010**, *3* (4), 981−990.

(22) Vecera, Z.; Dasgupta, P. K. Measurement of atmospheric nitric and nitrous acids with a wet effluent diffusion denuder and low-pressure ion chromatography-postcolumn reaction detection. *Anal. Chem.* **1991**, *63* (20), 2210−2216.

(23) Heland, J.; Kleffmann, J.; Kurtenbach, R.; Wiesen, P. A new instrument to measure gaseous nitrous acid (HONO) in the atmosphere. *Environ. Sci. Technol.* **2001**, *35* (15), 3207−3212.

(24) Zellweger, C.; Ammann, M.; Hofer, P.; Baltensperger, U. NOy speciation with a combined wet effluent diffusion denuder − aerosol collector coupled to ion chromatography. *Atmos. Environ.* **1999**, *33* (7), 1131−1140.

(25) Zhou, X.; Qiao, H.; Deng, G.; Civerolo, K. A method for the measurement of atmospheric HONO based on DNPH derivatization and HPLC analysis. *Environ. Sci. Technol.* **1999**, *33* (20), 3672−3679.

(26) Kleffmann, J.; Wiesen, P. Technical Note: Quantification of interferences of wet chemical HONO LOPAP measurements under simulated polar conditions. *Atmos. Chem. Phys.* **2008**, *8* (22), 6813−6822.

(27) Kleffmann, J.; Lörzer, J. C.; Wiesen, P.; Kern, C.; Trick, S.; Volkamer, R.; Rodenas, M.; Wirtz, K. Intercomparison of the DOAS and LOPAP techniques for the detection of nitrous acid (HONO). *Atmos. Environ.* **2006**, *40* (20), 3640−3652.

(28) Tsikas, D. Analysis of nitrite and nitrate in biological fluids by assays based on the Griess reaction: Appraisal of the Griess reaction in

the l-arginine/nitric oxide area of research. *J. Chromatogr. B: Anal. Technol. Biomed. Life Sci.* **2007**, *851* (1−2), 51−70.
(29) Huang, G.; Zhou, X.; Deng, G.; Qiao, H.; Civerolo, K. Measurements of atmospheric nitrous acid and nitric acid. *Atmos. Environ.* **2002**, *36* (13), 2225−2235.
(30) Peterson, B. J.; Fry, B. Stable isotopes in ecosystem studies. *Annu. Rev. Ecol. Syst.* **1987**, 18293−320.
(31) Murphy, D. V.; Recous, S.; Stockdale, E. A.; Fillery, I. R. P.; Jensen, L. S.; Hatch, D. J.; Goulding, K. W. T. Gross nitrogen fluxes in soil: theory, measurement and application of ^{15}N pool dilution techniques. In *Adv. Agron.*; Sparks, D., Ed.; Academic Press: Salt Lake City, 2003; Vol. *79*, pp 69−118.
(32) Houlton, B. Z.; Sigman, D. M.; Hedin, L. O. Isotopic evidence for large gaseous nitrogen losses from tropical rainforests. *Proc. Natl. Acad. Sci. U. S. A.* **2006**, *103* (23), 8745−8750.
(33) Green, L. C.; Wagner, D. A.; Glogowski, J.; Skipper, P. L.; Wishnok, J. S.; Tannenbaum, S. R. Analysis of nitrate, nitrite, and [^{15}N]nitrate in biological fluids. *Anal. Biochem.* **1982**, *126* (1), 131−138.
(34) Yakushiji, H.; Kanda, J. Determination of experimentally enriched ^{15}N in nitrate nitrogen based on an improved method of azo dye formation. *J. Oceanogr.* **1998**, *54* (4), 337−342.
(35) Florian Stange, C.; Spott, O.; Apelt, B.; Russow, R. W. B. Automated and rapid online determination of ^{15}N abundance and concentration of ammonium, nitrite, or nitrate in aqueous samples by the SPINMAS technique. *Isot. Environ. Health Stud.* **2007**, *43* (3), 227−236.
(36) Pérez, T.; Trumbore, S. E.; Tyler, S. C.; Matson, P. A.; Ortiz-Monasterio, I.; Rahn, T.; Griffith, D. W. T. Identifying the agricultural imprint on the global N_2O budget using stable isotopes. *J. Geophys. Res.: Atmos.* **2001**, *106* (D9), 9869−9878.
(37) Ozkan, U. S.; Cai, Y. P.; Kumthekar, M. W. Investigation of the reaction pathways in selective catalytic reduction of NO with NH_3 over V_2O_5 catalysts: isotopic labeling studies using $^{18}O_2$, $^{15}NH_3$, ^{15}NO, and $^{15}N^{18}O$. *J. Catal.* **1994**, *149* (2), 390−403.
(38) Nielsen, L. P. Denitrification in sediment determined from nitrogen isotope pairing. *FEMS Microbiol. Lett.* **1992**, *86* (4), 357−362.
(39) Moore, H. The isotopic composition of ammonia, nitrogen dioxide and nitrate in the atmosphere. *Atmos. Environ. (1967−1989)* **1977**, *11* (12), 1239−1243.
(40) Coplen, T. B. Guidelines and recommended terms for expression of stable-isotope-ratio and gas-ratio measurement results. *Rapid Commun. Mass Spectrom.* **2011**, *25* (17), 2538−2560.
(41) Biemann, K. *Mass spectrometry: organic chemical applications*; McGraw-Hill: New York, 1962; pp 223−225.
(42) Caimi, R. J.; Brenna, J. T. Quantitative evaluation of carbon isotopic fractionation during reversed-phase high-performance liquid chromatography. *J. Chromatogr. A* **1997**, *757* (1−2), 307−310.
(43) Lalor, S. T. *Soils of UCD research farm*; University College Dublin: Lyons Estate, Celbridge, Co. Kildare, 2004.
(44) Persson, X.-M. T.; Błachnio-Zabielska, A. U.; Jensen, M. D. Rapid measurement of plasma free fatty acid concentration and isotopic enrichment using LC/MS. *J. Lipid Res.* **2010**, *51* (9), 2761−2765.
(45) Shinn, M. B. Colorimetric method for determination of nitrite. *Ind. Eng. Chem., Anal. Ed.* **1941**, *13* (1), 33−35.
(46) Pai, S.-C.; Yang, C.-C.; P. Riley, J. Formation kinetics of the pink azo dye in the determination of nitrite in natural waters. *Anal. Chim. Acta* **1990**, *232* (0), 345−349.
(47) Lu, L.; Han, W.; Zhang, J.; Wu, Y.; Wang, B.; Lin, X.; Zhu, J.; Cai, Z.; Jia, Z. Nitrification of archaeal ammonia oxidizers in acid soils is supported by hydrolysis of urea. *ISME J.* **2012**, *6* (10), 1978−1984.
(48) Di, H. J.; Cameron, K. C.; Shen, J. P.; Winefield, C. S.; O/'Callaghan, M.; Bowatte, S.; He, J. Z. Nitrification driven by bacteria and not archaea in nitrogen-rich grassland soils. *Nat. Geosci.* **2009**, *2* (9), 621−624.
(49) Mobley, H. L.; Hausinger, R. P. Microbial ureases: significance, regulation, and molecular characterization. *Microbiol. Rev.* **1989**, *53* (1), 85−108.
(50) Thornton, F. C.; Shurpali, N. J.; Bock, B. R.; Reddy, K. C. N_2O and NO emissions from poultry litter and urea applications to Bermuda grass. *Atmos. Environ.* **1998**, *32* (9), 1623−1630.
(51) Li, D.; Wang, X. Nitrogen isotopic signature of soil-released nitric oxide (NO) after fertilizer application. *Atmos. Environ.* **2008**, *42* (19), 4747−4754.
(52) Anthonisen, A. C.; Loehr, R. C.; Prakasam, T. B. S.; Srinath, E. G. Inhibition of nitrification by ammonia and nitrous acid. *J. − Water Pollut. Control Fed.* **1976**, *48* (5), 835−852.
(53) Müller, C.; Stevens, R. J.; Laughlin, R. J. A ^{15}N tracing model to analyse N transformations in old grassland soil. *Soil Biol. Biochem.* **2004**, *36* (4), 619−632.
(54) Dong, W.; Hu, C.; Zhang, Y.; Wu, D. Gross mineralization, nitrification and N_2O emission under different tillage in the North China Plain. *Nutr. Cycl. Agroecosyst.* **2012**, *94* (2−3), 237−247.
(55) Santoro, A. E.; Sakamoto, C. M.; Smith, J. M.; Plant, J. N.; Gehman, A. L.; Worden, A. Z.; Johnson, K. S.; Francis, C. A.; Casciotti, K. L. Measurements of nitrite production in and around the primary nitrite maximum in the central California Current. *Biogeosciences* **2013**, *10* (11), 7395−7410.
(56) Buchwald, C.; Casciotti, K. L. Isotopic ratios of nitrite as tracers of the sources and age of oceanic nitrite. *Nat. Geosci.* **2013**, *6* (4), 308−313.

SUPPORTING INFORMATION

A novel tracer method to measure isotopic labeled gas-phase nitrous acid ($HO^{15}NO$) in biogeochemical studies

Dianming Wu,[*,†,‡,@] Christopher J. Kampf,[*,I] Ulrich Pöschl,[I] Robert Oswald,[†,x] Junfang Cui,[§,⊥] Michael Ermel,[†,x] Chunsheng Hu,[‡] Ivonne Trebs,[†,#] Matthias Sörgel[†]

[†]Biogeochemistry Department, Max Plank Institute for Chemistry, P. O. Box 3060, 55020 Mainz, Germany

[‡]Key Laboratory of Agricultural Water Research, Center for Agricultural Resources Research, Institute of Genetic and Developmental Biology, The Chinese Academy of Sciences, 050021 Shijiazhuang, China

[I]Multiphase Chemistry Department, Max Plank Institute for Chemistry, P. O. Box 3060, 55020 Mainz, Germany

[§]UCD School of Biosystems Engineering, University College Dublin, Dublin 4, Ireland

[⊥]Institute of Mountain Hazards and Environment, The Chinese Academy of Sciences, 610041 Chengdu, China

[@]University of the Chinese Academy of Sciences, 100049 Beijing, China

[X]Institute for Inorganic and Analytical Chemistry, Johannes Gutenberg University Mainz, 55128 Mainz, Germany

[#]Now at: Centre de Recherche Public - Gabriel Lippmann, Department Environment and Agro-biotechnologies, 41 rue du Brill, L-4422 Belvaux, Luxembourg

The supporting information comprises 9 pages, 5 figures and 2 tables.

MANUSCRIPT TEXT

nanoHPLC-nanoESI-QToF analysis of $\psi(^{15}N)$

In addition to the analysis of $\psi(^{15}N)$ using the HPLC-DAD-ESI-MS system described in the main text, the $\psi(^{15}N)$ of the azo dye was also investigated using a nanoHPLC-nanoESI-QToF system (Agilent Technologies, USA). The system consisted of a nano pump (G2226A, Agilent) with 4-channel micro-vacuum degasser (G1379B, Agilent), a microfluidic chip cube (G4240-64000, Agilent) interfaced to a Q-ToF mass spectrometer (6520, Agilent; nominal mass resolution 20000 at a scan rate of 5 s^{-1}), a capillary pump (G1376A, Agilent) with degasser (G1379B, Agilent), and an autosampler with thermostat (G1377A, Agilent). The injection volume of 0.4 µL was transferred from the autosampler to the chip cube interface by the capillary pump operated at a flow rate of 4 µL min^{-1} with 0.1% formic acid in water as the eluent. Enrichment column (9 mm, 160 nL) and analytical column (150 mm x 75 µm) share 5 µm Zorbax 300SB-C18 particles and are located on the chip (G4240-62010, Agilent). Nano pump eluents were 0.1% formic acid in water with 3% acetonitrile (eluent A) and acetonitrile with 3% of 0.1% formic acid in water (eluent B). Chromatographic separation was performed using a gradient elution starting at 3% B for 3 min, linearly increasing to 90% B in the next 17 min, maintaining 90% B for 4 min and flushing back to 3% B in 1 min. The MS QToF settings were as follows: dry gas temperature 325 °C, dry gas flow rate 5 L min^{-1}, Capillary potential 1900 V, acquisition in positive ion polarity MS mode (4 GHz, HiRes) with a mass range of 100 - 500 m/z. Each chromatographic run was repeated three times.

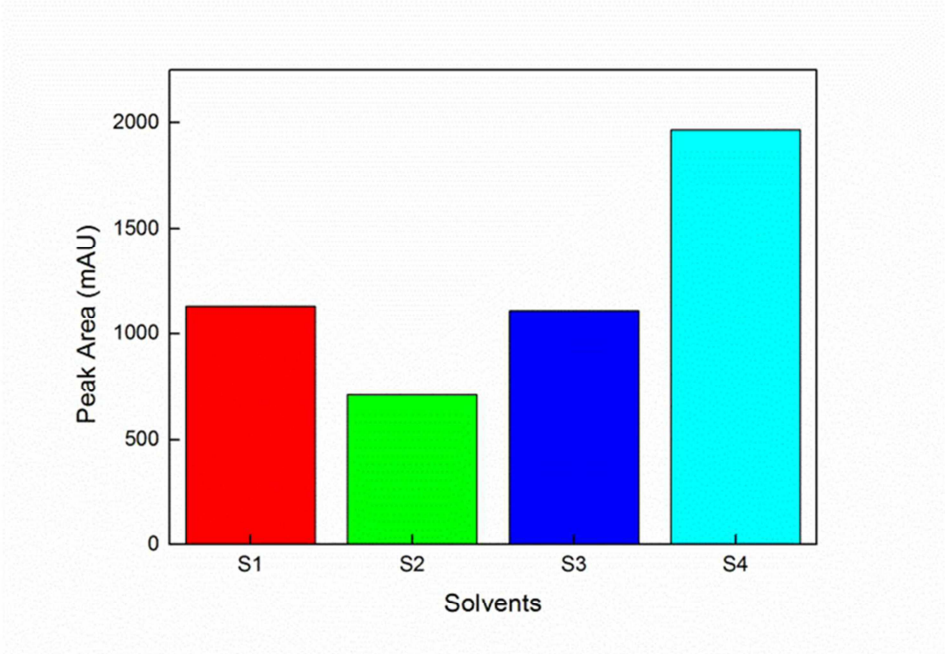

Figure S1. The effect of different solvents on the peak area signal (DAD) of the extracted azo dye. The concentration of the unlabeled dye was 4.53 µM. The solvents S1, S2, S3 and S4 were 2 mL 70/30 (v/v) of acetonitrile (ACN) / 0.1% (v/v) trifluoroacetic acid in water (TFA), 2 mL 75/25 (v/v) of ACN / 0.1% TFA, 1 mL 70/30 (v/v) of ACN / 0.1% TFA + 1 mL 0.1% TFA and 2 mL 35/65 (v/v) of ACN / 0.1% TFA, respectively.

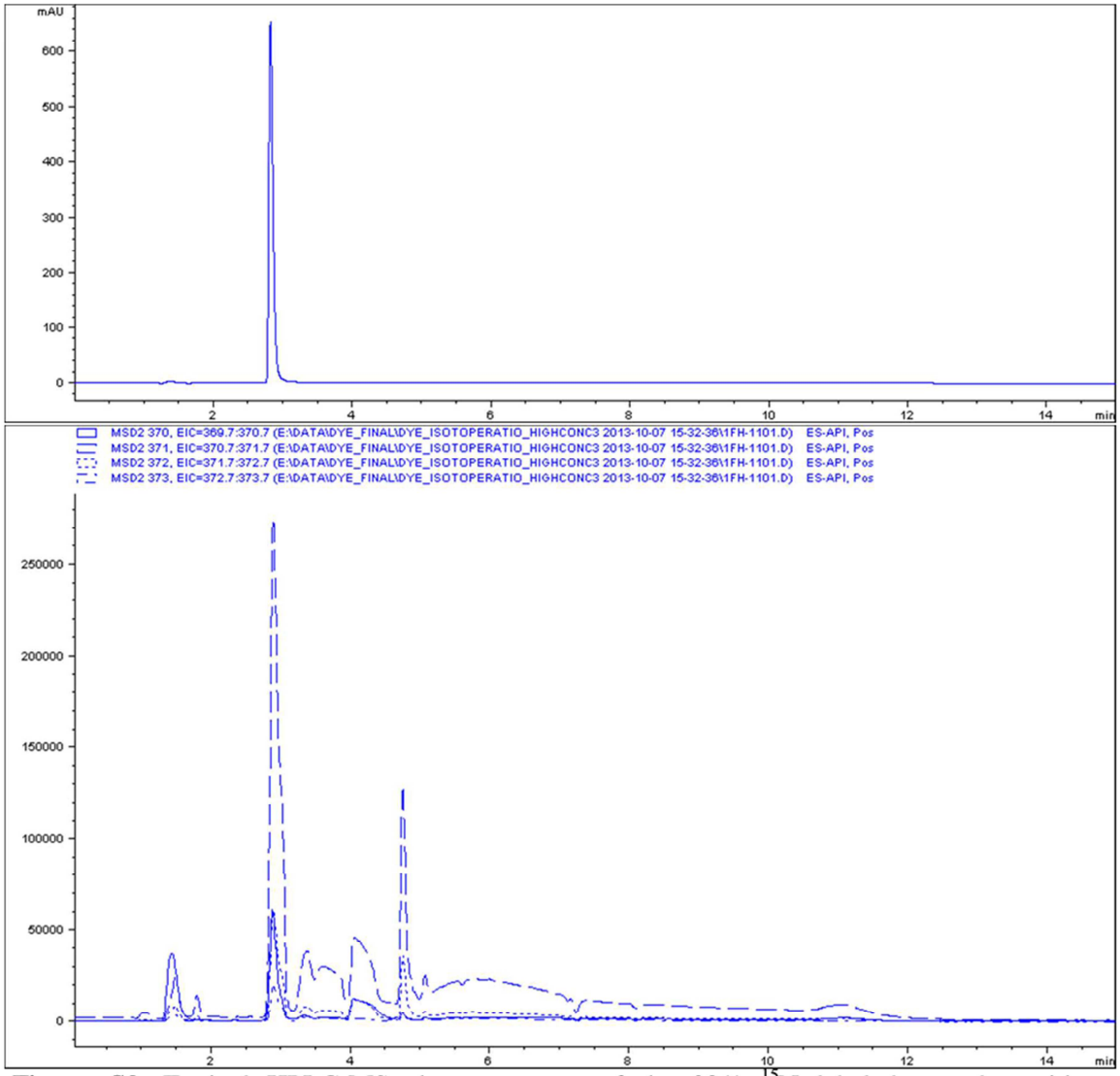

Figure S2. Typical HPLC-MS chromatograms of the 98% ^{15}N labeled azo dye with a concentration of 9 µM. The upper panel shows the UV/vis signal of the azo dye at its maximum absorption wavelength of 540 nm. The lower panel shows the extracted ion chromatograms (EIC) of *m/z* 370, *m/z* 371, *m/z* 372 and *m/z* 373.

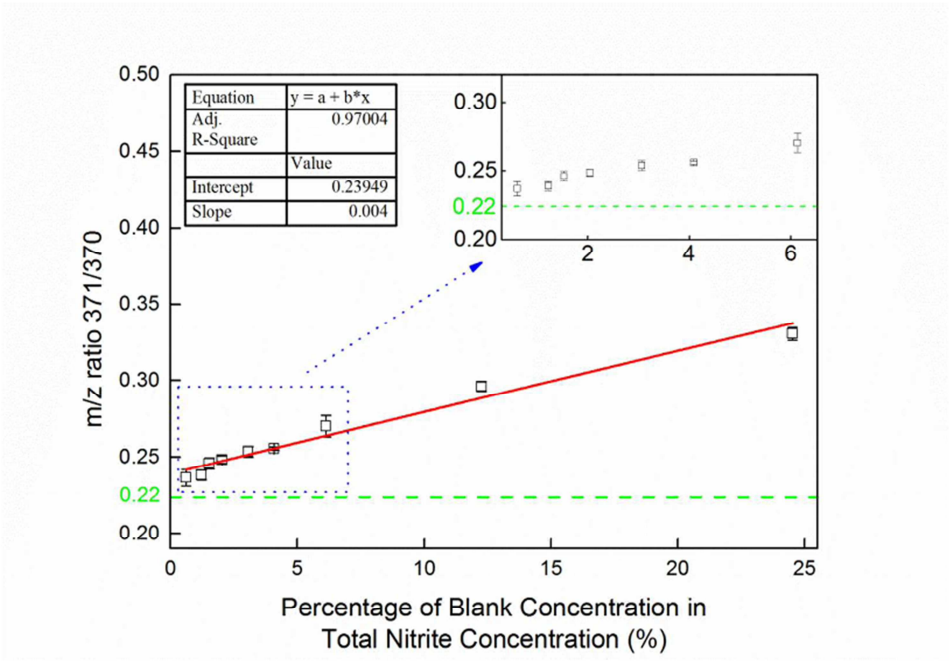

Figure S3. Correlation between percentage of blank concentration in total nitrite concentration (%) and *m/z* ratio 371/370. Shown are mean values and standard deviations at different dye concentrations (0 - 19 µM). The green dashed line shows the theoretical value of *m/z* ratio 371/370, obtained using an online Isotope Distribution Calculator: http://www.sisweb.com/mstools/isotope.htm.

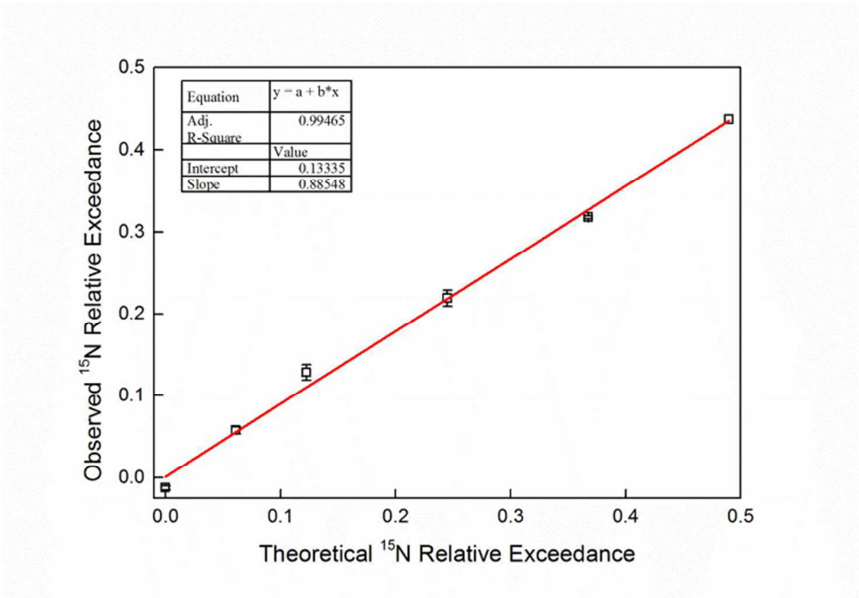

Figure S4. Correlation (y = 0.8855x + 0.1334) between $\psi(^{15}N)$ of calibration standards and measured values by nanoHPLC-nanoESI-QToF. Shown are mean values and standard deviations of three replicates at a dye concentration of 0.91 µM.

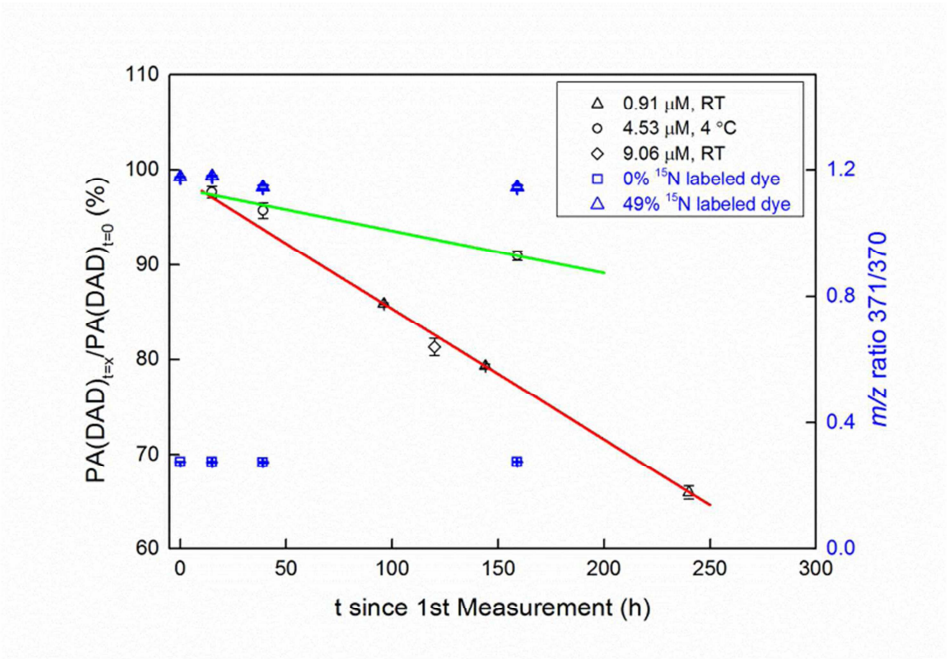

65

66 **Figure S5.** The effects of storage temperature and time on of the relative peak area
67 ($PA(DAD)_{t=x}/PA(DAD)_{t=0}$) and *m/z* ratio 371/370 of the 0% labeled and 49% labeled azo dye.
68 The dye solutions with concentrations of 0.91 and 9.06 µM (red line) were stored at room
69 temperature (RT), while the dye solution with a concentration of 4.53 µM was stored at 4 °C
70 (green line) before being analyzed by HPLC-MS. Error bars show the standard deviation of the
71 mean (n = 3).

Table S1. The matrix effect of *N*-(1- naphthyl)-ethylenediamine dihydrochloride (NED) on the 540 nm signal peak area of azo dye and its $\psi(^{15}N)$. The NED solution samples were exposed to sunlight from 0 to 60 min. Means followed by the same lowercase letters are not significantly different at $P < 0.05$ according to the ANOVA t-test (n = 3).

Exposure Time (min)	Peak Area of NED (mAU)	Peak Area of Azo Dye (mAU)	$\psi(^{15}N)$
0	13675	141.8 ± 1.6 a	0.77 ± 0.01 a
1	13426	141.2 ± 1.6 a	0.77 ± 0.01 a
5	13361	140.3 ± 1.5 a	0.76 ± 0.01 a
10	13047	140.6 ± 1.3 a	0.76 ± 0.01 a
30	11479	139.6 ± 0.7 a	0.74 ± 0.01 a
60	8357	143 ± 0.8 a	0.76 ± 0.02 a

77 **Table S2.** The nutrient content before and after the soil experiments.

Soil Sample	NH_4^+-N	NO_2^--N	NO_3^--N
		mg kg^{-1}	
Before Measurement	1.4	0.27	6.8
After Measurement (unfertilized)	2.1	0.75	8.7
After Measurement (fertilized)	25.3	1.57	9.2

78

B4. Ermel et al, BGD to be submitted, 2014

Bidirectional exchange of HONO between soil and air

Authors: M. Ermel[1,2], R. Oswald[1], T. Behrendt[1,3], D. Wu[1,4], S. Hohlmann[1], F. X. Meixner[1], I. Trebs[5] and M. Sörgel[1]

[1] Biogeochemistry Department, Max Planck Institute for Chemistry, P.O. Box 3060, 55020 Mainz, Germany
[2] Institute for Inorganic and Analytical Chemistry, Johannes Gutenberg University Mainz, 55128 Mainz, Germany
[3] Multiphase Chemistry Department, Max Planck Institute for Chemistry, P.O. Box 3060, 55020 Mainz, Germany
[4] Key Laboratory of Agricultural Water Research, Center for Agricultural Resources Research, Institute of Genetic and Developmental Biology, The Chinese Academy of Sciences, 050021 Shijiazhuang, China
[5] Centre de Recherche Public - Gabriel Lippmann, Department Environment and Agro-biotechnologies, 41 rue du Brill, L-4422 Belvaux, Luxembourg

Abstract

Recent studies showed that nitrous acid (HONO) can be emitted by soils in significant amounts. The microbial and chemical processes in soil leading to the release of HONO have a considerable influence on the chemistry of the lower troposphere. Recent field experiments found bidirectional fluxes of HONO from the ground surface, but up to now only one laboratory study investigated bidirectional fluxes of HONO. In this study, we used a dynamic chamber system to determine the bidirectional flux of HONO by exposing each of six soil samples collected in the field to two different HONO mixing ratios. We observed bidirectional fluxes for all samples. HONO fluxes were found to be constant with increasing soil layer thickness and, thus, we discuss the application of the compensation point concept. Due to the various processes involved in emission and uptake of HONO, we introduce the "ecosystem specific compensation mixing ratio of HONO", χ_{comp}, which is a function of the soil water content. We observed χ_{comp} to be in a range of 0.09 – 239.9 ppb. During our experiments we found uptake of HONO that is subsequently followed by a strong release when HONO free air was applied. Our results support a recent finding that adsorbed HONO during nighttime can strongly contribute to its daytime release and, hence, might explain part of the missing daytime source. We identified four processes in soils, which are responsible for the release and uptake of HONO. These processes are portioning of HONO between gas and liquid phase, bacterial formation from hydroxylamine (NH_2OH), adsorption and desorption, which are all phyisco-chemical processes. We show their contribution in a conceptual model as a function of the soil water content.

1. Introduction

The cycling of reactive nitrogen (N_r) in soil is mainly driven by nitrification and denitrification, which both are carried out by bacteria (Meixner and Yang, 2006). It is well known that during both processes the trace gases nitric oxide (NO) (Pilegaard, 2013) and nitrous oxide (N_2O) (Bouwman et al., 2013) are produced and emitted to the atmosphere. About 20% of the global NO release can be attributed to soil emissions (Stocker et al., 2013). Hence, the factors controlling this process were investigated in detail previously. The production and destruction of tropospheric ozone (O_3), a pollutant hazardous to plants (Lamaud et al., 2009) and humans (Uysal and Schapira, 2003), is driven by NO and volatile

organic compounds (VOC) (Crutzen and Lelieveld, 2001), hence, soils can have severe effects on atmospheric chemistry and human health.

It was recently shown that emission fluxes of nitrous acid (HONO)from arid and arable soils can be in the same order of magnitude as those of NO (Oswald et al., 2013). The photolysis of HONO during daytime produces NO and OH, the major oxidant of the atmosphere (Lammel and Cape, 1996). Consequently, HONO has a strong influence on the reactivity of the atmosphere and was recently shown to have a significant influence on cloud formation (Elshorbany et al., 2014). This additional "source" of NO from HONO emitted by soil might explain the discrepancy between the soil NO_x (NO and NO_2) emission determined with global models and satellite-based approaches (Oswald et al., 2013). HONO formed in soil can be released or taken up from the partitioning of nitrous acid between the soil solution and the gas phase, which is formed from soil nitrite (Su et al., 2011) and by ammonia-oxidizing bacteria (AOB) via the intermediate hydroxylamine (Ermel et al., 2014). Several recent field studies suggested that HONO fluxes from soil are bidirectional (Twigg et al., 2011;Wong et al., 2012;VandenBoer et al., 2013).

Recent laboratory studies showed that soil can indeed act as a sink for HONO (Donaldson et al., 2014;Oswald, 2014). Donaldson et al. (2014) coated a flow tube reactor with dry soil and investigated the uptake coefficient of HONO as result of a heterogeneous reaction at different relative humidity and HONO mixing ratios. In contrast, (Oswald, 2014) studied the uptake of HONO on soil in a laboratory dynamic chamber system as a function of the soil water content (SWC) and used the production and consumption concept, which has been applied for soil-air exchange of NO and other trace gases for many decades (Remde et al., 1989;Feig et al., 2008;Behrendt et al., 2014). However, the prerequisite for the application of this concept is that production and consumption of the trace gas occur in the same soil layer (Conrad, 1994). In this case, the net release rate (J) of NO or any other trace gas determined with a dynamic chamber system is a function of production (P) and consumption (U):

$$J = \frac{Q}{m_{soil} V_m} (\chi_{out} - \chi_{in}) \quad (1)$$

$$J = P - U \quad (2)$$

where J (nmol kg^{-1} s^{-1}) is calculated from the purging flow Q (m^3 s^{-1}), the mixing ratio of the trace gas at the inlet χ_{in} and at the outlet χ_{out} of the chamber (ppb), the mass of the soil (kg) and the molar volume of air V_m (m^3 mol^{-1}) (Pape et al., 2008;Behrendt et al., 2014). An important parameter is the compensation mixing ratio χ_{comp}, at which the production and consumption equal each other (Behrendt et al., 2014;Remde et al., 1989;Conrad, 1994). It can

be calculated from a set of two experiments with different inlet mixing ratios of the trace gas (Breuninger et al., 2012;Behrendt et al., 2014):

$$\chi_{comp} = \frac{\chi_{out,1}}{1-\frac{\chi_{out,2}-\chi_{out,1}}{\chi_{in,2}-\chi_{in,1}}} \quad (3)$$

where indices 1 and 2 refer to the two experiments and $\chi_{in,2} > \chi_{in,1}$. In contrast to NO, for which a constant compensation mixing ratio for all SWC was found (Behrendt et al., 2014), Oswald (2014) showed that the HONO mixing ratio compensation point is a function of SWC. This implies that, although their production processes are strongly related (Oswald et al., 2013), different consumption mechanisms for NO and HONO exist.

To investigate this further, we measured HONO soil-air exchange fluxes for different soil samples with a laboratory dynamic chamber system. Furthermore, one selected soil sample was studied intensively by exposing it to h different HONO mixing ratios, and by investigating this effect on bidirectional HONO fluxes. We provide a detailed discussion on the applicability of the compensation point concept for HONO and resolve major drawbacks of the classic concept.

2. Materials and Methods

2.1 Soil samples

The soil samples were taken from the upper soil layer (0-5 cm). HONO release of samples S2 and S3 was previously investigated by Oswald et al. (2013). Sample S5 was intensively investigated by Su et al. (2011);Oswald et al. (2013);Ermel et al. (2014);Oswald et al. (2014a). HONO emission from Sample S1 was investigated by Oswald et al. (2014b).

Samples S1 (Boreal forest, Hyytiälä, Finland, 61.846°N, 24.295°E) was sieved to 16 mm instead of 2 mm after sampling, due to the high organic content (Bargsten et al., 2010).

Samples S2 (eucalyptus forest, Grose Valley, Australia, 33.61°S, 150.63°E), S3 (pasture, Hawkesbury River flood plain, Australia, 33.57°S, 150.77°E), and S5 (wheat field, Mainz-Finthen, Germany, 49.97°N, 8.16°E;) were dried at 40 °C for 24 h, sieved to 2 mm and stored at 4 °C in open plastic bags before measurement.

Samples S4 (White millet field, Rajasthan, India, 28.07°N, 73.65°E) and S6 (Sugar cane, Punjab, India, 30.65°N, 76.55°E) were collected dry. The samples were sieved to 2 mm and stored at 4°C in open plastic bags until measurement.

Standard DIN and ISO procedures were used to characterize the chemical and physical properties of the soil samples: bulk pH of soil was measured according to ISO 10390, nitrite, nitrate and ammonium according to ISO/TS 14256-1, loss on ignition according to DIN 19684-3 (Blume et al., 2000). All soil extracts were prepared with potassium chloride (KCl).

2.2 Experimental setup

The dynamic chamber setup used in this study is identical to one from Ermel et al. (2014), except for adding the HONO source and the valve controlling the HONO inlet mixing ratio. The system consists of the chamber itself, a compressed air purification system, an analyzer system and a valve system. The chamber is coated with Teflon (PFE) foil and has a volume of 0.008 m³. It was purged with $1 \cdot 10^{-4}$ m^3 s^{-1} of purified compressed air, further denoted as zero air, which was obtained from a pure air generator (PAG 003, EcoPhysics, Switzerland) and was free of NO_x (NO + NO_2), O_3, HONO, hydrocarbons and water vapor (dew point -30°C). Before the compressed air entered the PAG, it was pre-dried by a membrane dryer (Clearpoint and Drypoint M, BEKO Deutschland GmbH, Germany) and exposed to an UV lamp (OG-1, Ultra-Violet Products Ltd, USA) to photolyse HONO. The air leaving the chamber was analyzed by a differential H_2O and CO_2 analyzer (LI-7000, Li-Cor Biosciences GmbH, Germany), which used zero air as reference. Furthermore, NO_x was measured by a chemiluminescence NO analyzer (CLD 780TR, ECOPHYSICS, Switzerland; Limit of Detection (LOD_{NO}) ≈ 35 ppt), using a specific photolytic converter for NO_2 (Photolytoc NO_2 converter, Air Quality Desogn, Inc., USA; LOD_{NO2} ≈ 120 ppt). An UV-absorption photometer (Model 49c, Thermo Electron Corporation, USA; LOD ≈ 0.5 pbb) was used to measure O_3. Data of these instruments was acquired by a datalogger (CR3000, Campbell Scientific, Inc., USA) every 60 s. A long path absorption photometer (LOPAP, QUMA Elektronik & Analytik GmbH, Germany; LOD ≈ 5 ppt) (Kleffmann et al., 2002;Heland et al., 2001) measuring HONO was directly connected to the chamber to avoid artefacts due to wall losses on long tubing. HONO was produced from hydrochloric acid (HCl, 37%, Sigma-Adlrich, Germany) and potassium nitrite (KNO_2, cryst. for analysis, Merck KGaA, Germany) after the method of Febo et al. (1995) at a flow of $8.3 \cdot 10^{-3}$ m^3 s^{-1}. In order to expose the soil samples to different HONO mixing ratios during a single experiment, a time controlled valve switched the HONO flow into the chamber every 45 min. The entire dynamic chamber system was placed in a large temperature controlled cabinet (KB115, Binder GmbH, Germany).

The NO_x and O_3 analyzer were calibrated with NO standard gas (25.1 ± 0.5 ppb NO, Linde, Germany) and gas phase titration unit (Sonimix 6000, Schmidlin, Switzerland), which has a built-in O_3 generator. A dew point generator (Li-610, Li-Cor Biosciences GmbH, Germany) was used to calibrate the H_2O analyzer. The LOPAP was calibrated by using a nitrite standard solution (CertiPUR, ß(NO_2^-) = 999 ± 5 mg/l, Merck KGaA, Germany).

2.3 Measurement procedure

The background signal of the LOPAP instrument was determined before and after the measurement by introducing purified air directly to the inlet. The mixing ratios of HONO and NO at the chamber inlet, $\chi_{in,2,HONO}$ and $\chi_{in,2,NO}$, were also determined prior and after the experiment by flushing the empty chamber until constant mixing ratios were achieved. Continuous measurement of the HONO mixing ratio from the HONO source during an entire experiment showed that a linear function can be used to describe the HONO mixing ratio change over time.

To conduct an experiment, a soil subsample of 50 g were homogeneously distributed in a petri dish (100 x 20 mm, Duran Group, Germany) and wetted to reach water holding capacity (whc) (Oswald et al., 2013;Behrendt et al., 2014). The sample was then placed in the dynamic chamber. Two different types of experiments were conducted. First, a standard experiment was made with each subsample using only purified air during the experimental course ($\chi_{in,1}$ = 0 ppb). Second, a discontinuous experiment was made during which the HONO source was activated via the time controlled valve, which switched from HONO free air ($\chi_{in,1}$ = 0 ppb) to an elevated mixing ratio of HONO ($\chi_{in,2}$ = 14-125 ppb). After dry-out of the sample during the experiment the residual water content was determined by drying (105°C) until constant weight was reached. For each BFE experiment two data sets were retrieved due to the switching of the valve and, hence, measurements are discontinuous over the whole SWC range. We applied fit functions using mathematical models provided by the software ORIGIN 8.6G to fill in the missing data for further analysis.

2.4 Calculations

2.4.1 Soil water content

The described measurement setup does not allow for online measurements of any quantity used to describe the water content of the soil. However, the gravimetric soil moisture before and after the measurement can be easily measured. The loss of water during the experiment

can be calculated by the water released as water vapour, which is measured at the chamber exit. According to Bargsten et al. (2010), the gravimetric soil moisture can be calculated:

$$\theta_g(t) = \theta_g(\mathrm{whc}) - \theta_g(t_{max}) \cdot \frac{\int_0^t \mathrm{RH}\cdot \mathrm{d}t}{\int_0^{t_{max}} RH\cdot \mathrm{d}t} \quad (4)$$

With $\theta_g(t)$ (%) the gravimetric water content at time t (min), $\theta_g(whc)$ the gravimetric water content at water holding capacity, t_{max} is the total experiment time and RH is the relative humidity.

For further discussion and comparison of different soils, which feature different $\theta_g(whc)$, it is more suitable to use the soil water content (SWC) expressed as % of whc (for details see Oswald et al. (2014a):

$$\mathrm{SWC} = \frac{\theta_g \cdot 100}{\theta_g(\text{at WHC})} \quad (5)$$

2.4.2 Net flux

Net fluxes F (nmol m^{-2} s^{-1}) of HONO and NO are calculated as:

$$F = \frac{Q}{A\cdot V_m}(\chi_{out} - \chi_{in}) \quad (6)$$

where A is the surface area of the petri dish (m^2), V_m the molar volume of air, Q the purging air flow rate (m^3 s^{-1}), χ_{in} the inlet and χ_{out} the outlet mixing ratio. Errors were calculated according to Gaussian error propagation (Ermel et al., 2014).

2.4.3 Compensation mixing ratio

The compensation mixing ratio χ_{comp} for soil measured at two different values for χ_{in} was calculated according to eq. (3). In a graph with χ_{in} as abscissa and χ_{out} as ordinate, a linear regression can be used to calculate χ_{comp}:

$$m = \frac{\chi_{out,2} - \chi_{out,1}}{\chi_{in,2} - \chi_{in,1}} \quad (7)$$

and

$$b = \chi_{out,1} \quad (8)$$

resulting in

$$\chi_{comp} = \frac{b}{1-m} \quad (9)$$

The error of χ_{comp} is then derived from the error of m and b:

$$\Delta\chi_{comp} = \sqrt{\left(\frac{1}{1-m}\Delta b\right)^2 + \left(\frac{b}{(1-m)^2}\Delta m\right)^2} \quad (10)$$

3. Results

The soil samples S1 – S6 cover a wide range of different soil properties like pH, nutrients and loss on ignition (LOI) (Tab. 1).

Table 1: Summary of soil properties: pH, nutrients, LOI and whc of soil samples S1 – S6 (see Sect. 2.3). Values marked with * are below the limit of detection (LOD) and the LOD is shown.

Sample	**pH**	**N-NH_4^+**	**N-NO_2^-**	**N-NO_3^-**	**whc**	**LOI**
		mg kg^{-1}	mg kg^{-1}	mg kg^{-1}	kg kg^{-1}	%
S1	3.0	1.6	0.07	2.0	595	52.3
S2	3.7	1.3	0.15*	12.3	68.8	4.4
S3	5.4	2.9	0.15*	17.5	62.7	3.5
S4	7.1	3.0	2.00	1.9*	29.4	1.0
S5	7.2	18.1	1.00	77.7	63.5	5.2
S6	7.2	5.4	0.09	1.9*	25.4	1.4

3.1 Net flux and χ_{comp}

Applying a mixing ratio of HONO of 0 ppb at the chamber inlet $\chi_{in,1}$ during the discontinuous experiment (Fig. 1) causes only very low, but relatively constant emissions at high SWC and high emission at low SWC for soil sample S5. This optimum curve of the HONO release from soil was recently described in several studies (Oswald et al., 2013;Ermel et al., 2014;Oswald et al., 2014a). A similar pattern can be found at an elevated HONO mixing ratio at the chamber inlet $\chi_{in,2}$ = 14 ppb (Fig. 1). However, the slope of the linear part at high SWC is different from the slope at 0 ppb. In the SWC range from 33 to 100 % of whc, $\chi_{out,2}$ is below the inlet mixing ratio $\chi_{in,2}$, which implies an uptake of HONO by the soil. Consequently, net emission of HONO from the soil was found at low SWC (0 – 32 % of whc).

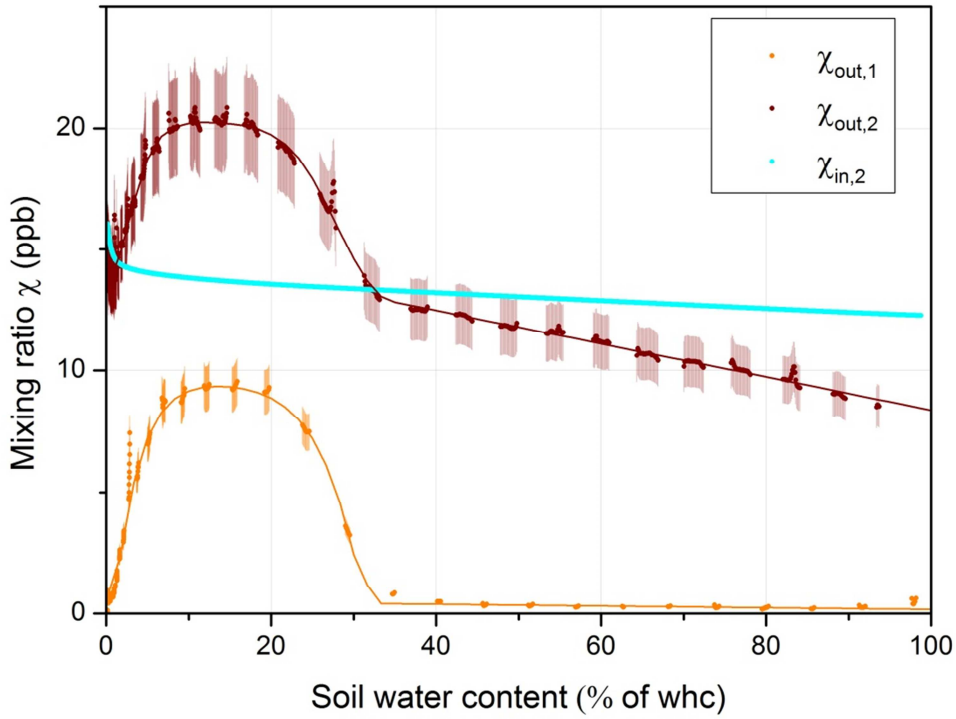

Figure 1: Mixing ratios of HONO during a discontinuous experiment with S5. HONO inlet mixing ratio χ_{in} was controlled by a valve (see text). The inlet mixing ratio of HONO $\chi_{in,1}$ was 0 ppb. The inlet mixing ratio $\chi_{in,2}$ provided by the HONO source is shown as a cyan colored solid line. Orange and brown dots represent the measured mixing ratios of HONO $\chi_{out,1}$ and $\chi_{out,2}$, respectively. The fit functions (see section 2.3) are shown as solid lines of the respective color. An optimum function was used to model the maximal emission at optimum SWC and a linear function was applied to the lower emissions at higher SWC. Error bars denote the measurement uncertainty of the LOPAP instrument (10 % + 2 σ).

However, during subsequent discontinuous experiments using higher values for $\chi_{in,2}$, we found that $\chi_{out,1}$ varies with $\chi_{in,2}$ at HONO inlet mixing ratios of 0 ppb (Fig. 2). This effect causes (a) different shapes of the optimum emission curves, (b) a different pattern of the constant emission at higher SWC and (c) different net fluxes. Additionally, a near-linear relationship between $\chi_{out,1}$ and $\chi_{in,2}$ was found for different soil moistures (not shown). For this reason, we decided to use the $\chi_{out,1}$ from the standard experiment with purified air ($\chi_{in,1}$ = 0 ppb, see section 2.3) to calculate net fluxes and also to determine compensation mixing ratios. A detailed discussion about the unexpected variation of $\chi_{out,1}$ will be presented in the following sections.

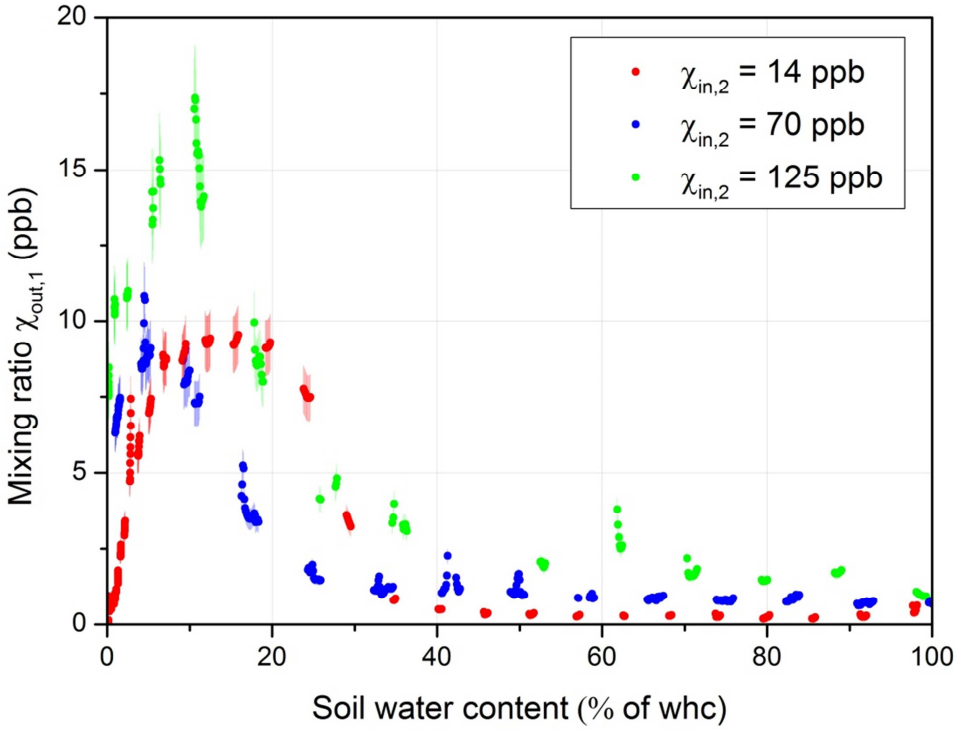

Figure 2: HONO outlet mixing ratio $\chi_{out,1}$ at 0 ppb inlet mixing ratio of soil sample S5 during switching of the valve to elevated inlet mixing ratios of HONO $\chi_{in,2}$ = 14 ppb (red), 70 ppb (blue) and 125 ppb (green). Error bars denote the measurement uncertainty of the LOPAP instrument (10 % + 2 σ).

The net flux of HONO F_2(HONO) from soil sample S5 at an ambient HONO mixing ratio of 14 ppb (Fig. 2), was calculated according to equation (6). Net deposition of HONO to the soil is indicated by negative fluxes F_2(HONO) at high SWC, while HONO net emission is indicated by positive F_2(HONO) . At $\chi_{in,1}$ = 0 ppb F_1(HONO) is always positive. Hence, the direction and magnitude of the HONO net flux depends on the ambient HONO mixing ratio, which has been frequently observed for other trace gases such as e.g., NO (Behrendt et al., 2014), CH_4 (Seiler et al., 1983) and N_2O (Chapuis-Lardy et al., 2007).

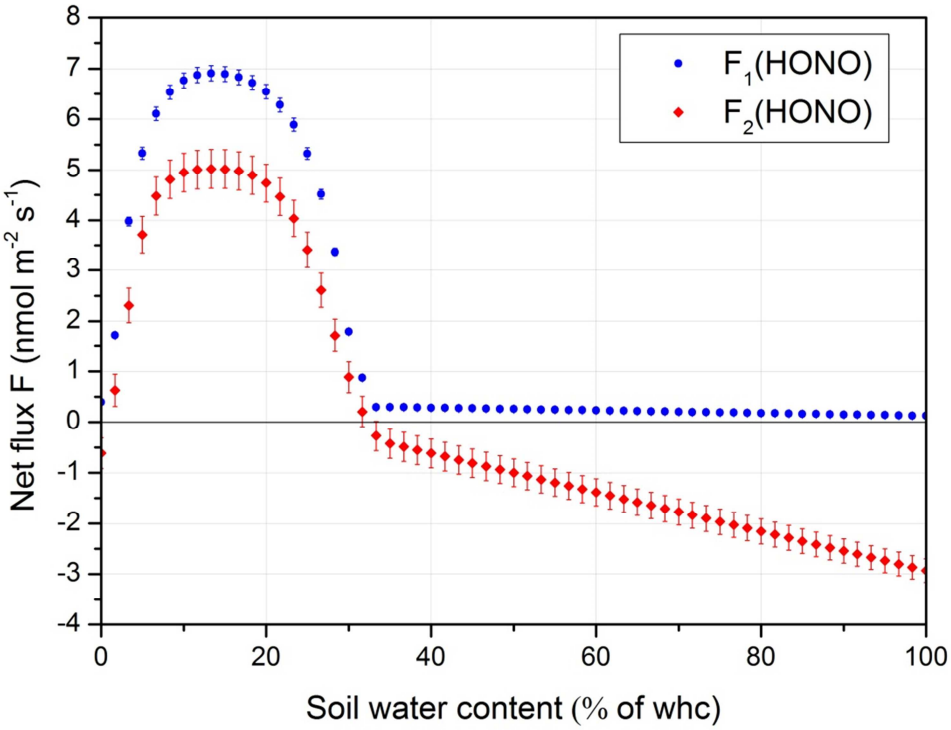

Figure 3: The net fluxes F_1(HONO) for $\chi_{in,1}$ = 0 ppb and F_2(HONO) for $\chi_{in,2}$ = 14 ppb of soil sample S5 are shown as a function of the soil water content. The error bars represent the uncertainty derived from Gaussian error propagation.

At SWC values of ~32 % of whc F_2(HONO) is about 0 nmol m^{-2} s^{-1}, thus emission (production) and uptake (consumption) compensate each other. According to classical microbial theory, the corresponding ambient mixing ratio is called the compensation point (Conrad, 1994). As discussed in detail in Sect. 4.2, we will use the term “ecosystem specific compensation mixing ratio” instead of compensation point mixing ratio χ_{comp}. The four mixing ratios, $\chi_{in,1}$, $\chi_{in,2}$, $\chi_{out,1}$ and $\chi_{out,2}$, and equations (7) – (9) can be used to calculate χ_{comp} for the entire SWC range (Fig. 4). Similar to $\chi_{in,1}$ and $\chi_{in,2}$, χ_{comp} shows an optimum curve with a maximum at lower SWC and a near-linear decrease towards higher SWC.

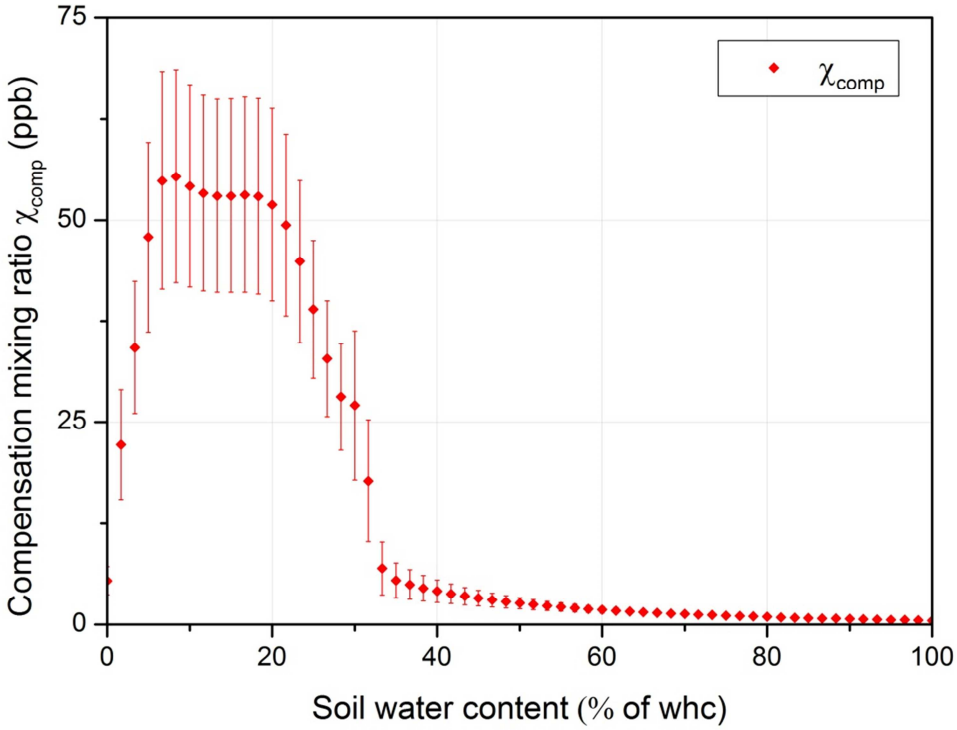

Figure 4: The ecosystem specific compensation mixing ratio χ_{comp} of soil sample S5 for $\chi_{in,2}$ = 14 ppb is shown as a function of the soil water content. The error bars of χ_{comp} denote the uncertainty derived from Gaussian error propagation.

3.2 Net fluxes for different soil layer thickness

As a result of different emission and uptake processes the net flux of a trace gas from soil can vary with increasing soil layer thickness. We investigated the relationship between F_2(HONO) and the soil layer thickness of S5 (Fig. 5). The samples were analysed at 100 % of whc and F_2(NO) was measured as a reference, since the soil-air exchange of NO is well characterized. The error of χ_{in} and χ_{out} was obtained from the standard deviation of 10 data points, which equal 10 min of measurement. The net fluxes of HONO and NO are both negative and, hence, only net deposition was observed at $\chi_{in,2}$(HONO) = 28 ppb and $\chi_{in,2}$(NO) = 43 ppb (Fig. 5). F_2(HONO) and F_2(NO) appear to be constant with increasing soil layer thickness (2 – 40 mm).

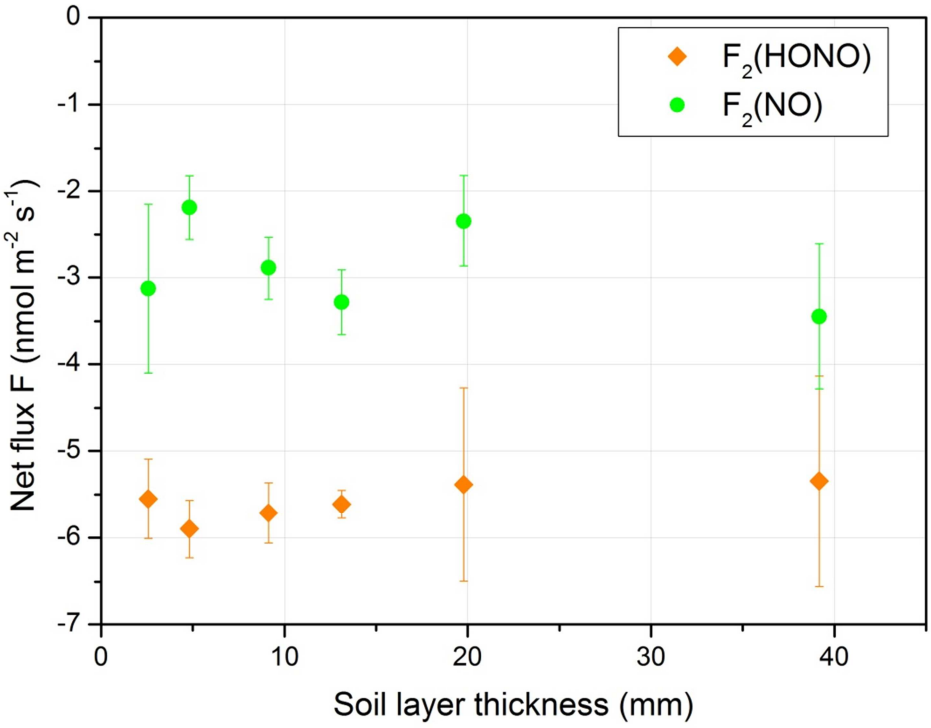

Figure 5: Net fluxes of HONO (orange diamonds) and NO (green circles) as a function of soil layer thickness. Soil sample S5 was wetted to reach whc and exposed to inlet mixing ratios of $\chi_{in,2}$(HONO) = 28 ppb and $\chi_{in,2}$(NO) = 43 ppb. The error bars of the net flux represent the uncertainty derived from Gaussian error propagation.

The experiment was repeated for S5 at low SWC values (SWC < 1 %, Fig. 6). Inlet mixing ratios were $\chi_{in,2}$(HONO) = 25 ppb and $\chi_{in,2}$(NO) = 49 ppb. Repeatedly, F_2(HONO) is negative for all soil layer thickness. However, the uptake increases with increasing thickness of the soil layer up to 21 mm, but remained constant up to 40 mm, which is the maximal possible layer thickness in the used measurement setup. In contrast, the net NO flux changed from uptake within the first 10 mm to emission with increasing layer depth.

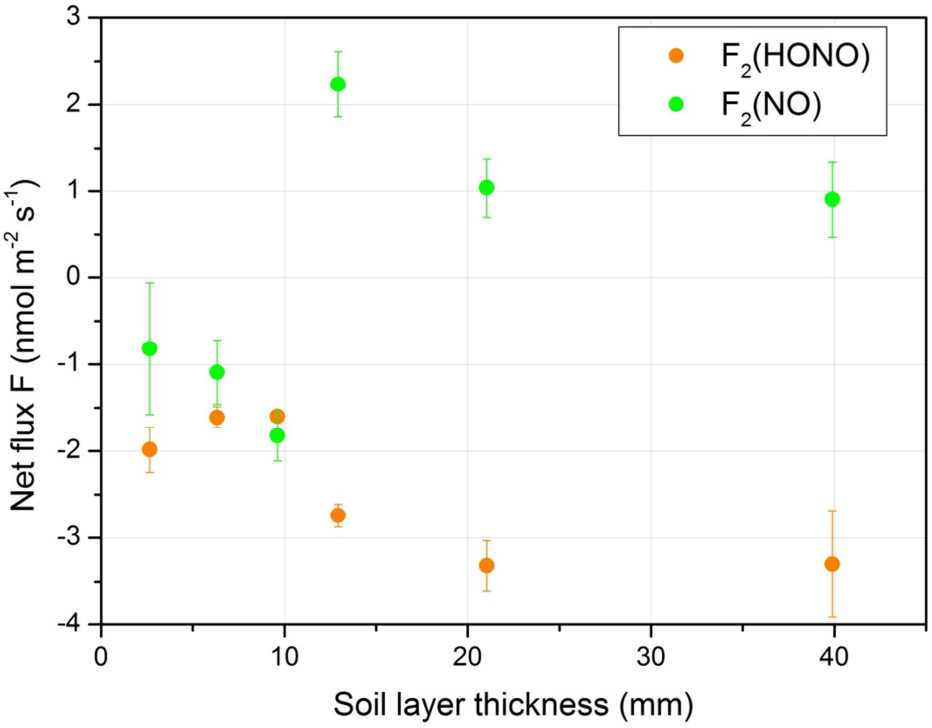

Figure 6: Net fluxes F_2(HONO) (orange diamonds) and F_2(NO) (green circles) as a function of soil layer thickness. Dry soil samples (SWC < 1 %) of S5 were investigated at inlet mixing ratios of $\chi_{in,2}$(HONO) = 25 ppb and $\chi_{in,2}$(NO) = 48 ppb. The error bars of the net flux represent the uncertainty derived from Gaussian error propagation.

3.3 Net fluxes for different χ_{in}

The discontinuous experiment was repeated for soil sample S5 at different $\chi_{in,2}$(HONO) of 14 ppb, 70 ppb and 125 ppb. The net fluxes derived from the measurements with $\chi_{in,2}$(HONO) = 14 ppb and 70 ppb show a comparable pattern (Fig. 7) and at $\chi_{in,2}$(HONO) = 70 ppb the soil is nearly a complete sink for HONO. The kink in F_2(HONO) at $\chi_{in,2}$(HONO) = 70 ppb can be attributed to the merging of the fit functions. A completely different pattern for the net flux is found for $\chi_{in,2}$(HONO) = 125 ppb, which exhibits a net deposition maximum at 25 % of whc. This is the only experiment with $\chi_{in,2} > \chi_{comp}$ over the whole SWC range. The HONO emission optimum might be masked by the dominance of adsorption.

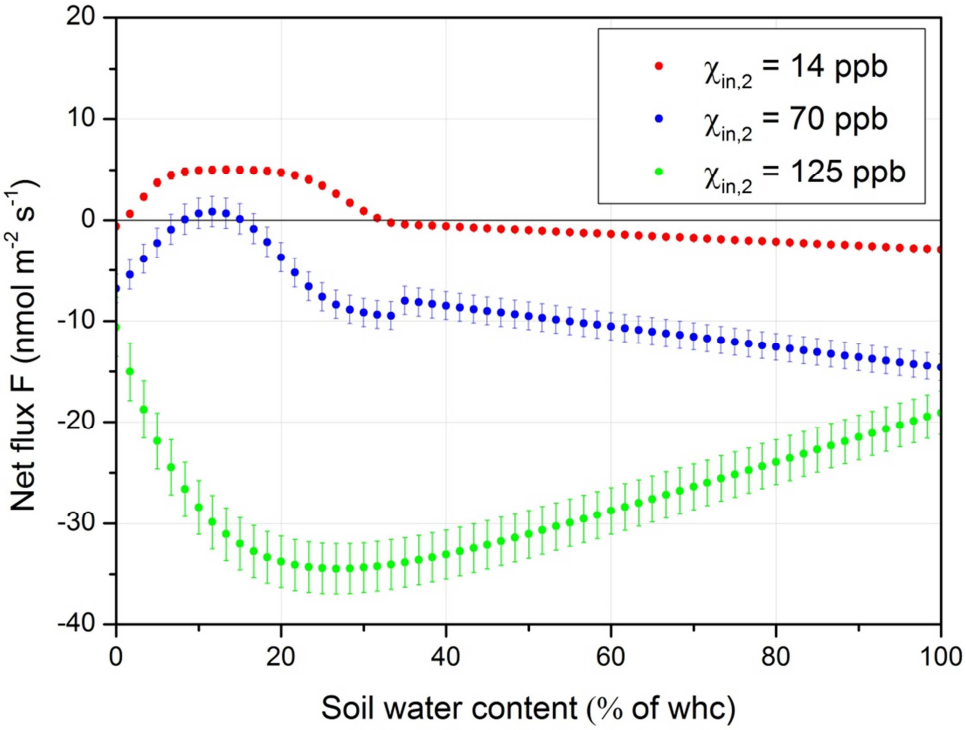

Figure 7: Net fluxes F_2(HONO) of soil sample S5 at different inlet mixing ratios of HONO $\chi_{in,2}$= 14 ppb (red), 70 ppb (blue) and 125 ppb (green). The error bars of the net flux represent the uncertainty derived from Gaussian error propagation.

From the three sets of experiments with $\chi_{in,2}$(HONO) = 14 ppb, 70 ppb and 125 ppb, we calculated the ecosystem specific compensation mixing ratio χ_{comp} using $\chi_{in,1}$ = 0 ppb from the standard experiment (Fig. 8). All three experiments show a strong overlap in χ_{comp} for the SWC range from 60% of whc to 100% of whc. This, however, leads to χ_{comp}, which is much smaller than HONO*. The experiments with $\chi_{in,2}$(HONO) = 70 ppb and 125 ppb show a good agreement in χ_{comp} from 33 % to 100 % of whc. The ecosystem specific compensation mixing ratio for $\chi_{in,2}$(HONO) = 14 ppb is higher at soil moistures between 33 % and 50 % of whc. At lower SWC, where the emission occurs, values of χ_{comp} differ strongly in magnitude and shape from each other, although experiments with $\chi_{in,2}$ = 14 ppb and 70 ppb show a better overall agreement in χ_{comp}.

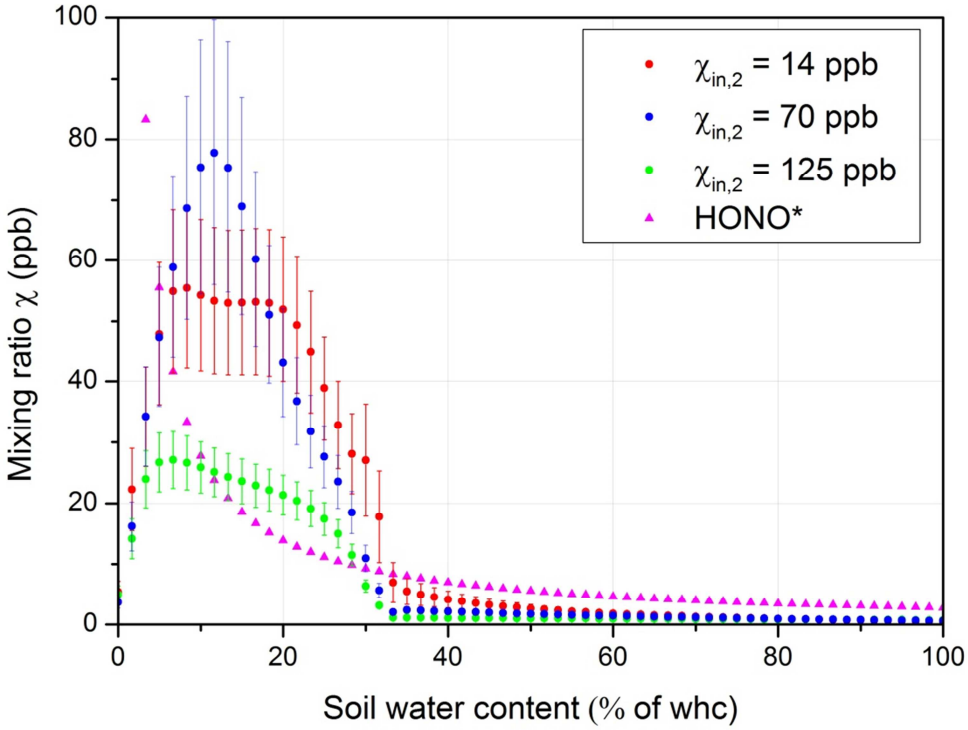

Figure 8: The ecosystem specific compensation mixing ratio χ_{comp} of soil sample S5. The inlet mixing ratios of HONO are $\chi_{in,1}$ = 0 ppb (standard experiment), $\chi_{in,2}$ = 14 ppb (red), 70 ppb (blue) and 125 ppb (green). The HONO gas phase equilibrium mixing ratio HONO* (pink triangles) was calculated according to Su et al. (2011). The error bars of χ_{comp} represent the uncertainty derived from Gaussian error propagation.

3.4 Net fluxes and χ_{comp} for different soils

A comparison of investigated net fluxes of HONO for the six different soil samples used in this study is not straightforward because $\chi_{in,2}$ was different for each experiment. Hence, we use the ecosystem specific compensation point χ_{comp} to compare the six samples. Since χ_{comp} varies with soil moisture we will use the three most prominent points of the curve to compare χ_{comp}. These are (1) at water holding capacity ($\chi_{comp,whc}$), (2) at the emission optimum ($\chi_{comp,Fopt}$) and (3) at dry conditions ($\chi_{comp,dry}$) (Table 2).

Table 2: Summary of the optimum net flux and ecosystem specific compensation mixing ratios of soil samples S1 – S6 based on experiments with $\chi_{in,1}$ = 0 ppb (standard experiment) and the shown $\chi_{in,2}$. For each soil sample χ_{comp} is shown at water holding capacity ($\chi_{comp,whc}$), at optimum emission ($\chi_{comp,Fopt}$) and under dry conditions ($\chi_{comp,dry}$). Samples S4 and S6 were investigated with one discontinuous experiment.

Soil sample	$\chi_{in,2}$.	F_{opt}	$\chi_{comp, whc}$		$\chi_{comp, Fopt}$		$\chi_{comp, dry}$	
	ppb	nmol m^{-2} s^{-1}	ppb		ppb		ppb	
S1	157.1	0.243	1.62	± 0.38	1.59	± 0.87	0.09	± 0.08
S2	9.5	0.324	1.42	± 0.13	1.53	± 0.30	0.76	± 0.20
S3	8.6	0.237	0.54	± 0.11	1.94	± 0.51	8.70	± 8.80
S4	17.2	25.46	0.09	± 0.01	239.9	± 22.7	8.12	± 1.91
S5	14.1	8.731	0.49	± 0.08	53.02	± 11.98	5.44	± 1.73
S6	168.2	4.554	1.27	± 0.17	9.26	± 1.14	4.57	± 0.69

The observed F_{opt}(HONO) for the soil samples are in good agreement with the findings of Oswald, et al. (2013), taking land use type (Sect. 2) and pH into account (Table 1). The ecosystem specific compensation mixing ratio χ_{comp} for soil samples S1 – S6 varies from the low ppt range up to several hundred ppb. Highest χ_{comp} are found at F_{opt}(HONO) for all soils, which is caused by the strong microbial formation of HONO. As this process appears to be irreversible, high ambient mixing ratios are required to compensate this release by uptake through adsorption or Henry's law. Consequently, the best correlation between soil properties and χ_{comp} was found for the mixing ratio at the optimum flux χ_{opt} and $\chi_{comp,Fopt}$, as the release dominates over the uptake.

It is noteworthy, that some of the χ_{comp} values are below typical nighttime mixing ratios of HONO (1 – 3 ppb) or even typical daytime mixing ratios of HONO (30 – 300 ppt) (Wong et al., 2012;Li et al., 2012;Villena et al., 2011;Acker et al., 2006). For instance, soil sample S4 reveals χ_{comp} below 1 ppb for a SWC $\geq$ 35% of whc (Fig. 9). Hence, this soil will be mostly a sink for HONO.

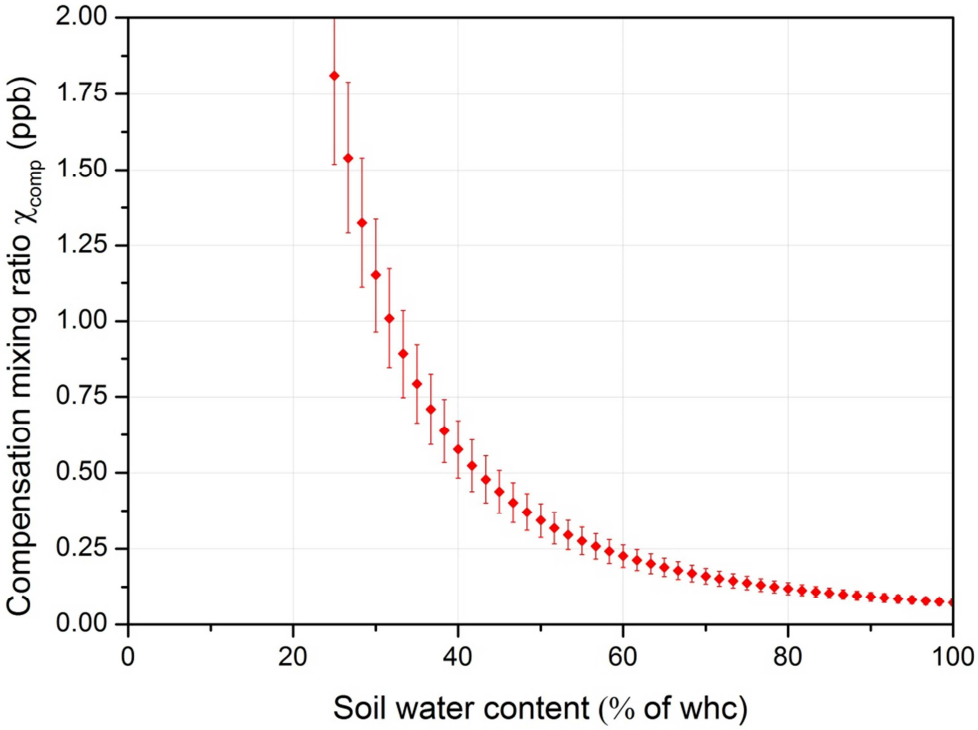

Figure 9: The ecosystem specific compensation mixing ratio χ_{comp} of soil sample S4 is below 1 ppb at SWC ≥ 35% of whc. The error bars of χ_{comp} represent the uncertainty derived from Gaussian error propagation.

3.5 Adsorption and desorption of HONO

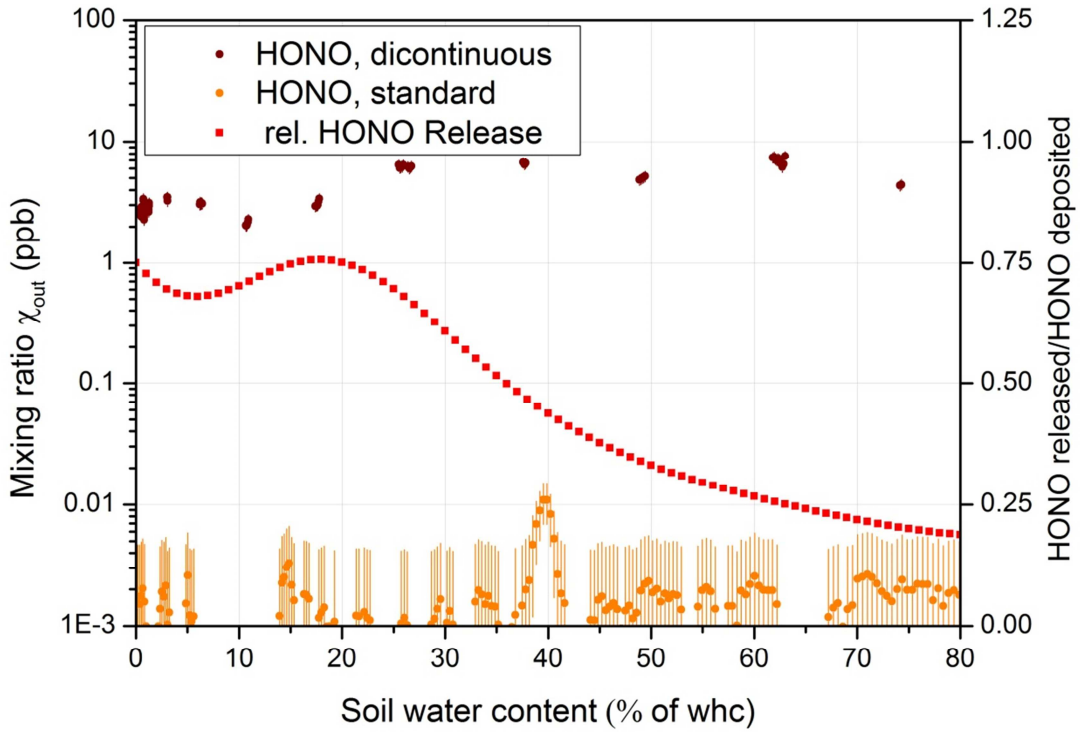

Figure 10: The mixing ratio of HONO at the chamber exit for the standard experiment (orange circles) is much lower than during a discontinuous experiment with the switching valve system (brown circles) for soil sample S1, although both are measured at $\chi_{in,1}$(HONO) = 0 ppb. The ratio between the additionally released HONO during the discontinuous experiment with $\chi_{in,1}$(HONO) = 0 ppb and the HONO taken up by the soil during the experiment with $\chi_{in,2}$(HONO) = 157 ppb (red squares) varies with the SWC. The error bars of the mixing ratios of HONO denote the uncertainty of the LOPAP instrument.

Soil sample S1 was measured with the standard experiment ($\chi_{in,1}$(HONO) = 0 ppb)and with the discontinuous experiment ($\chi_{in,2}$(HONO) = 157 ppb). Figure 10 shows the difference between the mixing ratios of HONO at the chamber outlet for $\chi_{in,1}$ = 0 ppb from these two experiments. During the standard experiment χ_{out}(HONO) for S1 is in the range of a few ppt (close to the detection limit). However, for the discontinuous experiment $\chi_{out,1}$ is about three order of magnitude higher. These findings are comparable to the observed increase of $\chi_{out,1}$ at elevated $\chi_{in,2}$ for soil sample S5 (Figure 2) and indicate that HONO can be adsorbed by soil and is subsequently released when lower ambient mixing rations prevail. We calculated the ratio between the additionally released HONO (during $\chi_{in,1}$ = 0 ppb) and the HONO adsorbed / taken up by the soil (during $\chi_{in,2}$ = 157 ppb). This ratio is approaching unity with decreasing soil moisture.

3.6 Elevated ambient HONO mixing ratios influence NO emission

The NO release from soil sample S1 was determined during a standard and discontinuous experiment (Fig. 11). Very low NO emissions (few ppt)were found during the standard experiment.However, exposing the soil to elevated HONO mixing ratios ($\chi_{in,2}$ = 140 ppb) led to an optimum shaped emission of NO of up to 4.2 ppb. We calculated the ratio between the additionally emitted NO and the HONO taken up by the soil. The ratio is a function of the SWC and varies between 0 % and > 100 %. At SWC below 25 % of whc the uncertainties of the ratio, which were derived by Gaussian error propagation, increase strongly because less HONO was taken up. The difference between two high HONO mixing ratios in the denominator leads to errors that are larger than the possible maximum of 100 %.

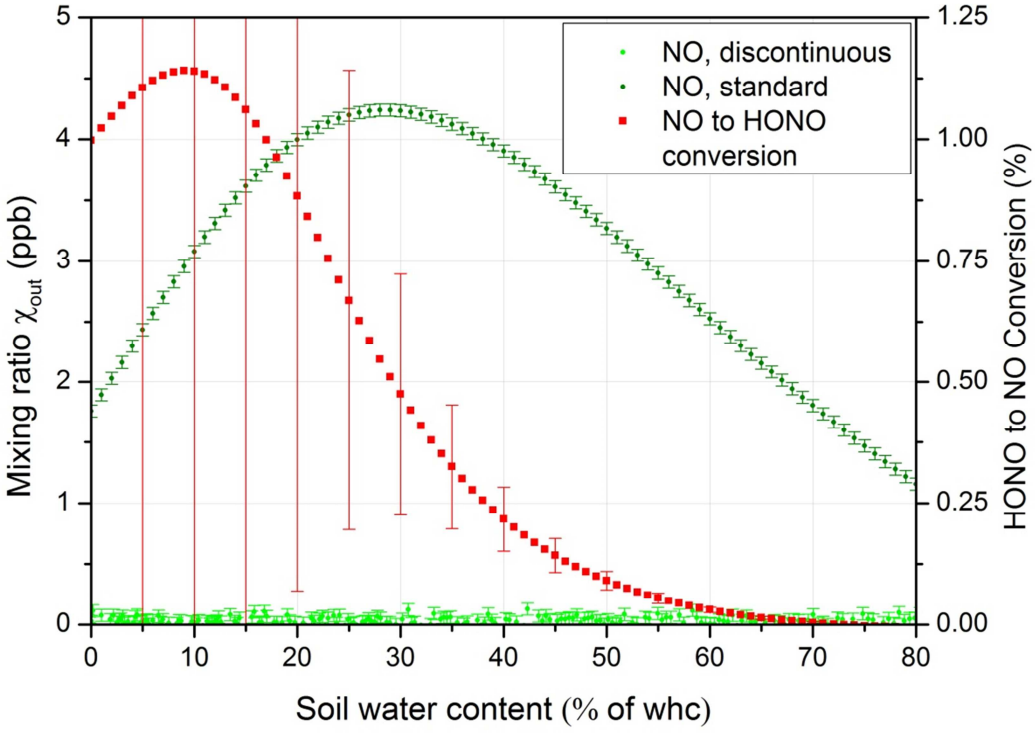

Figure 11: The mixing ratio of NO at the chamber outlet for a standard experiment (light green circles) is much lower than during the discontinuous experiment (dark green circles) for soil sample S1, although both are measured at χ_{in} = 0 ppb HONO. The ratio between the additionally released NO and the HONO taken up by the soil during the discontinuous experiment (red squares) varies with SWC. The error bars of the HONO mixing ratios denote the uncertainty of the LOPAP instrument. For the HONO to NO conversion every fifth error bar derived from Gaussian error propagation is shown.

4. Discussion

4.1 Bidirectional fluxes of HONO from soil

We investigated six soil samples with a laboratory dynamic chamber system and found distinct responses of HONO soil-air exchange to SWC and the ambient HONO mixing ratios. Oswald (2014) reports bidirectional fluxes of HONO from a pasture soil, which was exposed to two different ambient HONO mixing ratios in two separate experiments. Our results are in general agreement with those findings and emphasize the ambiguous role of HONO fluxes from soil. Our laboratory results support some recent field studies that reported bidirectional HONO fluxes between ground surface and atmosphere (VandenBoer et al., 2013;Wong et al., 2012;Twigg et al., 2011).

4.2 Defining the compensation mixing ratio of HONO

The occurrence of bidirectional fluxes of a trace gas implies the existence of the so called compensation point (Conrad, 1994). This point, which can be either expressed as concentration or as mixing ratio, describes the ambient mixing ratio of a trace gas at which the net flux is zero. Two prerequisites are vitally important for the application of this concept: (i) production and consumption occur simultaneously and (ii) both processes are located in the same soil layer. According to these definitions by Conrad (1994), the concept is mainly applicable to microbial production and consumption processes of trace gases, for instance CO, H_2, N_2O, NO, NO_2 and OCS.

Contrary, the production and consumption of HONO is related to several different processes. The partitioning of nitrous acid between gas phase and aqueous phase within soils (Su et al., 2011) is both depending on the nitrite concentration in the soil solution and on the ambient HONO mixing ratio. This partitioning by Henry's law might explain the strong uptake of HONO at high SWC (Fig. 3). HONO formation from hydroxylamine (NH_2OH) released by ammonia-oxidizing bacteria (Ermel et al., 2014) is only an indirect source of HONO, as a reaction of NH_2OH on a surface at low SWC is necessary. This process is mainly responsible for strong emissions of HONO in soils at neutral pH (Oswald et al., 2013). However, this process is only a production term, as the reverse reaction of HONO to NH_2OH is unlikely. Uptake of HONO by deposition on soil particles is an important consumption process in soil (Donaldson et al., 2014). Up to now, only one laboratory study investigating this process was performed and was limited to dry soil samples. The desorption of deposited HONO on soil

was recently proposed as an additional source of HONO and might explain a large fraction of the missing HONO daytime source (VandenBoer et al., 2013). This process might be the result of the adsorption observed during our experiments (see Sect. 3.5 and also Sect. 4.4). Hence, bidirectional fluxes of HONO are controlled by at least four different processes. Since many of these processes were discovered recently, additional processes cannot be excluded. For example, uptake of HONO by nitrite-oxidizing bacteria or release by ammonia-oxidizing archaea might be possible. As all of the identified processes are not of (direct) microbial nature and are not necessarily occurring simultaneously the criterion (i) for the application of the compensation point concept according to Conrad (1994) is not fulfilled.

We demonstrated that HONO net fluxes are constant for soil sample S5 at 100 % whc for increasing soil layer thickness (Fig. 5). This finding is essential to allow the application of the dynamic chamber system (Remde et al., 1989). Under dry conditions, we found constant HONO net fluxes for a soil layer thickness above 20 mm. This is likely related to adsorption of HONO on dry soils (Donaldson et al., 2014). Since the diffusion of HONO is higher at low SWC for dry soils, deeper layers are better accessible for gaseous HONO (Oswald et al., 2014a) and have to be considered in contrast to for soils at whc. Hence, the two experiments show that uptake of HONO is related to at least two different processes, namely partitioning of HONO according to Henry's law and adsorption of HONO. The uptake of HONO appears to be constant for increasing thickness of the soil layer. Under this assumption, prerequisite (ii) is fulfilled. However, the relevant processes at different SWC are not yet completely understood and our experimental setup is restricted to a maximum soil layer thickness of ˜ 40 mm. Further studies on this subject with higher soil layer thickness are required.

Consequently, according to the definition by Conrad (1994) the application of the classical compensation point concept is not advisable. However, we believe that it is still possible to calculate a compensation mixing ratio with the retrieved data. The resulting compensation mixing ratios of HONO, however, are not constant with SWC as known for e.g., the compensation point of NO (Behrendt et al., 2014;Conrad, 1994;Remde et al., 1989). Nevertheless, the significance of a variable compensation mixing ratio has to be questioned. For instance, the NO compensation mixing ratio determined for different soil samples is usually comparable for a certain land use type. For HONO, however, the compensation mixing ratio can vary by several orders of magnitude within one experiment, e.g. S4 (Table 2 and Fig. 9). As the processes, underlying the ecosystem specific compensation mixing ratio of HONO, depend much on site specific conditions and soil properties, the use of these values for global upscaling is not recommended. However, it appears to be a useful tool to improve

the knowledge of the still not fully understood role in the biogeochemical nitrogen cycle and the chemistry of HONO in the atmosphere. For instance, the compensation mixing ratio of HONO could be determined for several soil samples during a field campaign. This would clearly define the role of soil for the HONO exchange fluxes at the measurement site and, if SWC is also measured, it could help to interpret measured vertical profiles of HONO.

As noted above, the compensation mixing ratio of HONO can vary strongly with SWC for one soil sample. Therefore, we suggest using the term ecosystem specific compensation mixing ratio of HONO, as it exhibits a clear distinction from the compensation point by the definition of Conrad (1994).

4.3 Determination of χ_{comp}

For the calculation of the ecosystem specific compensation mixing ratio of HONO, χ_{comp}, it is necessary to perform at least two experiments with different HONO inlet mixing ratios. As shown in Fig. 9, the resulting χ_{comp} strongly depends on the experimental conditions, such as the inlet mixing ratio $\chi_{in,2}$, in case a valve is used that switches χ_{in} during the experiment. This is a result of adsorption and subsequent desorption of HONO (see Sect. 4.4), yielding different results for χ_{in} = 0 ppb for standard and discontinuous experiment. For this reason, we recommend to use a standard and a discontinuous experiment to determine resulting χ_{comp}, although this may introduce uncertainties due to subsample variability. A valve for switching between different HONO inlet mixing ratios is necessary to avoid accumulation of nitrite in the soil and, hence, an alteration of soil nutrients, as nitrite is quickly transformed to other forms of N_r. Since adsorption and desorption of HONO on soil are not fully understood yet, switching of HONO mixing ratio should also be preferred as surface saturation effects cannot be precluded yet.

It is possible to conduct a linear regression for each SWC out of several experiments, in order to increase accuracy of χ_{comp} by the use of a larger data set from several individual experiments with different values for $\chi_{in,2}$. The variation in the strength and shape of the optimum emission, however, leads to large errors for this SWC range (see Fig. 8). It is likely, that this problem can be attributed to subsample variability, which is well known for e.g. NO flux measurements (Bargsten et al., 2010;Gelfand et al., 2009;Laville et al., 2009;Yu et al., 2010). This variability is usually associated with differences in the microbial activity and, hence, also important soil parameters such as the NO_2^- concentration. Behrendt et al. 2014 solved this problem by conducting all required experiments on one subsample. Unfortunately, this concept, which integrates the valve system as shown for the discontinuous experiments,

needs an additional standard experiment for HONO. For the linear range of the deposition (Fig. 12), the regression of data from several experiments with different χ_{in} will likely result in more accurate χ_{comp}. However, it needs to be considered that at least four processes are involved in the resulting bidirectional HONO flux (see Sect. 4.2) and none of them appears to be sufficiently characterized to ensure a linear relationship of χ_{comp} to χ_{in}. We propose that multiple experiments at two inlet mixing ratios of HONO, e.g., 0 ppb and 10 ppb should be conducted for the determination of χ_{comp}. We suggest 10 ppb HONO, as this is still relatively close to atmospheric conditions, but yields a large difference between HONO taken up and inlet mixing ratio. This results in comparably low uncertainties from Gaussian error propagation.

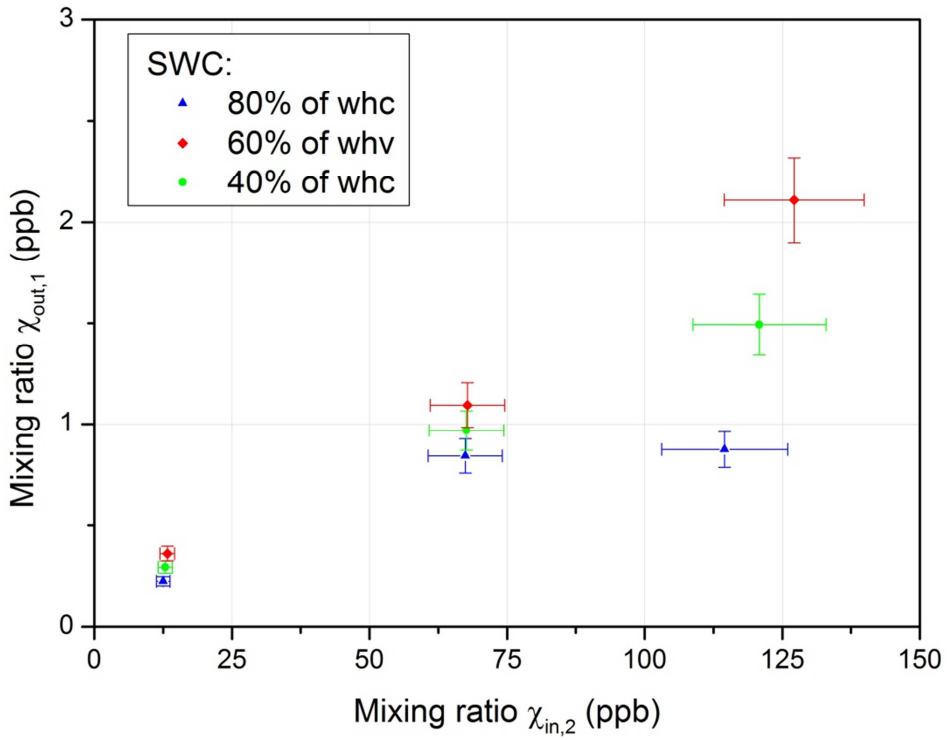

Figure 12: The mixing ratio of HONO $\chi_{out,1}$ as a function of the inlet mixing ratio $\chi_{in,2}$ at soil water contents 40% of whc (red diamonds), 60% of whc (green circles) and 80% of whc (blue triangles). Error bars denote uncertainties of the LOPAP instrument.

For the six measured soil samples only one correlation for the investigated χ_{comp} was found. It has to be noted that for S4 and S6a standard experiment could not be conducted and, hence, the desorption effect was not eliminated. However, a relationship between the optimum emission of HONO and the ecosystem specific compensation mixing ratio of HONO at the

optimum emission was found (Tab.2). This indicates, that the optimum emission is a non-reversible process, as more HONO needs to be deposited with increasing F_{opt}(HONO) and, hence, the release dominates over the uptake processes. Our results support the recent findings of bacterial HONO formation from hydroxylamine (Ermel et al., 2014), which appears to be irreversible.

Su et al. (2011) proposed HONO* as equilibrium gas phase mixing ratio of HONO, which is derived from partitioning of HONO between gas and liquid phase. We calculated HONO* and found that χ_{comp} below HONO* for soil sample S5 (Fig. 8), while for other soil samples HONO* was several orders of magnitude larger than χ_{comp}. The discrepancy was especially large for soil samples with low pH. However, HONO* resembles the shape of χ_{comp} at higher SWC well. Hence, the release and uptake of HONO by wet soil might be explained the concept of Su et al. (2011), which is based on Henry's law. At lower SWC, χ_{comp} is above the calculated HONO*, indicating that a different process becomes dominant. It has to be considered, that the nitrite pool in soil is an intermediate in the fast transformation from ammonia to nitrate and back (Russow et al., 2009). Thus, the nitrite concentration used to determine HONO* might vary during the experiment, which would result in different HONO*. Further studies with continuous monitoring of soil nitrite concentrations are required to determine the contribution of soil nitrite to HONO emission.

4.4 Adsorption and desorption of HONO

The adsorption of HONO on the soil surface has been reported from field studies (VandenBoer et al., 2013) and was also observed in the laboratory (Donaldson et al., 2014). At high ambient HONO mixing ratios we found net deposition fluxes of HONO occurring in the whole investigated SWC range (Fig. 7). Thus, uptake of HONO can occur by dry and wet soil. The partitioning from soil nitrite (Su et al., 2011) can only be considered at higher SWC, as it is based on Henry's law, which implies "infinite dilution" (Henry, 1803;Smith and Harvey, 2007). For dry soils, the competitive adsorption of HONO and water described by Donaldson et al. (2014) appears to be more reasonable. This process, however, is strongly depending on the relative humidity. Therefore, the representativeness of χ_{comp} at low SWC has to be questioned. As the humidity drops at the end of an experiment, where SWC is low and, hence, close to the conditions of Donaldson et al. (2014), the adsorption is maximal. Consequently, the calculated χ_{comp} values are minimal estimates.

The discontinuous experiments yielded higher emissions at $\chi_{in,1}$ = 0 ppb, than a standard experiment at χ_{in} = 0 ppb without the change of the ambient mixing ratio of HONO. Hence,

desorption of adsorbed HONO as postulated by (VandenBoer et al., 2013) can be measured directly. For soil sample S1 the ratio between the mixing ratios of desorbed and adsorbed HONO (Fig. 10) was a function of SWC and values reached unity at a certain SWC, which implies that desorption can be as strong as adsorption. However, it has to be considered that the ambient mixing ratio of HONO was switched every 45 minutes and, hence, desorption likely was not completed. This might explain the higher desorption at the end of the experiment (at lower SWC), as adsorbed HONO accumulated. At higher SWC, adsorption via Henry's law is subject to the acid base equilibrium of nitrite and nitrous acid, which will buffer the desorption process by the accumulation of soil nitrite. Further experiments will be needed to investigate the temporal and quantitative scales of desorption and adsorption of HONO on soil surfaces. The ^{15}N tracer method of Wu et al. (2014) might be a suitable tool. The strength of the desorption supports the findings of VandenBoer et al. (2013), who attribute a large fraction of the missing daytime source to desorption of HONO.

The production of NO from adsorbed HONO on soil was shown recently by Donaldson et al. (2014), who reported a yield of 16 % on dry soil. We found the HONO to NO conversion to vary between 0 and 100 %, although values in the lower SWC range are prone to large errors (see Sect. 3.6). As most other measured or calculated quantities, the conversion of HONO to NO is a function of SWC. Lower yields at high SWC might be attributed to the uptake via the acid-base mechanism forming a reservoir of nitrite, which can be accumulated and released at lower ambient mixing ratios. In contrast, adsorption has no coupled additional equilibrium at low SWC, which acts as a storage for HONO. This process might be relevant for field measurements, as an upward NO flux derived from conversion of adsorbed HONO might be measured at the site, while the measurement of soil samples in a laboratory dynamic chamber system with HONO free air might reveal lower fluxes. This implies that adsorption of ambient HONO can influence emission fluxes of NO from soil.

4.5 Implications of low χ_{comp} for atmospheric chemistry

Mixing ratios of HONO are usually in the range of 30 – 300 ppt during daytime and 0.5 – 5 ppb at night (VandenBoer et al., 2014;VandenBoer et al., 2013;Zhang et al., 2012;Sörgel et al., 2011;Villena et al., 2011). Our results show that many of the observed χ_{comp} at very low and high soil water contents are below typical values of nocturnal HONO mixing ratios. Consequently, soils can indeed act as a sink during nighttime, which was previously proposed by several field studies (VandenBoer et al., 2013;Wong et al., 2011;Su et al., 2008b;Su et al., 2008a;Stutz et al., 2004;Stutz et al., 2002;Sörgel et al., 2011). However, for some of the soil

samples, for instance S4 (Fig. 10), we found that χ_{comp}(HONO) can also be lower than typical daytime HONO mixing ratios. Hence, soils can also act as sinks during daytime. This has important implications for the atmospheric chemistry of HONO, as the missing HONO daytime source (Sörgel et al., 2011;Oswald et al., 2013;Kleffmann et al., 2003) could be larger than expected for some field sites, since soil can be an additional sink term in the budget. However, the previously discussed adsorption and desorption processes need to be considered. Obviously, a soil with low χ_{comp} will take up even more HONO at night and, hence, might be a strong desorption source during the following day. Further studies are required to evaluate which of these two processes will dominate and how this will influence atmospheric chemistry.

4.6 A conceptual model for HONO soil-air exchange

We previously identified four different processes controlling the bidirectional fluxes of HONO. All of these are a function of the SWC and, hence, the contribution to the net flux varies with the SWC as well. The partitioning of HONO between gaseous and aqueous phase, is restricted to higher SWC due to the principles of Henry's law. We found χ_{comp} to exceed HONO* at 30% of whc (Fig. 8), where bacterial HONO formation starts to dominate. Therefore, we assume that the gas-liquid partitioning is only relevant in the SWC range from 30 – 100% of whc. From the studies of Oswald et al. (2013) we know that bacterial formation is restricted to the lower SWC range from 0 – 30% of whc, with an optimum at about 15% of whc. Additionally, bacterial formation is only a release process (Ermel et al., 2014). Adsorption of HONO was recently shown to occur on dry soils, but an upper limit was not reported up to now (Donaldson et al., 2014). It also appears difficult to distinguish adsorption and uptake by Henry's law. As the maximal emission of HONO from NH_2OH is related to the water limitation of AOB, we assume that adsorption is only relevant in the strongly water limited SWC from 0 – 15% of whc. As our results in Figs. 2 and 10 show, desorption of HONO can occur at all SWC from 0 – 100% of whc. However, we do not differentiate between release from soil nitrite and release from adsorbed HONO, as no clear distinction is possible. Further experiments with isotope labelled HONO and nitrite are necessary to distinguish the contribution of both processes. Fig. 15 summarizes the discussed processes in a conceptual model.

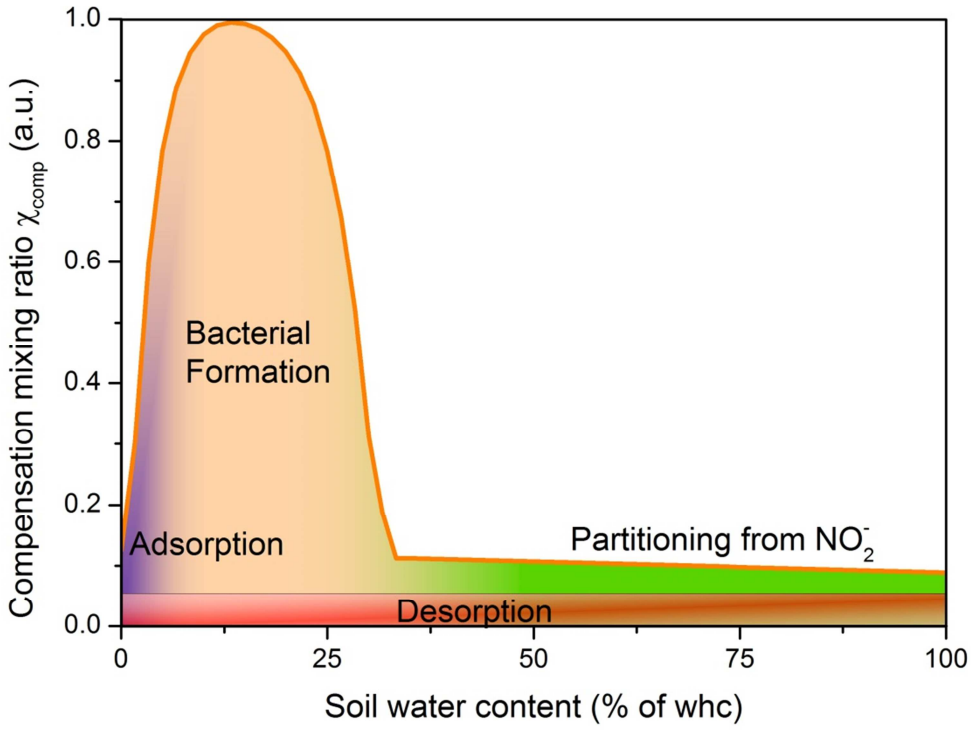

Figure 15: Simplified scheme of the contribution of the different processes involved in HONO release and uptake as a function of SWC. While adsorption, bacterial formation and partitioning from soil nitrite dominate at a certain SWC, desorption can occur at all SWC, depending on the ambient HONO mixing ratio.

5. Summary and Conclusions

In the present study, HONO exchange fluxes of six different soils were investigated in a laboratory dynamic chamber system. We found bidirectional fluxes for all analysed samples. A soil sample from a wheat field in Germany was intensively studied to investigate bidirectional fluxes with increasing soil layer thickness and varying ambient HONO mixing ratios. As the flux of HONO was found to be constant with increasing soil layer thickness, an important prerequisite for the application of the compensation point concept was fulfilled. However, we introduced the new term “ecosystem specific compensation mixing ratio of HONO”, χ_{comp}, because the classical concept by Conrad et al. (1994) requires biological production and consumption to occur simultaneously. This prerequisite was not fulfilled for HONO and we identified at least four mainly physicochemical processes influencing bidirectional HONO fluxes. These are (a) partitioning from soil nitrite, (b) HONO formation

from NH_2OH released by bacteria, (c) adsorption and (d) desorption of HONO. These processes all depend on the soil water content and each dominates within a certain SWC range. Hence, χ_{comp} is a function of the soil water content and is not constant as found for e.g. NO (Behrendt et al., 2014). The application of a valve system to switch between two different HONO levels (0 ppb and 10 – 150 ppb) and comparison with measurements using only purified air during the experimental course showed that HONO is adsorbed at higher ambient mixing ratios and desorbed from the soil when exposing the sample to HONO free air. The desorption rate was found to vary with soil water content and can reach the magnitude of the adsorption rate. This confirms recent findings from a field study (VandenBoer et al., 2013), revealing a strong contribution of HONO desorption from the ground to the unknown daytime source. In addition, we found the conversion yield of adsorbed HONO to NO to be a function of the soil water content and yields of up to 100 % for an acidic soil sample. This reveals the influence of HONO on NO emission fluxes from soil. The low χ_{comp} found at high soil water content for several soil samples indicates that soil can act as a HONO sink even during daytime when low mixing ratios (30 – 300 ppt) prevail. Hence, soil can also increase the unknown daytime source. However, the relation between low χ_{comp} and desorption of nocturnally accumulated HONO requires further experiments to draw final conclusions. We have investigated fundamental insights providing a basis for future studies on soil-air exchange of HONO that is highly relevant for atmospheric chemistry.

Acknowledgements

This project was funded by the Max Planck Society. The work was supported by the Max Planck Graduate Center with the Johannes Gutenberg-Universität Mainz (MPGC). We are grateful to M. Welling and A. Moravek for supporting the experiments and helping to collect the soil samples.

References

Acker, K., Febo, A., Trick, S., Perrino, C., Bruno, P., Wiesen, P., Moller, D., Wieprecht, W., Auel, R., Giusto, M., Geyer, A., Platt, U., and Allegrini, I.: Nitrous acid in the urban area of Rome, Atmos Environ, 40, 3123-3133, DOI 10.1016/j.atmosenv.2006.01.028, 2006.

Bargsten, A., Falge, E., Pritsch, K., Huwe, B., and Meixner, F. X.: Laboratory measurements of nitric oxide release from forest soil with a thick organic layer under different understory types, Biogeosciences, 7, 1425-1441, 10.5194/bg-7-1425-2010, 2010.

Behrendt, T., Veres, P. R., Ashuri, F., Song, G., Flanz, M., Mamtimin, B., Bruse, M., Williams, J., and Meixner, F. X.: Characterisation of NO production and consumption: new insights by an improved laboratory dynamic chamber technique, Biogeosciences Discuss., 11, 1187-1275, 10.5194/bgd-11-1187-2014, 2014.

Blume, H., Deller, B., Leschber, R., Paetz, A., Schmidt, S., and Wilke, B.: Handbuch der Bodenuntersuchungen, Terminologie, Verfahrensvorschriften und Datenblätter. Physikalische, chemische, biologische Untersuchungsverfahren. Gesetzliches Regelwerk, Grundwerk. Berlin, Wien, Zürich, 2000.

Bouwman, A. F., Beusen, A. H. W., Griffioen, J., Van Groenigen, J. W., Hefting, M. M., Oenema, O., Van Puijenbroek, P. J. T. M., Seitzinger, S., Slomp, C. P., and Stehfest, E.: Global trends and uncertainties in terrestrial denitrification and N_2O emissions, Philosophical Transactions of the Royal Society B: Biological Sciences, 368, 10.1098/rstb.2013.0112, 2013.

Breuninger, C., Oswald, R., Kesselmeier, J., and Meixner, F. X.: The dynamic chamber method: trace gas exchange fluxes (NO, NO_2, O_3) between plants and the atmosphere in the laboratory and in the field, Atmos Meas Tech, 5, 955-989, 10.5194/amt-5-955-2012, 2012.

Chapuis-Lardy, L., Wrage, N., Metay, A., Chotte, J.-L., and Bernoux, M.: Soils, a sink for N_2O? A review, Global Change Biology, 13, 1-17, 10.1111/j.1365-2486.2006.01280.x, 2007.

Conrad, R.: Compensation concentration as critical variable for regulating the flux of trace gases between soil and atmosphere, Biogeochemistry, 27, 155-170, 10.1007/bf00000582, 1994.

Crutzen, P. J., and Lelieveld, J.: Human impacts on atmospheric chemisty, Annu Rev Earth Pl Sc, 29, 17-45, 2001.

Donaldson, M. A., Berke, A. E., and Raff, J. D.: Uptake of gas phase nitrous acid onto boundary layer soil surfaces, Environ Sci Technol, 48, 375-383, 10.1021/es404156a, 2014.

Elshorbany, Y. F., Crutzen, P. J., Steil, B., Pozzer, A., Tost, H., and Lelieveld, J.: Global and regional impacts of HONO on the chemical composition of clouds and aerosols, Atmos. Chem. Phys., 14, 1167-1184, 10.5194/acp-14-1167-2014, 2014.

Ermel, M., Behrendt, T., Oswald, R., Derstroff, B., Wu, D., Hohlmann, S., Stönner, C., Pommerening-Röser, A., Williams, J., Meixner, F. X., Andreae, M. O., Sörgel, M., and Trebs, I.: Hydroxylamine released by ammonia-oxidizing bacteria as precursor for HONO emission from soils submitted to Proceedings of the National Academy of Sciences, 2014.

Febo, A., Perrino, C., Gherardi, M., and Sparapani, R.: Evaluation of a high-purity and high-stability continuous generation system for nitrous acid, Environ Sci Technol, 29, 2390-2395, 1995.

Feig, G. T., Mamtimin, B., and Meixner, F. X.: Soil biogenic emissions of nitric oxide from a semi-arid savanna in South Africa, Biogeosciences, 5, 1723-1738, 2008.

Gelfand, I., Feig, G., Meixner, F. X., and Yakir, D.: Afforestation of semi-arid shrubland reduces biogenic NO emission from soil, Soil Biol. Biochem., 41, 1561-1570, 10.1016/j.soilbio.2009.04.018, 2009.

Heland, J., Kleffmann, J., Kurtenbach, R., and Wiesen, P.: A new instrument to measure gaseous nitrous acid (HONO) in the atmosphere, Environ Sci Technol, 35, 3207-3212, 2001.

Henry, W.: Experiments on the quantity of gases absorbed by water, at different temperatures, and under different pressures, Philosophical Transactions of the Royal Society of London, 29-276, 1803.

Kleffmann, J., Heland, J., Kurtenbach, R., Lorzer, J., and Wiesen, P.: A new instrument (LOPAP) for the detection of nitrous acid (HONO), Environ Sci Pollut R, 48-54, 2002.

Kleffmann, J., Kurtenbach, R., Lorzer, J., Wiesen, P., Kalthoff, N., Vogel, B., and Vogel, H.: Measured and simulated vertical profiles of nitrous acid - Part I: Field measurements, Atmos Environ, 37, 2949-2955, Doi 10.1016/S1352-2310(03)00242-5, 2003.

Lamaud, E., Loubet, B., Irvine, M., Stella, P., Personne, E., and Cellier, P.: Partitioning of ozone deposition over a developed maize crop between stomatal and non-stomatal uptakes, using eddy-covariance flux measurements and modelling, Agr Forest Meteorol, 149, 1385-1396, DOI 10.1016/j.agrformet.2009.03.017, 2009.

Lammel, G., and Cape, J. N.: Nitrous acid and nitrite in the atmosphere, Chem Soc Rev, 25, 361-+, 1996.

Laville, P., Flura, D., Gabrielle, B., Loubet, B., Fanucci, O., Rolland, M. N., and Cellier, P.: Characterisation of soil emissions of nitric oxide at field and laboratory scale using high resolution method, Atmos Environ, 43, 2648-2658, http://dx.doi.org/10.1016/j.atmosenv.2009.01.043, 2009.

Li, X., Brauers, T., Haseler, R., Bohn, B., Fuchs, H., Hofzumahaus, A., Holland, F., Lou, S., Lu, K. D., Rohrer, F., Hu, M., Zeng, L. M., Zhang, Y. H., Garland, R. M., Su, H., Nowak, A., Wiedensohler, A., Takegawa, N., Shao, M., and Wahner, A.: Exploring the atmospheric chemistry of nitrous acid (HONO) at a rural site in Southern China, Atmospheric Chemistry and Physics, 12, 1497-1513, DOI 10.5194/acp-12-1497-2012, 2012.

Meixner, F., and Yang, W.: Biogenic Emissions of Nitric Oxide and Nitrous Oxide from Arid and Semi-arid Land, in: Dryland Ecohydrology, edited by: D'Odorico, P., and Porporato, A., Springer Netherlands, 233-255, 2006.

Oswald, R., Behrendt, T., Ermel, M., Wu, D., Su, H., Cheng, Y., Breuninger, C., Moravek, A., Mougin, E., Delon, C., Loubet, B., Pommerening-Roser, A., Sorgel, M., Poschl, U., Hoffmann, T., Andreae, M. O., Meixner, F. X., and Trebs, I.: HONO emissions from soil bacteria as a major source of atmospheric reactive nitrogen, Science, 341, 1233-1235, 10.1126/science.1242266, 2013.

Oswald, R.: Formation and surface exchange of nitrous acid, Universitätsbibliothek Mainz, 2014.

Oswald, R., Behrendt, T., Ermel, M., Wu, D., Breuninger, C., Moravek, A., Loubet, B., Hoffmann, T., Andreae, M. O., Meixner, F. X., Sörgel, M., and Trebs, I.: Influence of soil properties and ambient mixing ratios on HONO emission, submitted to Biogeosciences, 2014a.

Oswald, R., Ermel, M., Hens, K., Novelli, A., Ouwersloot, H. G., Paasonen, P., Petäjä, T., Sipilä, M., Keronen, P., Bäck, J., Königstedt, R., Hosaynali Beygi, Z., Fischer, H., Bohn, B., Kubistin, D., Harder, H., Martinez, M., Williams, J., Hoffmann, T., Trebs, I., and Sörgel, M.: Comparison of HONO budgets for two measurement heights at a field station within the boreal forest (SMEAR II - HUMPPA-COPEC 2010), Atmos. Chem. Phys. Discuss., 14, 7823-7857, 10.5194/acpd-14-7823-2014, 2014b.

Pape, L., Ammann, C., Nyfeler-Brunner, A., Spirig, C., Hens, K., and Meixner, F.: An automated dynamic chamber system for surface exchange measurement of non-reactive and reactive trace gases of grassland ecosystems, Biogeosciences Discussions, 5, 2008.

Pilegaard, K.: Processes regulating nitric oxide emissions from soils, Philosophical Transactions of the Royal Society B: Biological Sciences, 368, 10.1098/rstb.2013.0126, 2013.
Remde, A., Slemr, F., and Conrad, R.: Microbial production and uptake of nitric oxide in soil, Fems Microbiology Letters, 62, 221-230, 1989.

Russow, R., Stange, C. F., and Neue, H. U.: Role of nitrite and nitric oxide in the processes of nitrification and denitrification in soil: Results from ^{15}N tracer experiments, Soil Biol. Biochem., 41, 785-795, DOI 10.1016/j.soilbio.2009.01.017, 2009.

Seiler, W., Holzapfel-Pschorn, A., Conrad, R., and Scharffe, D.: Methane emission from rice paddies, J Atmos Chem, 1, 241-268, 1983.

Smith, F. L., and Harvey, A. H.: Avoid common pitfalls when using Henry's law, Chem Eng Prog, 103, 33-39, 2007.

Sörgel, M., Regelin, E., Bozem, H., Diesch, J. M., Drewnick, F., Fischer, H., Harder, H., Held, A., Hosaynali-Beygi, Z., Martinez, M., and Zetzsch, C.: Quantification of the unknown HONO daytime source and its relation to NO_2, Atmospheric Chemistry and Physics, 11, 10433-10447, DOI 10.5194/acp-11-10433-2011, 2011.

Stocker, T. F., Qin, D., Plattner, G.-K., Tignor, M., Allen, S. K., Boschung, J., Nauels, A., Xia, Y., Bex, V., and Midgley, P. M.: Climate change 2013: The physical science basis, Intergovernmental Panel on Climate Change, Working Group I Contribution to the IPCC Fifth Assessment Report (AR5)(Cambridge Univ Press, New York), 2013.

Stutz, J., Alicke, B., and Neftel, A.: Nitrous acid formation in the urban atmosphere: Gradient measurements of NO_2 and HONO over grass in Milan, Italy, J Geophys Res-Atmos, 107, Artn 8192 Doi 10.1029/2001jd000390, 2002.

Stutz, J. C., Wang, S. H., and Hurlock, S. C.: Formation of nitrous acid in the urban nocturnal boundary layer., Abstr Pap Am Chem S, 228, U203-U203, 2004.

Su, H., Cheng, Y. F., Cheng, P., Zhang, Y. H., Dong, S., Zeng, L. M., Wang, X., Slanina, J., Shao, M., and Wiedensohler, A.: Observation of nighttime nitrous acid (HONO) formation at a non-urban site during PRIDE-PRD2004 in China, Atmos Environ, 42, 6219-6232, 2008a.

Su, H., Cheng, Y. F., Shao, M., Gao, D. F., Yu, Z. Y., Zeng, L. M., Slanina, J., Zhang, Y. H., and Wiedensohler, A.: Nitrous acid (HONO) and its daytime sources at a rural site during the 2004 PRIDE-PRD experiment in China, Journal of Geophysical Research: Atmospheres (1984–2012), 113, 2008b.

Su, H., Cheng, Y., Oswald, R., Behrendt, T., Trebs, I., Meixner, F. X., Andreae, M. O., Cheng, P., Zhang, Y., and Poschl, U.: Soil nitrite as a source of atmospheric HONO and OH radicals, Science, 333, 1616-1618, 10.1126/science.1207687, 2011.

Twigg, M., House, E., Thomas, R., Whitehead, J., Phillips, G., Famulari, D., Fowler, D., Gallagher, M., Cape, J., and Sutton, M.: Surface/atmosphere exchange and chemical interactions of reactive nitrogen compounds above a manured grassland, Agr Forest Meteorol, 151, 1488-1503, 2011.

Uysal, N., and Schapira, R. M.: Effects of ozone on lung function and lung diseases, Curr Opin Pulm Med, 9, 144-150, 2003.

VandenBoer, T. C., Brown, S. S., Murphy, J. G., Keene, W. C., Young, C. J., Pszenny, A., Kim, S., Warneke, C., Gouw, J. A., and Maben, J. R.: Understanding the role of the ground surface in HONO vertical structure: High resolution vertical profiles during NACHTT-11, Journal of Geophysical Research: Atmospheres, 118, 10,155-110,171, 2013.

VandenBoer, T. C., Markovic, M. Z., Sanders, J. E., Ren, X., Pusede, S. E., Browne, E. C., Cohen, R. C., Zhang, L., Thomas, J., Brune, W. H., and Murphy, J. G.: Evidence for a nitrous acid (HONO) reservoir at the ground surface in Bakersfield, CA during CalNex 2010, Journal of Geophysical Research: Atmospheres, n/a-n/a, 10.1002/2013jd020971, 2014.

Villena, G., Kleffmann, J., Kurtenbach, R., Wiesen, P., Lissi, E., Rubio, M. A., Croxatto, G., and Rappengluck, B.: Vertical gradients of HONO, NO_x and O_3 in Santiago de Chile, Atmos Environ, 45, 3867-3873, DOI 10.1016/j.atmosenv.2011.01.073, 2011.

Wong, K. W., Oh, H. J., Lefer, B. L., Rappengluck, B., and Stutz, J.: Vertical profiles of nitrous acid in the nocturnal urban atmosphere of Houston, TX, Atmospheric Chemistry and Physics, 11, 3595-3609, DOI 10.5194/acp-11-3595-2011, 2011.

Wong, K. W., Tsai, C., Lefer, B., Haman, C., Grossberg, N., Brune, W. H., Ren, X., Luke, W., and Stutz, J.: Daytime HONO vertical gradients during SHARP 2009 in Houston, TX, Atmospheric Chemistry and Physics, 12, 635-652, DOI 10.5194/acp-12-635-2012, 2012.

Wu, D., Kampf, C. J., Pöschl, U., Oswald, R., Cui, J., Ermel, M., Hu, C., Trebs, I., and Sörgel, M.: Novel Tracer Method To Measure Isotopic Labeled Gas-Phase Nitrous Acid ($HO^{15}NO$) in Biogeochemical Studies, Environ Sci Technol, 10.1021/es501353x, 2014.

Yu, J., Meixner, F. X., Sun, W., Mamtimin, B., Wang, G., Qi, X., Xia, C., and Xie, W.: Nitric oxide emissions from black soil, northeastern China: A laboratory study revealing significantly lower rates than hitherto reported, Soil Biology and Biochemistry, 42, 1784-1792, http://dx.doi.org/10.1016/j.soilbio.2010.06.016, 2010.

Zhang, N., Zhou, X., Bertman, S., Tang, D., Alaghmand, M., Shepson, P. B., and Carroll, M. A.: Measurements of ambient HONO concentrations and vertical HONO flux above a northern Michigan forest canopy, Atmospheric Chemistry and Physics, 12, 8285-8296, DOI 10.5194/acp-12-8285-2012, 2012.